

Copyright

by

Arielle Simone Mimouni

2014

**The Thesis Committee for Arielle Simone Mimouni  
Certifies that this is the approved version of the following thesis :**

**Impact of salt-tolerant friction reducers on shale stability  
and fracture conductivity**

**APPROVED BY  
SUPERVISING COMMITTEE:**

---

Lynn E. Katz, Supervisor

---

Eric van Oort, Co-Supervisor

---

Mukul M. Sharma, Co-Supervisor

**Impact of salt-tolerant friction reducers on shale stability  
and fracture conductivity**

**by**

**Arielle Simone Mimouni**

**Thesis**

Presented to the Faculty of the Graduate School of

The University of Texas at Austin

in Partial Fulfillment

of the Requirements

for the Degree of

**Master of Science in Engineering**

**The University of Texas at Austin**

**August 2014**

## **Acknowledgements**

I would like to thank my advisors Dr. Katz, Dr. van Oort and Dr. Sharma for their guidance and support during the past two years. Nicholas Kuzmyak provided me with a lot of help, especially doing hot rolling oven tests, and viscosity measurements, and preparing presentations and papers. Thank you to Rod Russell who taught me how to conduct fracture conductivity tests and who helped troubleshoot the equipment. I am grateful to Dr. Chenevert, and Arthur Hale for their expertise on shale research and their advice. Thanks to Justin Gabuten, Seung-hwan, Celina Dozier, Joon Kyoung Han, Alyssa Offutt, Junhao Zhou, JP Gips, and Shashvat Doorwar from my research groups for their help in the lab.

I would like to acknowledge my funding source, Shell, who gave me the opportunity to work on this research and study for my masters at the University of Texas at Austin.

Lastly, thank you to my family and friends for their support and encouragement.



## **Abstract**

### **Impact of salt-tolerant friction reducers on shale stability and fracture conductivity**

Arielle Simone Mimouni, M.S.E.

The University of Texas at Austin, 2014

Supervisors: Lynn E. Katz, Eric van Oort, Mukul M. Sharma

One of the main challenges of hydraulic fracturing is the reuse of flowback waters. While it alleviates the disposal and treatment costs of these concentrated brines, it also limits the environmental impacts of the fracking industry by reducing the amounts of fresh water necessary to produce gas. This research aims at optimizing this process by assessing the impacts of salt-tolerant friction reducers on shale stability and fracture conductivity. Polyacrylamide and polyethylene oxide based friction reducers were assessed over a wide range of NaCl and CaCl<sub>2</sub> concentrations, using a hot rolling oven and fracture conductivity experiments. The commonly used polyacrylamide based DR3046 was found to be a good shale stabilizer but did not efficiently reduce friction in the presence of divalent salts. While high molecular weight polyethylene oxides showed a high friction reduction in all brines, and reduced shale cuttings dispersion in the presence of salts, they did not maintain fracture conductivity. The newly developed Dispersion Polymer Friction Reducer (DPFR) showed the best and most consistent results for all salt

concentrations, in terms of friction reduction, shale stabilization efficiency, and ability to maintain the highest fracture conductivity.

## Table of Contents

List of Tables .....	x
List of Figures .....	xii
Chapter 1: Introduction .....	1
1.1 Background .....	1
1.2 Scope .....	2
1.3 Approach .....	3
Chapter 2: Literature review .....	4
2.1 Hydraulic fracturing overview .....	4
2.2 Flowback water reuse .....	5
2.2.1 Quantity and quality .....	5
2.2.2 Flowback water reuse challenges .....	11
2.2.3 Flowback water reuse technologies .....	12
2.3 Shale stability .....	14
2.3.1 Shale instability mechanisms .....	14
2.3.2 Clay mineralogy and problems related to water interactions ...	16
2.3.3 Solutions .....	19
2.4 Fracture conductivity .....	25
2.4.1 Definition .....	25
2.4.2 Mechanisms for reduction of fracture conductivity .....	26
2.5 Polyacrylamide .....	30
2.5.1 Degree of hydrolysis .....	31
2.5.2 Applications .....	32
2.5.3 Degradation .....	33
2.6 Polyethylene oxide .....	33
2.6.1 Cloud point effect observation and explanation .....	34
2.6.2 Applications .....	39
2.6.3 Degradation .....	40

Chapter 3: Experimental methods .....	45
3.1 Materials.....	45
3.1.1 Fluids .....	45
3.1.2 Shale samples .....	48
3.2 Material characterization.....	49
3.2.1 Fluids characterization .....	49
3.2.2 Shale storage .....	50
3.3 Shale instability visualization .....	51
3.4 Hot rolling oven dispersion tests.....	52
3.5 Fracture conductivity tests .....	54
3.5.1 Experimental design .....	54
3.5.2 Experimental procedure .....	57
Chapter 4: Results .....	62
4.1 Fluid and shale characterization.....	62
4.1.1 Fluid characterization.....	62
4.1.2 Shale characterization .....	69
4.2 Shale instability visualization .....	70
4.2.1 Swelling tests results .....	70
4.2.2 Beaker tests results .....	71
4.2.3 Conclusions .....	73
4.3 Hot rolling oven dispersion results .....	73
4.3.1 Effect of salt addition .....	73
4.3.2 Effects of PA addition .....	75
4.3.3 Effects of PEO addition .....	77
4.3.4 Comparison of the effects of PA and PEO.....	80
4.3.5 Effects of salt composition .....	82
4.3.6 Effect of time.....	83
4.3.7 Conclusions on the efficiency of salt-tolerant friction reducers at preventing shale cuttings dispersion .....	85
4.4 Fracture conductivity results .....	86

4.4.1 Preliminary experiments .....	87
4.4.2 Shale fluid sensitivity to one fluid injection .....	88
4.4.3 Shale fluid sensitivity to successive fluid injections .....	92
4.4.4 Conclusions on the efficiency of salt-tolerant friction reducers at maintaining fracture conductivity .....	96
Chapter 5: Conclusions .....	98
5.1 Summary .....	98
5.2 Future work .....	100
Appendix A - Cloud point temperatures in NaCl and CaCl <sub>2</sub> solutions at 0.1% and 0.01% PEO .....	102
Appendix B - Effect of PEO addition on the pH of CaCl <sub>2</sub> solutions .....	103
Appendix C – Viscosity data .....	104
Bibliography .....	105

## List of Tables

Table 1 - pH, $\text{Cl}^-$ , $\text{Ca}^{2+}$ , $\text{Na}^+$ and TDS concentrations in 56 flowback waters collected from the Marcellus Shale .....	6
Table 2 - Marcellus shale flowback water quality in Pennsylvania (Barbot et al., 2013) .....	7
Table 3 - Typical produced water TDS levels in some US shale plays (From USGS, 2011) .....	10
Table 4 - Classification of shales by clay content and related problems (adapted from O'Brien & Chenevert, 1973).....	19
Table 5 - Polyox grades and molecular weights .....	<b>Erreur ! Signet non défini.</b>
Table 6 – Label scheme .....	48
Table 7 - X-Ray diffraction mineralogy of GOM-12 and Pierre Shale I.....	69
Table 8 - CPT ( $^{\circ}\text{C}$ ) of 0.1% WSR-N10, 0.01% and 0.1% WSR-301, and 0.1% WSR-301 + 0.5% PPG in 10% and 20% NaCl.....	78
Table 9 –Propped fractures properties .....	88
Table 10 - Fracture conductivity test matrix .....	88
Table 11 - CPT ( $^{\circ}\text{C}$ ) of 0.1% PEO solutions in NaCl and $\text{CaCl}_2$ .....	102
Table 12 - CPT ( $^{\circ}\text{C}$ ) of 0.01% PEO solutions in NaCl and $\text{CaCl}_2$ .....	102

Table 13 - pH of CaCl <sub>2</sub> solutions with and without 0.1% PEO .....	103
Table 14 - Viscosity (cP) of PA and PEO solutions with no salt present and with 20% NaCl, at 25°C and 70°C .....	104
Table 15 - Viscosity (cP) of PA and PEO solutions with 10% NaCl, 10% CaCl <sub>2</sub> and the multi-solute brine, at 25°C and 70°C .....	104

## List of Figures

Figure 1 –The lower 48 US states shale plays (EIA, 2011) .....	9
Figure 2 - Evolution of TDS levels and flow rate of flowback waters versus time for Green County, PA (Hayes, 2009) .....	10
Figure 3 - Conceptual model of the sequential crystalline swelling process for smectite ( <i>Likos, 2004</i> ) .....	17
Figure 4 - Distribution of ions near a surface clay ( <i>Mitchell, 1993</i> ).....	18
Figure 5 - Monomeric amine (left), oligomeric amine (middle), polyamine (right) structures – (Adapted from Patel & Gomez, 2013) .....	24
Figure 6 - Schematic of a fracture ( <i>Adapted from Cinco-Ley &amp; Samaniego-V., 1981</i> ) .....	25
Figure 7 - Proppant embedment versus closure stress and dependence on clay content (Alramahi and Sundberg, 2012).....	27
Figure 8 - Impact of proppant size and time on retained porosity (Weaver et al., 2005) .....	28
Figure 9 - Proppant pack rearrangement (Terracina et al., 2010) .....	29
Figure 10 - SEM photo (514x) of formation fines spalling (circled) due to grain embedment (Terracina et al., 2010) .....	30



Figure 11 – HPAM chemical structure where m is the number of acrylic acid units and n-m is the number of acrylamide units (Adapted from Wever, Picchioni, & Broekhuis, 2011).....	30
Figure 12 - Chemical structure of polyethylene glycols and polypropylene glycols (Bland, 1994). R is a hydrogen or an alkyl group. Generally, $n+m \geq 4$ and represents the degree of polymerization. ....	34
Figure 13 - Order of effectiveness of ions in lowering the cloud point temperature (Adapted from Ataman, 1987) .....	37
Figure 14 - Cloud point temperature versus salt concentration for a 0.5% w/w PEO with a molecular weight of $4 \times 10^6$ g/mol (Bailey and Callard, 1959) ....	38
Figure 15 - Molecular weight distribution curves of PEO ( $M_w = 3.71 \times 10^6$ ) before and after application of 500 Pa and 1900 Pa shear stresses to 1 g/L aqueous solution at 30°C (D’Almeida and Dias, 1997) .....	41
Figure 16 – Effect of temperature on 1% PEO solution viscosity degradation (L’Hote-gaston et al., n.d.) .....	43
Figure 17 - Effect of humidity on 1% PEO solution viscosity degradation (L’Hote-gaston et al., n.d.) .....	43
Figure 18 - Polypropylene glycol chemical structure - n represents the average propylene oxide length ( <i>Fiume et al., 2012</i> ) .....	47

Figure 19 - A solution of 10 %CaCl <sub>2</sub> + 0.1% WSR-301 + 0.5% PPG 400 before the CPT (left) and at the CPT (right) .....	50
Figure 20 - Swelling test apparatus .....	52
Figure 21 – A solution of 20% NaCl + 0.1% WSR-301 + 0.5% PPG retained on the sieve with the cuttings before (left) and after (right) the shale was dried out. It had been hot-rolled for 8 hours at 70°C. ....	54
Figure 22 - Schematic of the core flood apparatus (Adapted from Pedlow, 2013) ....	55
Figure 23 - Core flood apparatus in oven .....	56
Figure 24 - Accumulator loaded with nitrogen .....	57
Figure 25 – Core preparation: Sand being packed between the half cores (left), and proppant pack, half cores, and screens tightly wrapped with Teflon tape (right) .....	57
Figure 26 - Schematic of the deviation from Darcy's Law at high flow rates .....	60
Figure 27 - Calculation of Y-intercept for permeability calculation .....	61
Figure 28 - Aspects of a PEO solution as the temperature increases (from the left to the right) - Solution of 10% CaCl <sub>2</sub> + 0.1% WSR-301 + 0.5% PPG – The cloud point temperature (CPT) is the first temperature above which the solution becomes cloudy .....	62

Figure 29 - Dependence of the CPT on NaCl concentration, the PEO concentration, and the PEO molecular weight.....	64
Figure 30 - Dependence of the CPT of 0.1% (w/w) WSR-301 on the salt species ....	65
Figure 31 - Dependence of the CPT of 0.1% (w/w) WSR-301 on the addition of PPG .....	65
Figure 32 - Viscosity of 20% NaCl solutions with 0.1% PA and 0.1% PEO at 70°C	66
Figure 33 - Adsorption isotherm of Pierre Shale I with a native water content of 5.7% .....	70
Figure 34 - Swelling of GOM-12 in DI Water, 0.1% WSR-301, and 4% NaCl. The strain is the ratio of the displacement of the clamp over the original length of sample shale.....	71
Figure 35 - Beaker test on GOM-12 at ambient temperature for 0.01% WSR-301 in the left jar and DI water in the right jar at 0h (left), 1.5 (middle) and 44h (right) – The red circles indicate the noticeable shale degradation.....	72
Figure 36 - Beaker test on GOM-12 at ambient temperature for 0.01% WSR-301 + 2.5% NaCl in the left jar and 2.5% NaCl in the right jar at 0h (left), and 1h30 (right) – The red circle indicates the noticeable shale degradation. .....	72

Figure 37 - Comparison of % shale retained in salt solutions (0, 10%, and 20% NaCl, 10% CaCl <sub>2</sub> , and the multi-solute brine) after 3h, 8h, and 12h in the HRO at 70°C.....	74
Figure 38 – Comparison of % shale retained in polyacrylamide-based solutions (0.1% DR3046 and 0.1% DPFR) with 0, 10% and 20% NaCl after 12 hours in the HRO at 70°C .....	76
Figure 39 – Comparison of % shale retained with 0.01% DPFR and 0.1% DPFR after 12 hours in the HRO at 70°C .....	77
Figure 40 – Comparison of % shale retained in polyethylene oxide-based solutions (0.1% WSR-301 and PEO-PPG dispersion) with 0, 10, and 20% NaCl after 12 hours in the HRO at 70°C .....	78
Figure 41 - % Shale retained after 12 hours in the HRO at 70°C vs the difference between 70°C and the CPTs of PEO-NaCl/CaCl <sub>2</sub> Solutions .....	79
Figure 42 - Comparison of % shale retained with 0.1% WSR-N10, 0.01% WSR-301, and 0.1% WSR-301 after 12 hours in the HRO at 70°C .....	80
Figure 43 - Comparison of % shale retained in 0.1% PA and 0.1% PEO solutions with 0, 10, and 20% NaCl after 12 hours in the HRO at 70°C .....	81
Figure 44 - % Shale retained after 12 hours in the HRO at 70°C vs viscosity at 70°C of the multi-solute brine, of 20% NaCl and in no salts .....	82

Figure 45 - % Shale retained after 12 hours in the HRO at 70°C vs salt concentrations and species (no salts, CaCl <sub>2</sub> , NaCl, multi-solute brine) for 0.1% DPFR, 0.1% DR3046, and 0.1% WSR-301 + 0.5% PPG .....	83
Figure 46 - Comparison of % shale retained in 20% NaCl and 0.1% WSR-N10, 0.1% WSR-301+ 0.5% PPG, 0.1% DPFR, and with no additive, after 3h, 8h, and 12h in the HRO at 70°C .....	84
Figure 47 - % Shale retained after 12h in the HRO at 70°C vs friction reduction % in 0.1% DR3046, 0.1% DPFR, and PEO-PPG dispersion with DI water, 10% NaCl, 20% NaCl, 10% CaCl <sub>2</sub> , and the multi-solute brine .....	86
Figure 48 - Comparison of the percentages of permeability retained after a first flood .....	89
Figure 49 – Fracture faces of cores 1 (left) and 2 (right) at the end of the test.....	90
Figure 50 - Microscope images showing faces of cores 1 (top) and 2 (down) after floods.....	91
Figure 51 - SEM image of core 2 after flood with fresh water .....	92
Figure 52 – Percentages of permeability retained after the successive injections in core 3 .....	94
Figure 53 – Percentages of permeability retained after the successive injections in core 4 .....	95

## **Chapter 1: Introduction**

### **1.1 Background**

Hydraulic fracturing or fracking is the process of fracturing of rocks via the pressurized injection of a liquid. In the last 10 years, this technology combined with horizontal drilling has enabled economic gas production from low permeability reservoirs such as shale plays. This has changed the energy landscape and made the US closer to achieving energy independence. While this process shows unequalled production rates and large resource reserves, it raises environmental concerns. Among them are the emissions of air pollutants, the pollution of groundwater, seismicity impacts, and large water consumption.

To extract the gas from the formation, fracturing fluids are injected at high pressure in the rocks. This creates fractures that allow the gas to flow to the surface. Up to six million gallons of water may be needed to fracture a well. These substantial volumes of water put a strain on water resources in arid areas by diverting supply away from agriculture, other industries and drinking water. After fracturing operations, flowback and produced waters flow back to the surface. Their water quality is highly variable and usually presents very high total dissolved solids concentrations (TDS), as well as oil and grease and scaling agents. As available water treatment technologies and especially desalination methods, are expensive and intensive, most of these waters are not returned to the watershed but disposed of in deep injection wells.

To minimize water consumption and to reduce wastewater management costs, water reuse practices constitute an attractive alternative. However, the performance of typical fracturing fluids is reduced when salts are present. Since progress is still

necessary to economically treat high TDS levels, salt-tolerant additives are being developed. Such additives will allow flowback water to be reused after it has been filtered and de-greased, without the need for desalination. This research provides a multifunctional assessment of three salt-tolerant friction reducers.

## **1.2 Scope**

Shell and the University of Texas at Austin have developed the Shell-UT Unconventional Research (SUTUR) program to study and optimize the exploration of unconventional oil and gas resources. Within this framework, this particular research is focused on enhancing flowback and produced water reuse in hydraulic fracturing, to significantly reduce water consumption and improve frac water management. One of the main challenges to reuse flowback waters is the incompatibility of typical fracturing fluids with salts. This research provides a multifaceted analysis of the efficiency of three additives in brines. Key properties of fracturing fluids are friction reduction efficiency, shale stabilization, and the ability to maintain fracture conductivity. Fracturing fluids should reduce friction losses to minimize injection costs. Additionally, clays are known to be particularly sensitive to water. Their degradation causes shale swelling and dispersion, which generates formation damage, and eventually productivity loss. Thus, fracturing fluids should enhance shale stability. Finally, high propped fractures permeability is essential to ensure significant gas production. Therefore, fracturing fluids need to be optimized to limit fluid sensitivity and proppant embedment. This paper builds on a project that tested the efficiency of three salt-tolerant friction reducers in several brines (Kuzmyak, 2014), and evaluate their shale stabilizing property and effects on the conductivity of propped fractures. Shale degradation was tested with hot rolling oven dispersion tests. Fracture conductivity was evaluated by measuring the change in

permeability of a propped fracture before and after fluid contact. Prior to these experiments, the viscosity and solubility properties of the test fluids were characterized and the mineralogy of the shale samples was determined. The results of this study provide a comparison of three salt-tolerant additives for use in flowback waters.

### **1.3 Approach**

Chapter 2 of this thesis contains background information on the hydraulic fracturing technology and on the flowback waters it produces. The topics developed in the literature review cover shale stabilization mechanisms and review fracture conductivity theory. It also describes some of the already known properties of the additives tested and focuses particularly on polyethylene oxide as it is not commonly used in the shale gas industry.

Chapter 3 reports the methods and materials used to conduct the hot rolling oven tests and fracture conductivity experiments.

Chapter 4 presents the results of the experiments and a discussion of the significance of these results for the usage of these additives as friction reducers as well as shale stabilizers.

Chapter 5 summarizes the results of this research and presents the implications of the work for the hydraulic fracturing industry. It also discusses the limitations and the possible future work.



## **Chapter 2: Literature review**

### **2.1 Hydraulic fracturing overview**

The use of hydraulic fracturing to produce natural gas involves several stages: exploration, drilling, fracturing, production, and well abandonment. During exploration, engineers design the fracturing and production stages based on the specific characteristics of the site, including geological, hydrological, and regulatory concerns. A hole is then drilled and several stages of casing and cement are installed to prevent any interaction between the formation and the wellbore. Once the casing is installed, explosives are used to perforate the casing, allowing access to the formation. Fracturing fluid is then injected down the wellbore and through the perforations, at a pressure sufficient to induce fractures in the formation, inducing horizontal fractures. Some of the injected fluid leaks into the formation; this is referred to as fluid loss. The pumping rate is maintained at a flow rate higher than the fluid loss rate to ensure that fractures propagate.

Most of the fracturing fluids used in North America are water-based fluids and include friction reducers and proppant; these are commonly referred to as slickwater fluids (Paktinat et al., 2011a). The other major types of fracturing fluids are oil-based, acid-based and foam-based fluids. Slickwater fluids are generally composed of a blend of additives beyond proppant and friction reducers, including viscosifiers, biocides, oxidative breakers, corrosive inhibitors, and clay stabilizers (Paktinat et al., 2011b). Water typically makes up 99.5% by volume of the fracturing fluid (Gregory et al., 2011).

Typically, friction reducers are high molecular weight polymers, which when placed in a turbulent flow regime, reduce the friction between the fracturing fluid and the walls of both the fracture and the wellbore piping. The power required for fluid injection

is therefore decreased by up to 75% (M. Blauch et al., 2009). After the injection of the fluid, granular agents called “proppant” are added to keep the fractures open. Once the desired fracture geometry is obtained, the proppant is pumped to ensure that the fractures remain open when the fluid pressure is released. Sand acts as a proppant by aggregating in natural fissures and maintaining the width of the fractures. In order to carry the proppant along the fracture and to minimize leak-off, the rheology of the fracturing fluid is enhanced by the addition of viscosifiers such as surfactants and polymers. At the end of the treatment, gel breakers break apart the viscosifying polymers. Biocides and anti-corrosive agents kill bacteria and reduce the tendency for corrosion, respectively. Finally, clay stabilizers are added to prevent clay swelling and degradation due to its sensibility to water (Paktinat et al., 2011b). When the hydraulic fracturing is completed, and the fluid has returned to the surface as flowback, the gas starts to travel up the well. Although the production lifetimes vary, it has been estimated that half of a well’s lifetime production is within its first five years (Clark et al., 2013). After the production decreases to the point that the well is no longer considered economically viable, the well is abandoned by plugging with cement.

## **2.2 Flowback water reuse**

### ***2.2.1 Quantity and quality***

According to Al-Muntasheri, fracturing operations require between 4 and 6 million gallons of water per well (Al-Muntasheri, 2014). Once the pressure is released, some water flows back to the surface. During the first two weeks (Haluszczak et al., 2013), this water is termed flowback water and mostly consists of the injection fluid: Silva and colleagues stated that, in the Marcellus Plays, this stage accounts for 15-25% of the total volume of water initially injected (Silva et al., 2012). However, flowback water

volumes are highly variable from play to play and can represent up to 40-50% of the initial water injected. The remaining water is referred to as produced water, and continues to flow to the surface once gas production has begun. The flow rates of flowback and produced waters are high during the first days; up to 70,000 gallons/day (gal/d) (Yoxtheimer, n.d.) and then diminish over time to 84-420 gal/d (Silva et al., 2012). In this thesis, flowback and produced water are not differentiated and will both be called flowback water.

Based on the water quality analysis of 56 flowback waters from the Marcellus Shale (M. E. Blauch et al., 2009; Haluszczak et al., 2013; Hayes, 2009), the concentrations of the prevalent ions, the total dissolved solids concentrations (TDS) and the pH were determined. Sodium and calcium are the most prevalent cations while anions are dominated by chloride (Hayes, 2009). As can be seen in Table 1, the data is quite varied, even within the Marcellus Shale play.

*Table 1 - pH, Cl<sup>-</sup>, Ca<sup>2+</sup>, Na<sup>+</sup> and TDS concentrations in 56 flowback waters collected from the Marcellus Shale*

<b>Concentration</b>	<b>Median</b>	<b>Average</b>	<b>Min</b>	<b>Max</b>
pH	6.4	6.5	5.1	7.8
Cl <sup>-</sup> (mg/L)	58,900	59,075	70,600	166,000
Ca <sup>2+</sup> (mg/L)	8,685	8,797	100	26,400
Na <sup>+</sup> (mg/L)	24,100	23,463	922	58,600
Total Dissolved Solids (mg/L)	106,608	104,447	3,010	298,000

In addition to TDS, oil and grease, scaling ions and naturally occurring radioactive materials (NORM) are usually detected as produced waters return to the surface; this can be seen in Table 2.

As can be seen in Figure 1, Table 3, and Figure 2, the composition of flowback waters depends on the time after the fracturing operations and on the formation characteristics. Thus, flowback waters sampled in the Marcellus Shale region show high levels of TDS - up to 180,000 mg/L - whereas typical TDS concentrations of flowback waters from the Eagle Ford play are only around 20,000 mg/L.

Table 2 – Marcellus shale flowback water quality in Pennsylvania (Barbot et al., 2013)

Constituent	Average concentration
Total dissolved solids (mg/L)	106,390
Total suspended solids (mg/L)	352
Oil and grease (mg/L)	74
COD (mg/L)	15,358
TOC (mg/L)	160
SO <sub>4</sub> <sup>2-</sup> (mg/L)	71
Br <sup>-</sup> (mg/L)	511
Mg <sup>2+</sup> (mg/L)	632
Ba <sup>2+</sup> (mg/L)	2,224
Sr <sup>+</sup> (mg/L)	1,695
Fe dissolved (mg/L)	40,8
Fe total (mg/L)	76
Alkalinity (mg/L as CaCO <sub>3</sub> )	165
Gross alpha (pCi/L)	1,509
Gross beta (pCi/L)	43,415
Ra <sup>226</sup> (pCi/L)	120
Ra <sup>228</sup> (pCi/L)	623
U <sup>235</sup> (pCi/L)	1
U <sup>238</sup> (pCi/L)	42



Table 3 - Typical produced water TDS levels in some US shale plays (From USGS, 2011)

Shale Play	Typical produced water TDS levels (mg/L)
Eagle Ford	20,000
Fayetteville	25,000
Barnett	60,000
Woodford	100,000
Haynesville-Bossier	120,000
Marcellus	180,000

In addition to spatial variations, flowback water composition also changes over the lifetime of the well. For example, Figure 2 shows the evolution of flowback waters volumes and TDS concentrations with time in a well in the Green County, PA (Marcellus Shale) (Hayes, 2009). Maximum TDS values observed in flowback waters are about 300,000 mg/L. This corresponds to the latest stages of flowback waters production, when the flow rate decreases down to 150 gal/d.

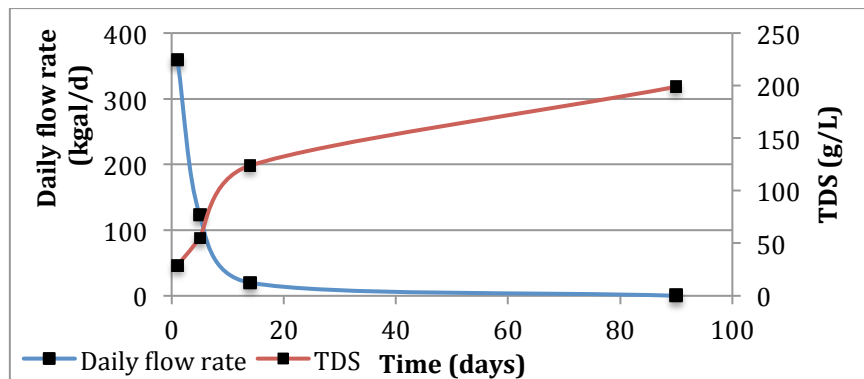


Figure 2 - Evolution of TDS levels and flow rate of flowback waters versus time for Green County, PA (Hayes, 2009)

### ***2.2.2 Flowback water reuse challenges***

In order to reuse flowback waters in hydraulic fracturing operations, contaminants of concern need to be treated. Particulates and suspended solids need to be removed to avoid the plugging of the equipment. High concentrations of scaling agents such as iron, magnesium, calcium, strontium, sulfates, silica and barium also affect equipment operation. Microbial growth needs to be controlled, and particularly, the sulfate reducing bacteria, which produce  $H_2S$  that causes pipeline corrosion. Finally, fluid stability is impacted by the presence of oil and grease, organics, TDS and chlorides. The performance of typical friction reducers is particularly dependent on TDS concentrations and divalent salts (Acharya et al., 2011). The most widely used friction reducers are high molecular weight ( $> 10^7$  g/mol) anionic polymers of acrylamide contained in an external oil emulsion (Paktinat et al., 2011c). When injected into the well, the emulsion inverts, allowing the polymer to go into solution and be an effective friction reducer. However, high salt concentrations often increase the inversion time to the extent that the polymer might not fully invert by the time it has reached the wellhead (Paktinat et al., 2011a). Thus, TDS concentration is probably the most problematic consideration when reusing flowback waters since the performance of the fracturing process is dramatically impaired by high salinity, thus potentially limiting reuse of flowback water. As described in Section 2.2.1, water quality of flowback waters varies considerably within a formation and over the lifetime of the well: This heterogeneity makes their reuse even more complex.



### ***2.2.3 Flowback water reuse technologies***

Currently, flowback waters are only reused when it is economically useful, taking the temporal evolution of flowback water flow rates and TDS concentrations into account. When the flow rate is low and the TDS concentration increases to a level where it is not cost-effective to treat, flowback waters are disposed of. Figure 2 illustrates this critical criterion that can be used to choose whether or not to treat and reuse. In this hydraulic fracturing well in Green County, PA, the period of reuse can be set at the first 15 days: After this, the daily flow rate drops below 20,000 gallons/day while the TDS concentration keeps increasing above 120,000 mg/L. This guideline shifts depending on the geologic formation.

When flowback waters are reused, their management is handled onsite. They are blended with fresh water, treated and then mixed with compatible additives. Available treatment processes include an oxidation/disinfection step to break oil emulsions and polymers, kill bacteria, and oxidize reduced compounds ( $\text{Fe}$ ,  $\text{Mn}$ ,  $\text{NH}_3$ ,  $\text{S}^{2-}$ ); a step to remove hydrocarbons using air flotation and granular activated carbon; and a chemical precipitation step to remove inorganic scaling agents. Additionally, membrane treatments and thermal evaporators are employed to remove TDS (Acharya et al., 2011; Gregory et al., 2011; Kimball, 2011; Silva et al., 2012; Xu, 2013). For TDS concentrations above 40,000 mg/L, evaporators using mechanical vapor recompression are the most common form of treatment (McLaughlin, 2013). Crystallizers, and thermal distillation are also recommended for these high concentrations (Bruff and Jikich, 2011; Kimball, 2011). However, these advanced processes are energy intensive, involve high capital costs, and generate a concentrated waste which needs to be disposed of.

To reduce the need to heavily treat flowback water, new friction reducers are being developed that are tolerant of high salt concentration, and include:

- Polyacrylamide-based oil emulsions which perform well for a specific salt composition. Examples include the Flojet DR 6000 and Flojet DR 9000 from SNF, Inc., effective in monovalent brines under 40,000 mg/L TDS and in complex brines above 50,000 mg/L, respectively (SNF, 2013),
- A liquid-polymer emulsion friction reducer (SCNFR), which uses nanoparticles and tolerates up to 12% by weight of NaCl in flowback waters (Blauch, 2010),
- FRPW, a water-based polyacrylamide friction reducer which showed promising results in produced waters of over 300,000 mg/L TDS (Zhou et al., 2014),
- A newly developed dispersion of polyacrylamide in concentrated brine called Dispersion Polymer Friction Reducer (DPFR) (Ferguson et al., 2013) which was shown to perform well at up to 110,000 mg/L TDS,
- Polyethylene oxides friction reducers (WSR series), which are developed by Dow Chemical; not currently used as friction reducers in hydraulic fracturing but consistently demonstrate performance in various brines, including in up to 20% (w/w) NaCl and 10% (w/w) CaCl<sub>2</sub> (Kuzmyak, 2014). Dow Wolf Cellulosics has recently released a technical note on the possible use of Polyslip OF-50 polymer in fracturing operations as a friction reducer.

### **2.3 Shale stability**

Major advancements in horizontal drilling and hydraulic fracturing has allowed gas production from low permeability shale reservoirs. However, some shales contain water-sensitive clays which can cause serious formation damage and productivity losses upon degradation when in contact with water.

#### ***2.3.1 Shale instability mechanisms***

Common borehole problems include hole closure, hole enlargement, collapse, fracturing, stuck pipe, and proppant embedment. Most of these problems are related to shale instability which is a major issue in the oil and gas industry (Eric van Oort et al., 1996). When a formation is drilled or fractured, engineered fluids fill the pore spaces created. The stress applied to the surrounding rocks is changed and creates an imbalance between the shale strength and applied stress. Additionally, the fluid interacts with the shale surface, increases pore pressure, and alters its strength.

Shale instability can be described as a two step process (Patel and Gomez, 2013; van Oort, 2003):

- The elevation of pore pressure: The fracturing fluid invades the pore space of the rocks. This changes the pore pressure and the mechanical stress on the formation. As the invading fluid interacts with the clay, it can cause swelling of the clay and this can cause mechanical instability.
- The hydraulic flow in the shale: The fluid enters the shale through fissures and fractures. The hydraulic pressure gradient might also cause the transport of the fluid through the pores, which in turn will soften the shale.

To prevent the shale from being damaged, van Oort proposed three solutions: ensure the proper mud weight, limit the fluid-shale invasion, and use a fluid that will react with the shale but enhance stability. First, the mud weight has to be determined so that it provides the proper mechanical stability. This support to the wellbore walls, which is a function of the mud density, is a requirement but is not always sufficient. The fluid-shale invasion must be minimized and delayed as well, usually by using viscous filtrates with low flow rates, which reduce shale permeability. Finally, since contact between the fluids and the shale is inevitable, it is advised to use fluids which will enhance shale stability when they react with the shale and the pore fluid. The difference between the invading fluid and the pore fluid compositions might create an osmotic flow out of the shale and thus reduce the water content of the shale. The reactions between the fluid and the shale include precipitation and cation exchange. Thus, the invading fluids can be designed to enhance cementation forces and reduce the swelling pressure. The object of interest is to minimize chemical alteration due to fluid-shale interactions and that result in swelling and dispersion (van Oort, 2003).

Swelling and dispersion are the two manifestations of shale instability due to chemical interaction. The adsorption of fluids and - particularly of water - causes the swelling of the softened shale resulting in heaving or sloughing. The other well-known problem consequent to the interaction of the shale and the fluid is the disintegration or dispersion of the shale. This may result in an accumulation of finely divided cuttings in the mud (O'Brien and Chenevert, 1973). Dispersion is often a consequence of swelling and of erosion of the shale. Both swelling and dispersion related problems add significant costs (10% of the well budget) to the drilling and fracturing operations (Khodja et al., 2010).

### ***2.3.2 Clay mineralogy and problems related to water interactions***

Shales are “sedimentary rocks that have been laid down over geologic time in marine basins” (O’Brien and Chenevert, 1973). When put in contact with slickwater fluids, shales become instable because of their clay-content. Clay minerals (e.g. montmorillonite, illite, chlorite) absorb water by two primary swelling mechanisms: crystalline swelling and osmotic swelling. In crystalline swelling, also called surface hydration, interlayer exchangeable cations of high hydration energy are considered. As the shales associate with water, they hydrate and a layer of water molecules is created in the clay interlayer. As the cations hydrate even more, a second molecular layer of water builds up (Wayllace, 2008). Norrish showed that up to four layers of water can be intercalated between clay mineral interlayers (Norrish, 1954). These short-range interactions result in an increased interlayer space between clay platelets (Figure 3).

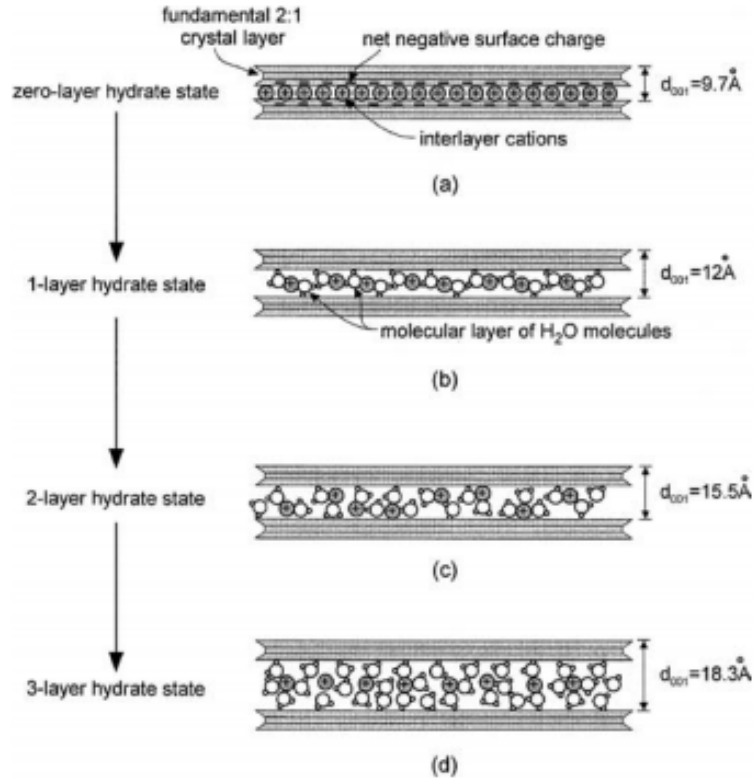


Figure 3 - Conceptual model of the sequential crystalline swelling process for smectite (Likos, 2004)

Although crystalline swelling is the most important physical swelling under downhole forces, osmotic swelling also impacts clay structure (Madsen and Müller-Vonmoos, 1989). Osmotic swelling is related to longer-range electrical double layer forces. An increase in the ionic concentration of an aqueous solution produces a decrease of the water activity  $a_w$ . As a result, the change in free energy from a state A with a given ionic concentration to a state B with a higher ionic concentration  $\Delta G_{A \rightarrow B} = RT \ln \frac{a_{w,B}}{a_{w,A}}$  is negative. This gives rise to a flow of water from the solution with the lowest ionic concentration A to the highest ionic concentration B. This phenomenon is commonly referred to as osmotic pressure. In clay interlayers system, cations are more concentrated at the surface of the clay than in the bulk solution since clay surfaces are negatively

charged. As a result, water moves from the bulk pore water to the interlayer because of a difference in ionic concentrations (Figure 4). This influx of water in the interlayer produces swelling. Additionally, when two negative potentials at the clay surface overlap, they create a repulsion which causes swelling (Madsen and Müller-Vonmoos, 1989).

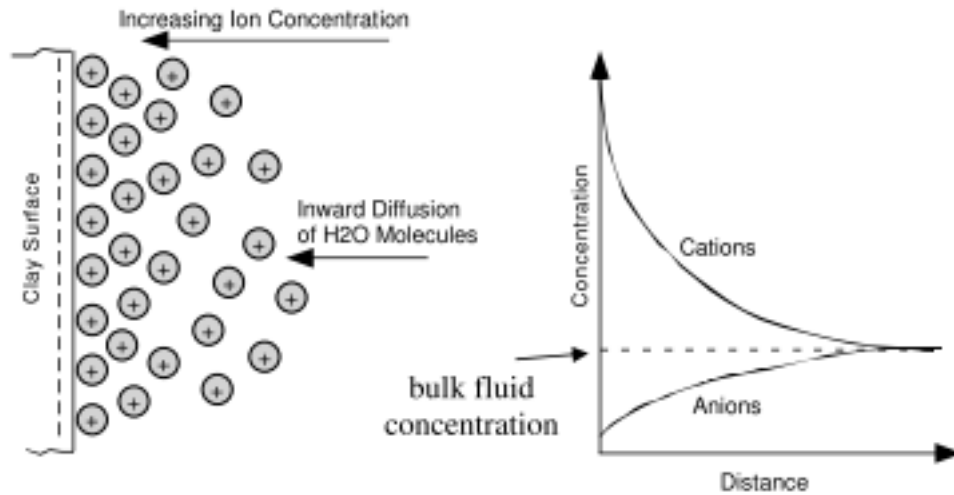


Figure 4 - Distribution of ions near a surface clay (Mitchell, 1993)

Dispersion is often a consequence of the swelling and of the erosion of the shale, and occurs when several interlayers of the clay hydrate at different degrees and thus weaken the overall structure of the shale. Additionally, Wingrave proposes that dispersion is enhanced in polar fluids such as water because water can “disturb the hydrogen-bonded silt contact points” by forming hydrogen bonds with the hydroxyl groups on the shale (Wingrave et al., 1987). Even if dispersion differs from swelling it is often included in shale swelling problems because the degree of dispersion usually represents the amount of swelling clay and because sloughing effects resulting from swelling are usually more important than dispersion effects (O’Brien and Chenevert, 1973).

The detailed interactions occurring between clays and water-based fluids depend on the clay mineralogy. O'Brien and Chenevert presented a classification of shales based on their clay content and the resulting problems, shown in Table 4. This table is not exhaustive but is a starting point to evaluate how reactive a shale is, based on its composition. The water-sensitive clays considered here are montmorillonite, illite, interlayered clays composed of both illite and montmorillonite, and chlorite.

*Table 4 - Classification of shales by clay content and related problems (adapted from O'Brien & Chenevert, 1973)*

Class	Characteristics	Clay Content
1	Soft, high dispersion	High in montmorillonite, some illite
2	Soft, fairly high dispersion	Fairly high in montmorillonite, high in illite
3	Medium-hard, moderate dispersion, sloughing tendencies	High in interlayered clays, high in illite, chlorite
4	Hard, little dispersion, sloughing tendencies	Moderate illite, moderate chlorite
5	Very hard, brittle, no significant dispersion, caving tendencies	High in illite, moderate chlorite

Shales with high montmorillonite content (25-40%) tend to swell and disperse considerably. If illite is also present, dispersion is expected to occur to a lesser extent. As illite and montmorillonite content decrease, the clay becomes harder and more brittle.

### **2.3.3 Solutions**

Shale inhibition has been extensively studied over the past 50 years, especially to stabilize shale during drilling processes. Highly concentrated salt solutions were first used as shale inhibitors (Patel and Stamatakis, 2007). They limit the water uptake by



shale by reducing the difference in ionic strength between the pore water and the drilling fluid and thus diminish or delay the osmotic transport of water. Moreover, the interaction of salts with shale involves cation exchange. The replacement of ions already present in the clay interlayers by ions which hydrate less than them, reduces the water inflow in the shale. KCl was found to be particularly effective at mitigating the impacts of water adsorption by shale (O'Brien and Chenevert, 1973). Montmorillonite, commonly found in swelling and dispersive shales, is a 2:1 clay mineral. While the average inside diameter of siloxane cavities of 2:1 clay minerals is 0.26nm, the ionic diameter of potassium ions is 0.266nm (Evangelou, 1998). Thus, when potassium ions enter the montmorillonite matrix and adsorb to the surface, very little space is left for hydration. Consequently, water uptake is decreased. Additionally, potassium has a low hydration energy, which enhances dehydration of the shale and compaction of the layers. For similar reasons, ammonium salts are good stabilizers (O'Brien and Chenevert, 1973).

Muds based on NaCl and starch (Patel and Stamatakis, 2007), silicate (Patel and Gomez, 2013), and lime (Hale and Mody, 1993) were also proposed as shale inhibitors. The impact of concentrated salt solutions on the environment and on the efficiency of the other components of the drilling fluid impelled researchers to develop less salt-dependent solutions.

In the 1960s, solutions of polymers and KCl began to be used as shale stabilizers and showed better efficiency than solutions of KCl alone (Patel and Stamatakis, 2007). As the polymer hydrates, its effective volume increases and forms a net near the shale which reduces the abrasion of the shale. Moreover, due to an increased viscosity of the solution, the transport of water through the pores into the shale matrix is delayed. Using

pressure transmission tests, it was observed that the pore pressure elevation was inversely proportional to the fluid viscosity (Bland et al., n.d.). This is in accordance with Darcy's law, which states that the rate of fluid invasion (and thus the elevation of pore pressure) is accelerated by a low viscosity solution. High molecular weight partially hydrolyzed polyacrylamides (PHPA) of  $6-8 \times 10^6$  g/mol were proven to be effective; in particular, 30% hydrolyzed polyacrylamides which consist of 30% of carboxylic groups and 70% of amide groups (Sheu and Perricone, 1988). In this case, Sheu and Perricone proposed that, once the polymer and the water enter the shale matrix, the carboxylic groups of the polymer chain adsorb on the positive charges of the clay surfaces and keep them together. This bridging might also occur via hydrogen bonds created between amid groups and clay sites. The addition of cations - especially  $K^+$  - to polyacrylamides improves the efficiency by limiting the water uptake via osmosis and hydration.

In the 1990s, glycol and polyglycol solutions raised interest among the drilling industry for their shale stabilization properties (Aston and Elliott, 1994; Bland, 1994; Bland et al., n.d.; Downs et al., 1993; van Oort and Bland, 1997). As can be seen in Figure 12, polyglycols are composed of repeating units of ethylene oxide and/or propylene oxide. Their unique property of inverse solubility raised interest: as the temperature increases, they lose their solubility and form an emulsion. The temperature of precipitation depends on the molecular weight of the polyglycol, on its concentration, and on the concentration of the other compounds in solution, particularly electrolytes (Bland, 1994). Downs, van Oort and Rothmann proposed the association of a conventional KCl-polymer stabilizing solution and of a relatively low molecular weight (500-1800 g/mol) polymeric surfactant composed of propylene and/or ethylene units, referred to as a "thermally active compound". It was observed that the addition of

propylene glycol and ethylene glycol reduced shale cuttings dispersion and water penetration, and that this improvement was a direct function of the concentration of the glycol additive (Downs et al., 1993). The temperature was monitored in these experiments but the relation between the phase separation at high temperature and the shale stabilization was not clearly determined. Bland states that the addition of polypropylene glycol (PPG) of molecular weight below 540 g/mol (i.e. PPG400) is beneficial to reduce shale swelling and the addition of higher molecular weight PPG serves more as a lubricant (Bland, 1992). In Aston's experiments, the cloud point property was not used and experiments were conducted below the precipitation temperature (Aston and Elliott, 1994). However, the addition of a glycol with ethylene oxide units and a molecular weight below 1000 g/mol to a KCl-PHPA solution greatly improved shale inhibition (dispersion and swelling) compared to solutions of KCl-PHPA and fresh water only.

Several explanations have been given for shale stabilization by glycols. Glycols could compete with water to form hydrogen bonds at the clay surface. Thus, they would replace the water around the shale and inside, leading to less hydration (Aston and Elliott, 1994). In the absence of hydroxyl groups, the methylene groups of polyglycols bond to the oxygen atoms of the shale via hydrogen bonding (Bradley, 1945). Through this mechanism, the polymers would form a barrier to the inflow of water. Another explanation involves the cloud point property. As the polymer clouds out of solution, it blocks the pore throats and prevents water inflow and pressure elevation within the pores. Since the shale stabilization effect has been observed below and above the cloud point temperature, the explanation is likely to be a combination of the proposed mechanisms. Given that the cloud point temperature of a concentrated polymer solution is lower than

of a less concentrated solution, not all the dissolved polymer precipitates at the same temperature. At a given temperature, only part of the polymer remaining in solution clouds out (Bland, 1994). When the fluid invades the shale matrix at a high temperature, part of the polymer is in solution, interacts with the clay via hydrogen bonding and stabilizes it, and part of the polymer clouds out and blocks the water inflow. Glycols act in synergy with salts and the inhibition effectiveness depends on the type of salts (Aston and Elliott, 1994).

Several authors note that the efficiency of shale stabilization by polyglycol will decrease with high molecular weight polyglycols (molecular weight > 100,000) because the large size of the polymer chains would prevent them from entering the shale (Aston and Elliott, 1994; Bland, 1994; Bland et al., n.d.; van Oort, 2003). However, no published experimental data was found to support this hypothesis and the only experiments reported involved polyglycols of molecular weight of 2000 g/mol or below.

In the mid 1990s, silicate/potassium additives were found to be effective stabilizers (Patel and Stamatakis, 2007; E van Oort et al., 1996) composed of silica ( $\text{SiO}_2$ ), Alkali ( $\text{Na}_2\text{O}$  or  $\text{K}_2\text{O}$ ) and water. Once at the pH of the formation, below 10.5, the silicates polymerize and form a gel. Additionally, the silicates precipitate when in contact with multivalent cations. Those two mechanisms block the entrance of water in the shale matrix (Patel and Gomez, 2013). While they have good inhibitive properties, silicates raise environmental concerns as they involve high pH fluids.

As mentioned earlier, ammonium and potassium are effective shale inhibitors. Using this idea of stabilization by cation exchange, nitrogen based clay stabilizers were developed. To compensate for the quick degradation of ammonium salts, their instability

above 150°F, and the odor resulting from dissociation into ammonia at high pH, higher molecular weight ammonium salts were developed (Patel and Stamatakis, 2007). These took the form of amine compounds: monomeric amines, oligomeric amines and polyamines (Figure 5). Monomeric amines have one nitrogen active site, oligomeric amines have two to four nitrogen active sites and polyamines can have over 100 nitrogen active sites. The more numerous the amine sites are, the more the polymer bridges with the clay, and prevents clay swelling by removing water molecules and reducing hydration. Moreover, higher molecular weight species provide more permanent stabilization. One disadvantage of polyamines is that their long chains prevent them from entering the clay matrix: they only adsorb to the clay surface. As a result, polyamines are generally less effective at reducing swelling of clays than oligomeric amines. Additionally, these cationic polymers may be incompatible with other additives such as anionic-based friction reducers, and are sometimes criticized for their toxicity (Patel and Gomez, 2013). Ammonium based clay stabilizers represent the most recent research development on clay stabilizers.

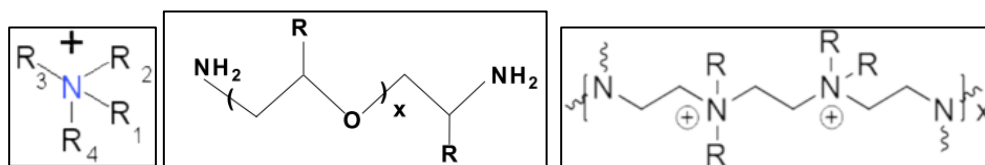


Figure 5 - Monomeric amine (left), oligomeric amine (middle), polyamine (right) structures – (Adapted from Patel & Gomez, 2013)

## 2.4 Fracture conductivity

### 2.4.1 Definition

During hydraulic-fracturing treatment, fractures are created to facilitate the production of gas from low permeability formations. While the pressure is released, it is essential to keep the fracture open. For this reason, most wells use granular agents called proppant to sustain fracture geometry. Fracture permeability ( $k_f$ ) describes the ability of the fracture to transmit a gas when it is packed with proppant.

To design hydraulic fracturing treatments, the dimensionless fracture conductivity parameter ( $F_{cd}$ ) is usually employed. Cinco-Ley and Samaniego defined this as the ratio of the permeability of the fracture ( $k_f$ ) times the fracture width ( $b_f$ ) to the permeability of the formation ( $k$ ) times the fracture half-length ( $x_f$ ):

$$F_{cd} = \frac{k_f * b_f}{k * x_f} \quad \text{Eq 1}$$

Figure 6 shows the schematic of a fracture and defines the parameters used in the fracture conductivity calculation.

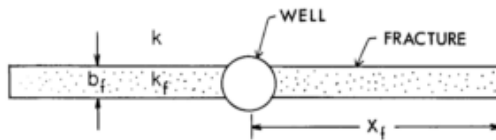


Figure 6 - Schematic of a fracture (*Adapted from Cinco-Ley & Samaniego-V., 1981*)

It represents the relative flow ability between the fracture and the formation (Cinco-Ley and Samaniego-V., 1981). It is generally accepted that an optimal  $F_{cd}$  ranges between 10 and 30 (Elbel and Britt, 2000). If a fracture half length is 100 feet (ft), a

fracture width is 0.002 ft and the reservoir permeability is 100 nanodarcy (nD), then the fracture permeability needs to be 50 millidarcy (mD) to obtain a  $F_{cd}$  of 10 (Pedlow, 2013).

#### ***2.4.2 Mechanisms for reduction of fracture conductivity***

The reduction of fracture permeability and thus the decrease in fracture conductivity indicates shale degradation, proppant pack degradation, or both.

When shale is degraded, it can soften and swell. Therefore, the proppant in contact with the shale might embed in the surface of the shale as the still relatively high pressure in the fracture pushes it towards the soft surface of the shale or as the shale swells around the proppant grains. As a consequence, the fracture tends to close up and the fracture conductivity decreases. Shales with high clay content and/or low Young's modulus, tend to soften more easily. Moreover, the higher the closure stress, the more the proppant embeds as can be seen in Figure 7. This means that, when the shale is degraded, and as the formation puts stresses on the fracture, the fracture conductivity lowers. Finally, shale stability depends on the fluid it is in contact with; this is explained in more detail in Sections 2.3.2 and 2.3.3. Therefore, fracture conductivity is better maintained when the fracturing fluid composition ensures shale stability.

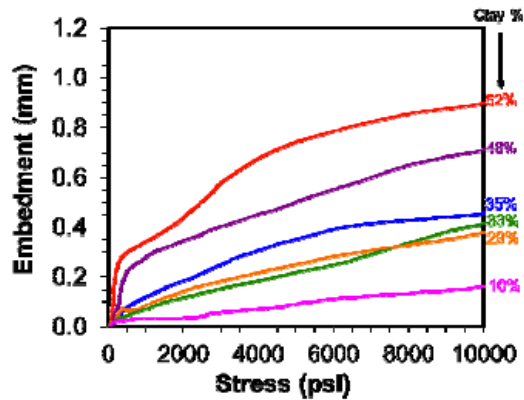


Figure 7 - Proppant embedment versus closure stress and dependence on clay content (Alramahi and Sundberg, 2012)

Proppant pack degradation includes proppant diagenesis and proppant flowback. Proppant diagenesis - also called proppant scaling - refers to the physical or chemical changes that the proppant undergoes when it is in contact with the fracturing fluid and the shale surface, at the temperature and pressure of the fracture. It can dissolve, precipitate, create mineral overgrowths at the surface of the granules or in between them, and be compacted. These geochemical interactions between the proppant, the shale, and the fluid result in a loss of proppant porosity and width which impact fracture conductivity. The longer the exposure time, the more severe the consequences are. Moreover, reaction rates increase at high temperature (LaFollette and Carman, 2010). Finally, it was observed that diagenesis increases when proppant sizes decrease (Figure 8) (Weaver et al., 2005).



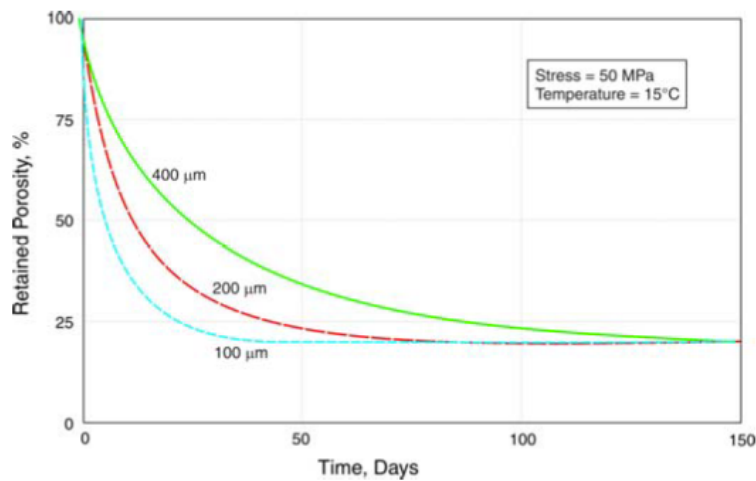


Figure 8 - Impact of proppant size and time on retained porosity (Weaver et al., 2005)

Weaver and colleagues showed that the coating of a polymer film can provide a protection against diagenesis effects on proppant grains (Weaver et al., 2005). It is less likely to undergo geochemical reactions and may be more resistant to impacts by forming grain-to-grain bonds.

Another problem that reduces fracture conductivity is proppant flowback and rearrangement, shown schematically in Figure 9. At high flow velocity, some proppant might flow out of the fracture and back into the wellbore. Not only might this allow the fracture to close, but it can cause costly damage to surface production equipment. The application of a resin coating onto the proppant grains to create a consolidated proppant pack is one of the solutions used to prevent proppant flowback and rearrangement (Terracina et al., 2010).

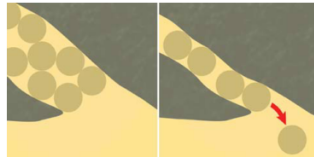


Figure 9 - Proppant pack rearrangement (Terracina et al., 2010)

Proppant and formation fines are the result of the deterioration of both materials. They are fines from formation spalling or crushed proppant particles released by mechanical forces resulting from high flow rates and high confining stresses. Proppant fines are generated when the fracturing fluid entrains these fines as it flows at non-Darcy conditions. When fines are mobilized, and transported, they might form pore restrictions and lead to permeability reduction. Gidley and colleagues showed that low density ceramic and coated sand are less susceptible to being crushed compared to uncoated sand and thus they better retain permeability (Gidley et al., 1995).

Formation fines are small particles already present in the formation, particles created during drilling, completing and high flow-rate fracturing operations, or particles created by the swelling and dispersion of the shale. Formation fines can also be generated by proppant embedment as can be seen in Figure 10. Muecke (1979) found that fines from sandstone formations are of various sizes (as small as 1  $\mu\text{m}$  and at larger than 37  $\mu\text{m}$  diameter) and compositions (mineral and non mineral). Like proppant fines, their transport into the fracture or the formation causes pores plugging and reduced permeability (Muecke, 1979). Palisch and colleagues state that the distribution of fines particles within the pore matrix depends on the proppant material and sizes as well as formation fines sizes (Palisch et al., 2007).

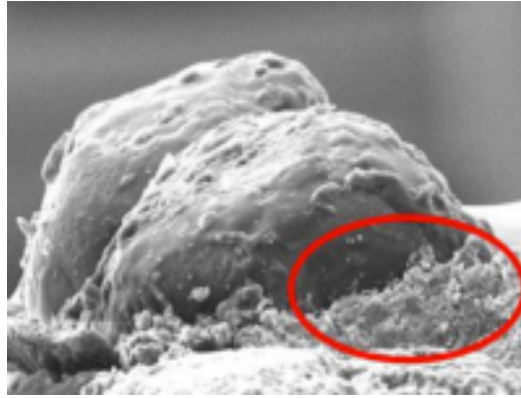


Figure 10 - SEM photo (514x) of formation fines spalling (circled) due to grain embedment (Terracina et al., 2010)

## 2.5 Polyacrylamide

Polyacrylamides (PAs) are high molecular weight water-soluble polymers that contain the repeating acrylamide unit  $C_3H_5NO$ . Partially Hydrolyzed Polyacrylamides (PHPAs) are copolymers of PA and polyacrylic acid. Their structure is shown on Figure 11. PAs are often manipulated to meet the requirements of the application; the hydrolysis and copolymerization are common operations (Leung et al., 1985). In this thesis, PAs and HPAMs will both be called PAs are PA-based polymers.

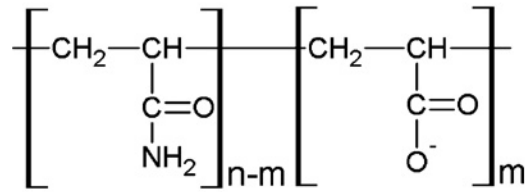


Figure 11 – HPAM chemical structure where  $m$  is the number of acrylic acid units and  $n-m$  is the number of acrylamide units (Adapted from Wever, Picchioni, & Broekhuis, 2011)

The degree of hydrolysis, the molecular weight of the PAs, the type of solvent, the temperature, and the pressure impact the properties of PA-based solutions (Wever et al., 2011). Only the degree of hydrolysis is discussed below because its effects were directly

observed in this research. Cationic, nonionic and anionic PAs are manufactured but cationic PAs are more rare.

### ***2.5.1 Degree of hydrolysis***

The degree of hydrolysis of PAs is the mole fraction of carboxylate groups (Taylor and Nasr-El-Din, 1994). It generally ranges between 2% and 40% (Green and Stott, 1999). It is an important determinant of PAs solution viscosity, and of their adsorption and flocculating abilities (Taylor and Nasr-El-Din, 1994). The carboxyl groups on the hydrolyzed polymer increase water solubility. When they dissociate, negative charges are left on the polymer backbone. Since charges of the same sign repulse each other, the chain stretches and the solution viscosity increases. Therefore, the higher the degree of hydrolysis is, the more viscous the solution will be. When the degree of hydrolysis is high, the viscosity of the solution is very sensitive to electrolytes: If cationic salts are added, they neutralize some of the negative charges. This results in the decrease of the hydrodynamic volume of the polymer, in the reduction of the solution viscosity, and may even cause the polymer precipitation (Choi, 2008; Taylor and Nasr-El-Din, 1994; Wever et al., 2011).

The degree of hydrolysis of PAs also controls their effectiveness to adsorb and flocculate. Cationic PAs mostly react with negatively charged suspensions. Anionic PAs bind to positively charged suspensions but also to negatively charged particles via intermediate cations, or to some neutral particles through hydrogen bonds (Green and Stott, 1999; Zeynali and Rabbii, 2002). Therefore, the interactions of the polymer with other particles depend on its degree of hydrolysis. A small degree of hydrolysis causes the polymer chain to shrink on itself and reduces its contact surface. Once the PA adsorb to a particle, it can act as a stabilizer or as a flocculating agent.

### **2.5.2      *Applications***

PAs are nontoxic additives used in various industries. Unlike its monomer acrylamide, which is a neurotoxic, a number of studies concluded that PA is not toxic (Caulfield et al., 2002). As an example, a cutaneous study and oral toxicity tests on rats and dogs showed that PA is safe to be in food, drugs and cosmetics when with less than 0.01% acrylamide monomer content. Since the average concentrations reported in cosmetics are less than 0.01%, PA is considered safe to use (Liebert, 1991).

The uses of PAs in biomedical research include tissue implant materials, gels for cell culture substrates, and carriers of drugs in animal studies (Gautreau et al., 2006; Liebert, 1991). In cosmetics, PA is used as a foam builder and shampoo stabilizer.

The main applications of PAs are related to its flocculating and thickening abilities. In water treatment processes, PAs are used as coagulants to remove pollutants. They enhance flocculation and destabilization of the aggregates (Rabiee et al., 2005). The applications of PAs as flocculants also include paper manufacturing, and mineral processing (SNF, n.d.). PA is also efficient in soil conditioners and is used in agriculture, in irrigation as well as in the Oil & Gas industry. Its viscosity and specific charges make it able to adsorb to the soil and maintain its integrity (Clark and Scheuerman, 1976; Green and Stott, 1999). In Enhanced Oil Recovery, PAs increase the viscosity of water. The “heavy” water pushes the oil in the reservoir towards the pump and this improves the productivity of the water-flooding process (Choi, 2008; Wever et al., 2011). PAs are also used in the hydraulic fracturing as friction reducers. Because of their high molecular weight, long-chain and high water solubility, PAs are efficient at reducing friction losses (Paktinat et al., 2011d).

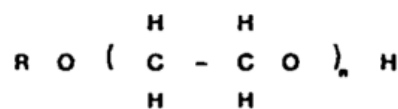
### **2.5.3      *Degradation***

The degradation of PAs is of concern because of the possibility of acrylamide release. Numerous studies investigated this subject. It was shown that under sunlight or UV irradiation, the residual monomer may be released but that the concentrations observed remain small and below the EPA standards (Caulfield et al., 2003; Smith et al., 1996; Woodrow et al., 2008).

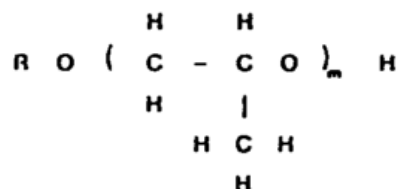
PA degradation processes include photo-degradation, biological processes, shear degradation, and chemical degradation (Caulfield et al., 2002). They cause changes of the physical and chemical properties of PAs such as the decrease of the molecular weight, a change in the degree of hydrolysis, and viscosity reduction. The absorption of light was found to generate free radicals. Microbial degradation produces  $\text{NH}_3$  and acrylic acid residues. Shear and elongational flows are responsible for bond scissions and creation of free radicals as well. Chemical degradation pathways include the action of free radicals and peroxides and the hydrolysis of the amide groups.

### **2.6 Polyethylene oxide**

Polyethylene oxide (PEO), also known as polyethylene glycol (PEG) is a linear and relatively non-polar polymer characterized by a repeating structure of ethylene oxide:  $\text{CH}_2\text{CH}_2\text{O}$ , as it is shown in Figure 12. The distinction between PEG and PEO depends on the molecular weight. PEG usually refers to polymers with a molecular weight below  $1 \times 10^5$  g/mol whereas PEO resins exist in a wide range of molecular weights, from  $1 \times 10^5$  to  $7 \times 10^6$  g/mol.



**Polyethylene Glycol**



**Polypropylene Glycol**

Figure 12 - Chemical structure of polyethylene glycols and polypropylene glycols (Bland, 1994). R is a hydrogen or an alkyl group. Generally,  $n+m \geq 4$  and represents the degree of polymerization.

While the PEO monomer ( $\text{CH}_2\text{CH}_2\text{O}$ ) is very close to methylene oxide ( $\text{CH}_2\text{O}$ ) or propylene oxide ( $\text{C}_3\text{H}_6\text{O}$ ), PEO is soluble in water at room temperature but polymethylene oxide (PMO) and polypropylene oxide (PPO) are not (Bailey and Callard, 1959). This is explained by the distances between oxygen atoms in the polymer chain. Unlike, in PMO and PPO, the inter-atomic (oxygen-oxygen) in the PEO backbone matches the oxygen-oxygen distance between an oxygen in the water structure and its nearest neighbor. For this reason, water molecules form a hydration shell around the polymer and enable its dissolution (Hammouda, 2006).

### **2.6.1 Cloud point effect observation and explanation**

PEO resins display an interesting property of inverse solubility in water. While it is soluble at room temperature, it precipitates when the temperature of the aqueous solution is increased. This temperature is called the cloud point temperature (CPT), since the solution takes on a cloudy appearance.

Several investigations were carried out to explain this phenomenon (Ataman, 1987; Bailey and Callard, 1959; Kjellander and Florin, 1981). It was suggested that a change in the entropy of dilution while the temperature increases is responsible for a change in the polymer-solvent interactions which causes the precipitation of the polymer in water (Bailey and Callard, 1959) . Kjellander showed that there is an enhanced structure of water near the polymer as compared with the bulk water. This increased structuring in the water is referred to as the hydration shell. Even though it is characterized by a negative change in entropy, the change in the enthalpy of dilution is negative enough at ambient temperature so that, the change in the free energy of dilution remains negative. This is shown in the Gibbs Free Energy Equation as follows:

$$\Delta G = \Delta H - T\Delta S \quad \text{Eq 2}$$

where  $\Delta G$  is the change in free energy of dilution,  $\Delta H$  is the change in the enthalpy of dilution,  $\Delta S$  is the change in the entropy of dilution, and  $T$  is the temperature.

As a consequence, water and PEO are miscible at ambient temperature, but, at higher temperature, the entropy decreases considerably. The more negative  $\Delta S$  and the higher  $T$  make the term  $-T\Delta S$  even greater, making the overall change in free energy  $\Delta G$  positive. The dilution is not spontaneous at this point so the hydration shells break down, hydrophobic units of polymer are exposed to the solution and the PEO precipitates (Ataman, 1987).

This temperature depends on the concentration and the molecular weight of the polymer; the more concentrated the solution is and the longer the polymer chains, the lower the CPT will be. Bailey showed that when the molecular weight of the polymer is above 50,000 g/mol and the concentration is above 0.3% by weight the precipitation temperature doesn't vary as much (Bailey and Callard, 1959).



The addition of salts has a strong effect on lowering the cloud point temperature. This is called the “salting out effect”. Bailey suggests that the addition of salts increases the activity of the neutral molecules of polymer, following the Debye-McAulay equation (Bailey and Callard, 1959):

$$\ln (f_n) = \frac{\beta}{2kTD_0} \sum_i \frac{n_i e_i}{r_i} \quad \text{Eq 3}$$

where  $f_n$  is the activity of the polymer molecule,  $\beta$  is a constant, characteristic of the nonelectrolyte, defined by the relation  $D = D_0 - \beta n$ ,  $D_0$  is the dielectric constant of the water,  $n$  is the number of molecules of polymer, and  $D$  is the dielectric constant of a solution of the polymer in water;  $n_i$ ,  $e_i$  and  $r_i$  are the number, charge, and ionic radii of the ions present, respectively.

An increased polymer activity would increase its effective concentration and thus favor polymer-polymer interactions versus polymer-solvent interactions. According to this theory, the lowering of the cloud point temperature would be proportional to the concentration of salts, and the valence of the ions, and inversely proportional to their size. However, as can be seen in Figure 13 (Ataman, 1987), while the size and the concentrations effects were clearly observed, the ionic strength principle was not followed. The effectiveness of an ion in lowering the cloud point temperature depends on the species.



Anions	Cations
$F^-$	
$PO_4^{3-}, CO_3^{2-}, SO_4^{2-}$	$Rb^+, K^+, Na^+, Cs^+$
$S_2O_3^{2-}$	$Ca^{2+}, Ba^{2+}$
$HCOO^-$	$NH_4^+$
$CH_3COO^-$	$Li^+$
$Cl^-$	
$NO_3^-$	
$Br^-$	
$I^-$	

Figure 13 - Order of effectiveness of ions in lowering the cloud point temperature (Adapted from Ataman, 1987)

As can be seen in Figure 14, the cloud point temperatures for potassium sulfate and magnesium sulfate solutions are very similar whereas potassium halides precipitate at much higher temperatures. Thus, the precipitation temperature depends more on the anion than on the cation of the salt.

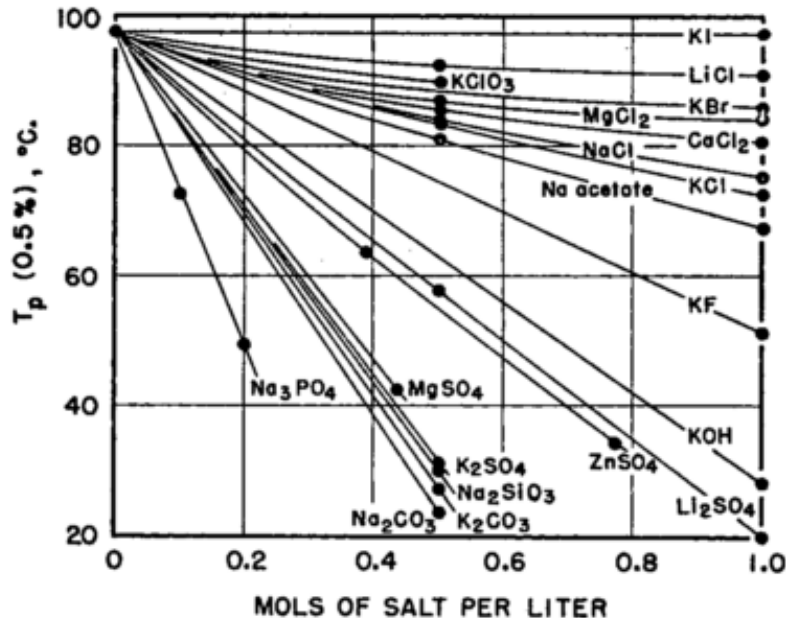


Figure 14 - Cloud point temperature versus salt concentration for a 0.5% w/w PEO with a molecular weight of  $4 \times 10^6$  g/mol (Bailey and Callard, 1959)

Other theories have been developed to describe the salting out effect. The addition of salt to water changes the water structure and particularly the normal hydrogen bonded structure of water. It is observed that the effectiveness of cations and of monovalent anions in lowering the CPT follows the same order as their ability to break water structure (Ataman, 1987). As the bulk water is affected by the addition of salts, the water-polymer interactions and the polymer-polymer interactions change and may be responsible for the precipitation.

Another explanation builds on Kjellander's model using the enhanced structure of water near the polymer. In an aqueous salt solution, it is shown that the PEO chains are surrounded by water containing a decreased salt concentration and that this is possibly caused by the high degree of structuring of the water in the vicinity of the PEO. This means that the water molecules will tend to transfer from the surroundings of the PEO to

the bulk solution (Florin et al., 1984). This disruption causes an increase in the hydrophobic characteristics of PEO and lowering of the precipitation temperature.

The salting out effect is likely to be the result of a combination of the mechanisms described above which involve ion-water, polymer-water and polymer-polymer interactions rather than direct ion-PEO interactions. It is noted that the effectiveness of salts in lowering the cloud point temperature follows the same order as the effectiveness of salts in lowering the intrinsic viscosity. This reflects the reduction of the polymer coil dimensions in solutions when salts are added (Bailey and Callard, 1959).

### **2.6.2      *Applications***

Polyethylene oxide resins are used in a wide range of applications from pharmaceutical and biomedical products to industrial processes. Their main properties include low toxicity, high solubility in water, thermoplasticity, complexation with organic acids, and viscoelasticity.

Polyethylene oxide has a low toxicity and thus is used in food, drugs and cosmetic products. A study on rats showed that the ingestion of polyethylene oxide of molecular weight of  $1 \times 10^5$  at concentrations of 3% and 2% does not produce sub-chronic nor chronic toxicity respectively (Leung et al., 2000). The U.S. Food and Drug Administration (FDA) has approved and recognized the use of PEOs for specific food packaging uses and as beer additives (FDA, 2013a, 2013b, 2013c, 2013d). Polyethylene oxide resins labeled as Polyox and of USP/NF grades which are produced by The Dow Chemical Co. meet the requirements of the United States Pharmacopeia/National Formulary (USP/NF) (Dow company, 2002a). Pharmaceutical and biomedical applications include denture adhesives, mucoadhesives, ophthalmic solutions, wound

dressings, oral drug release, biomaterials with low thrombogenicity, and lubricious coatings for biomaterials (Back and Schmitt, 2000).

PEOs are used in a wide range of industrial applications including in seed coatings for agriculture, in concrete mixtures for construction, as binders in ceramics, as thickeners in cleaners, as binders in batteries, as flocculants in the mining, paper and waste treatment industries. High molecular weight PEOs are used as drag reducers in fire hoses, in storm sewers (Back and Schmitt, 2000) and in well-fracturing fluids (Dow company, 2002). Uses of PEOs as friction reducers are described in Section 2.2.3.

### **2.6.3      *Degradation***

PEOs are subject to shear degradation and to oxidative degradation. PEO degradation is characterized by a decrease in friction reduction efficiency, a decrease in viscosity or a change in the molecular weight distribution. All three are related but can be measured independently. The breaking of molecular chains reduces molecular weight and therefore the viscosity of a polymer solution. Both the viscosity and the molecular weight are significant determinants of friction reduction efficiency.

In aqueous solutions subject to high shear, PEO chains can be broken. D'Almeida and Dias showed that shearing degrades high molecular weight fractions of PEO. Figure 15 represents the change in the molecular weight distribution before and after shearing was applied. After shearing, the distribution moves towards lower molecular weights. The distribution is shifted even more when the shear stress is increased. Thus, the degradation of high molecular weight chains produces chains of lower dimensions which are less likely to be impacted by the shear. With higher shear stress, more chains are likely to be degraded as the shear will also break chains of lower molecular weight.

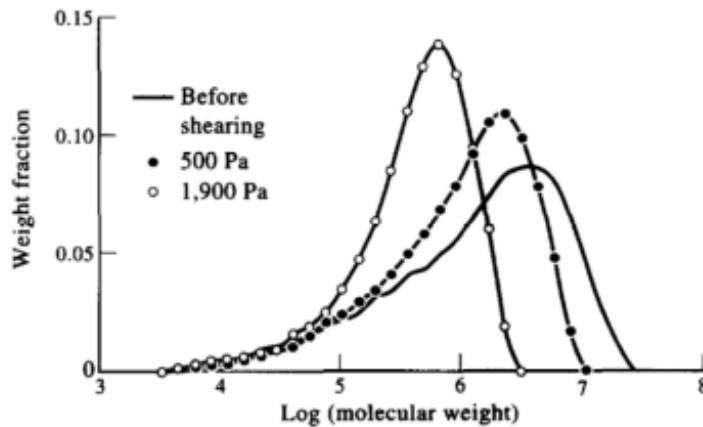


Figure 15 - Molecular weight distribution curves of PEO ( $M_w = 3.71 \times 10^6$ ) before and after application of 500 Pa and 1900 Pa shear stresses to 1 g/L aqueous solution at 30°C (D'Almeida and Dias, 1997)

D'Almeida and Dias also observed that the reduction of molecular weight of dissolved PEOs generates a reduction of viscosity and that decreasing the PEO concentration increases the degradation. Longer shear times increase the degradation up to a point where the molecular weight and the viscosity of the solution are constant. To explain these results, the authors note that energy is the product of shear stress and volume. They suggest that, for the same shear stress applied, higher molecular weight chains will absorb more energy than lower molecular weight molecules because they have a higher hydrodynamic volume. Thus, higher molecular weight molecules are more likely to degrade. After a certain time of shear, all the molecules have a molecular weight lower than the lowest molecular weight susceptible to degrade at a given shear stress so the molecular weight distribution doesn't change anymore (D'Almeida and Dias, 1997). Sung and coworkers looked at mechanical effects on drag reduction efficiency (DR%) in a turbulent flow for two high molecular weight PEOs ( $M_w = 5 \times 10^6$  and  $M_w = 4 \times 10^6$ ). They showed that the DR% of higher molecular weight decreases more rapidly at first,

but that the lower molecular weight and the lower concentrations produce a lower decrease in DR% over the entire shearing time (Sung et al., 2004). These findings confirm the results of D'Almeida and Dias as well as the conclusion that friction reduction efficiency is closely related to the highest molecular weight chains of PEO.

The American Society of Testing Materials (ASTM) defines a plastic as being oxidatively degradable when its degradation results from an oxidation in a natural environment. According to this definition, PEOs are oxidatively degradable. Experiments conducted by Dow showed that the viscosity of a solution of high molecular weight PEO is dependent on the exposure to the atmosphere, to UV light, to temperature and humidity (Dow company, 2002b; L'Hôte-gaston et al., n.d.). A 1% solution of POLYOX WSR-303 (molecular weight of  $7 \times 10^6$ ) had an initial viscosity of 8700 centipoise (cP). After UV exposure for 500 and 1000 hours, the solution viscosity dropped to 1300 cP and 20 cP respectively. After atmospheric exposure for 20 weeks, the viscosity was less than 15 cP. It was also shown via Gel Permeation Chromatography that the molecular weight of the polymer after 1000 hours of UV exposure or after 12 months of atmospheric exposure was below 21,000 g/mol. Moreover, when the solution was deoxygenated via nitrogen bubbling, the solution viscosity after 8 weeks was 6000 cP whereas it was 60 cP when simply exposed to the atmosphere. These experiments suggest that PEOs are subject to degradation via oxidation mechanisms in the presence of oxygen (Dow company, 2002b).

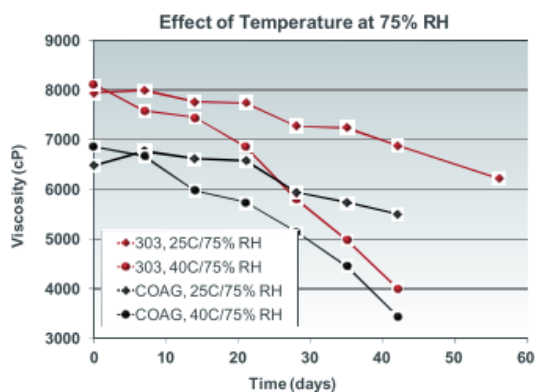


Figure 16 – Effect of temperature on 1% PEO solution viscosity degradation (L'Hote-gaston et al., n.d.)

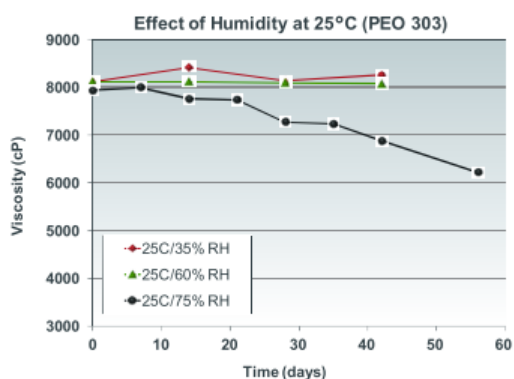


Figure 17 - Effect of humidity on 1% PEO solution viscosity degradation (L'Hote-gaston et al., n.d.)

Also, as can be seen in Figure 16 and Figure 17, 1% aqueous solutions of the POLYOX resins WSR303 and COAG with molecular weights of respectively  $7 \times 10^6$  and  $5 \times 10^6$  start degrading after 10 days as their viscosity decreases. Their viscosities decrease more at 40°C than at 25°C and at 75% relative humidity than at 35% relative humidity.

Finally, degradation is enhanced in the presence of certain metal ions such as  $\text{Cu}^+$ ,  $\text{Cu}^{2+}$ ,  $\text{Cu}^{3+}$ ,  $\text{Fe}^{3+}$ ,  $\text{Ni}^{2+}$  and by traces of chlorides, peroxides, permanganate or persulfate



(Back and Schmitt, 2000). In oxidative degradation processes, organic peroxides, carboxylic acids and ketones may form (Kutz, 2005).

The addition of antioxidants, storage under cool and low humidity conditions, and bubbling nitrogen through the solution stabilize PEOs and delays degradation, but PEOs will eventually degrade if left in the natural environment.

Given the large amounts of water consumed in the hydraulic fracturing industry and the costs related to the treatment of high TDS levels in flowback water, the development of salt-tolerant additives for flowback water reuse appears attractive. PAs have been used as friction reducers and to help stabilize shale for many years. Recently, salt-tolerant PA-based emulsions have been developed. High molecular weight PEOs are efficient friction reducers in all salt-concentrations but are not commonly used in the hydraulic fracturing industry. As the CPT property of low molecular weight PEOs has been shown to play a role in the enhancement of shale stabilization, it may as well help prevent shale degradation with high molecular weight PEOs. Therefore, both the newly developed PA emulsion and PEO solutions might provide friction reduction and shale stabilization. Moreover, salts are known to stabilize clay. The reuse of salty flowback waters is therefore expected to help shale stabilization even more. Finally, fracture conductivity is highly dependent on shale stability. If PEO and PA indeed efficiently stabilize shale, then they are likely to maintain fracture conductivity and thus be considered as multifunctional additives for flowback water reuse.

## Chapter 3: Experimental methods

The performance of PA and PEO based friction reducers as shale stabilizers and their ability to maintain fracture conductivity were evaluated. The physical state of the prepared fluids was first studied, and the mineralogy of the shale was determined. Then, preliminary experiments provided qualitative results about shale stabilization generated by salts and PEOs. Hot rolling oven tests showed the effects of PAs and PEOs on shale cuttings dispersion and thus on shale stability. Finally, the impacts of fluid-shale contact on fracture conductivity were assessed via permeability measurements.

### 3.1 Materials

#### 3.1.1 *Fluids*

PA friction reducers, PEO friction reducers, and polypropylene glycol (PPG) were tested in these experiments. They were diluted in the following brines: 5%, 10%, 15%, 20% and 25% by weight (w/w) of NaCl; 5%, 10%, 15%, and 20% w/w CaCl<sub>2</sub>; a multi-solute brine of both salts of 7.4%w/w NaCl and 1.8% w/w CaCl<sub>2</sub>.

PAs are described in Section 2.5. One of the PA friction reducers tested was the Flojet DR3046 provided by SNF (Riceboro, GA). It consists of an anionic 'high' molecular weight polymer of acrylamides contained in an external oil emulsion. Under high shear, the emulsion inverts, which allows the polymer to dissolve into solution. The concentration tested was 0.1% by volume (v/v), the optimal concentration for friction reduction (Kuzmyak, 2014). The DR3046 solutions were prepared by placing the 0.1 solution in a blender (OFITE, Houston, TX) for 3 minutes at 8000 rpm to pre-shear and invert the emulsion in the base fluid brine. The other polyacrylamide-based product was a dispersion of polyacrylamide stored in a concentrated brine. This novel friction reducer,

called Dispersion Polymer Friction Reducer (DPFR) and supplied by Nalco, was tested at the concentrations of 0.1% v/v and 0.01% v/v. The DPFR was dissolved in the brine using a stir plate at about 200 rpm and for 30 to 60 minutes.

The PEO solutions were prepared using Polyox powders supplied by The Dow Chemical Company (Midland, MI) Section 2.6 provides details about PEOs chemical structure and properties. The molecular weight of each product tested is listed in Table 5. WSR-301 has been used in the fracture conductivity tests, and in the hot rolling oven experiments. The effects of WSR-N10 on shale stability have been tested in hot rolling oven experiments to show the impacts of lower molecular weight PEOs on shale dispersion. The CPTs of all the PEOs listed in Table 5 have been evaluated. The PEO concentrations were 0.1% w/w and 0.01% w/w. To prepare the solutions, the PEO powder was gently poured in the base fluid brine while it was vigorously mixed on a stir plate. Once all the powder was dispersed in the solution, the stir rate was gradually reduced. Mixing continued until complete dissolution was visually apparent, between 3 and 12 hours depending on how well the PEO powder had initially been dispersed in the base fluid and on the molecular weight of the PEO. Since PEOs are subject to oxidative and shear degradations, they were continuously mixed until testing and used within three days of preparation.



PEO and 0.5% w/w PPG in the final solutions. Like PEO solutions, PEO-PPG solutions were continuously mixed until testing and used within three days of preparation.

The names of the chemicals the most tested in this research are listed in Table 6, along with their respective label used in this paper.

*Table 6 – Label scheme*

Brand Name	Label
Flojet DR3046	Conventional PA
DPFR	Novel PA
Polyox WSR-N10	WSR-N10
Polyox WSR-301	WSR-301
Polyox WSR-301 and PPG-400	PEO-PPG Dispersion

### **3.1.2      *Shale samples***

The beaker tests, the swelling tests, the hot rolling oven tests, and the fracture conductivity tests were run on different shales. The beaker tests and the swelling tests gave preliminary and qualitative results on the instability of shale due to fluid-shale contact, also called the shale fluid sensitivity. The hot rolling oven experiments generated quantitative results on shale dispersion. The changes in proppant pack permeability were measured in fracture conductivity tests. The preliminary tests, conducted in order to observe shale instability due to fluid sensitivity, were done on preserved shale samples from the Gulf of Mexico (GOM-12). Due to proprietary information, the particular formation they originate from cannot be disclosed. The dispersion and fracture

conductivity tests were run on outcrop shale samples: Pierre shale type I. These samples were maintained in a vacuum sealed desiccator to prevent any transfer of water in or out of the shale (see discussion on shale storage in Section 3.2.2 below). The mineralogy of the shales was determined using X-ray diffraction (Jung et al., 2013; O'Brien and Chenevert, 1973; Pedlow and Sharma, 2014).

## **3.2     Material characterization**

### **3.2.1     *Fluids characterization***

Cloud point and viscosity measurements were performed to evaluate the effects of temperature on the physical state of these fluids. The precipitation of a polymer with increased temperature - the cloud point effect – is a specific property of PEO and PEO-PPG solutions. Therefore, the cloud point temperature (CPT) of these solutions was determined, for various salt concentrations, polymer concentrations, and polymer molecular weights. The solutions were stirred and heated simultaneously. The CPT was measured with a thermometer at the temperature at which the solution became visually cloudy. Figure 19 shows an example of a CPT measurement, in which the solution appears clear below the CPT and cloudy above the CPT. Measurements of cloud point are critical to interpreting results of other tests such as the hot rolling oven tests and the fracture conductivity tests that were conducted at varied temperatures.

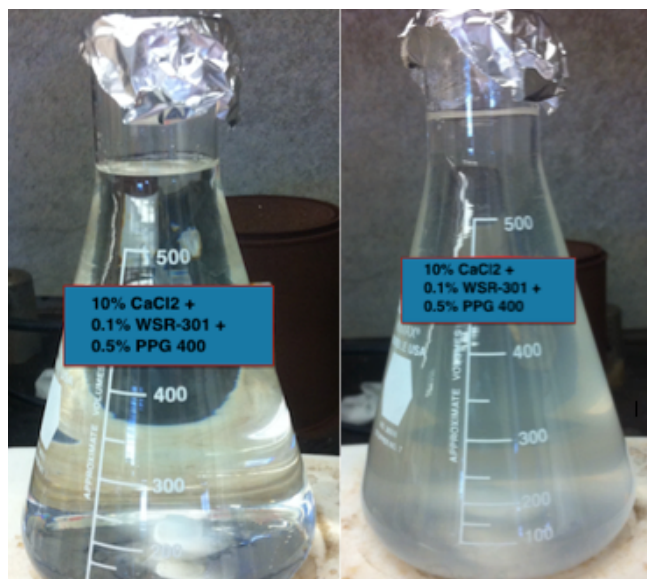


Figure 19 - A solution of 10 %CaCl<sub>2</sub> + 0.1% WSR-301 + 0.5% PPG 400 before the CPT (left) and at the CPT (right)

The PA and PEO fluids were further characterized using an AR-G2 magnetic bearing rheometer (TA Instruments) with the conical concentric cylinder model for the bob and the cup. The viscosities were measured at 25°C and at 70°C. High viscosity fluids are known to have a protective effect on shales by delaying the penetration time (See Section 2.3.1 and van Oort (2003)). Therefore, it was interesting to measure this parameter in order to better explain the results obtained with the hot rolling oven tests on shale stability.

### 3.2.2 *Shale storage*

In order to prevent any alteration to the shale's properties due to water uptake or loss, the shale samples were stored in desiccators at their native water activity (Chenevert, 1970a). Under laboratory conditions, the water activity is defined as the ratio of the vapor pressure of the water in contact with the shale and of the vapor pressure of pure water at the same temperature. It represents the adsorptive potential of a shale at a determined

water content (Osisanya, 1991). Therefore, to prevent any transfer of water in or out of the shale, it is essential to maintain it at its native water activity. Moreover, saturated salt solutions placed in desiccators are found to keep water activity levels constant (Winston and Bates, 1960) and can be used to determine the native water activities of the shales (Chenevert, 1970b; Jung et al., 2013; Osisanya, 1991; Zhou et al., 2013). This latter method, called the adsorption isotherm method, was used to evaluate the native water activity of GOM-12 shale and Pierre Shale I. Shale samples were weighed and stored in desiccators of various water activities ranging from 0.1 to 0.96. The mass of each sample increased or decreased upon adsorption or desorption of water respectively. Each sample was weighed every week until there was no apparent change in mass from the previous week. This condition was defined as equilibrium. The desiccator with a water activity in which the mass of shale varied the least was defined as the native water activity of the shale. This desiccator was chosen for storage of all of the samples.

### **3.3 Shale instability visualization**

Beaker tests and swelling tests were the preliminary tests that showed shale instability due to fluid sensitivity i.e. shale degradation because of fluid-shale contact. In a beaker test, a piece of GOM-12 shale was immersed in the test solution at ambient temperature. Pictures were taken at regular times to compare the evolution of the degradation. The beaker test method is a visual qualitative approach to assess shale stability. In addition, swelling tests were conducted to quantitatively evaluate shale swelling (Chenevert, 1970b; Zhou et al., 2013). For 24 hours, a piece of GOM-12 shale was immersed in a test solution and a sensor recorded the swelling of the shale at ambient temperature: As can be seen in Figure 20, a resistance probe measured the change in



shape of two C-clamps in the direction perpendicular to the bedding and in the direction parallel to the bedding.

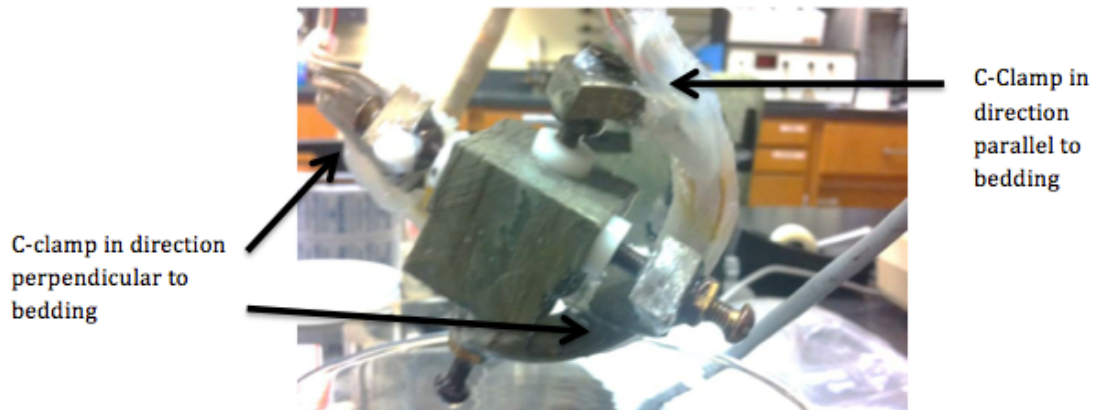


Figure 20 - Swelling test apparatus

### **3.4 Hot rolling oven dispersion tests**

The hot rolling oven dispersion (HRO) tests screened the effectiveness of additives to maintain the integrity of shale cuttings (Beihoffer et al., 1988; Hale, 1991). As shale dispersion is one of the consequences of water uptake, HRO tests provided an evaluation of shale cuttings stability. Forty-eight hours prior to testing, Pierre shale cuttings were ground, sieved and stored in the desiccator corresponding to their native water activity. The cutting sizes ranged between 0.5 mm to 2 mm (mesh 35 and 10). On the day of the experiment, 2g of cuttings were poured into a mason jar that containing 200 mL of the test solution. The exact mass of shale  $m_i$  in each jar was recorded. All the jars were then placed in a hot rolling oven (OFITE, inc., Houston,TX) at 70°C. The movement of the rollers in the oven was set at a constant speed of 25 rpm. At the end of 3h, 8h, and 12h, the cuttings were rinsed with 50 mL of deionized (DI) water, and poured onto 35 mesh sieves. The sieves were placed in a drying oven for 24h at 110°C. The retained dried shale was then weighed for each sieve. Additionally, at the beginning of

each HRO test, about 5g of shale cuttings were set aside for initial water content measurement: They were weighed before and after being dried out, and, using Eq 4, the native water content (%w) was calculated. The mass of initial cuttings is noted  $m_{w,i}$  and the mass of dry cuttings is noted  $m_{w,f}$ .

$$\%w = \frac{m_{w,i} - m_{w,f}}{m_{w,i}} * 100 \quad \text{Eq 4}$$

As can be seen in Eq 5, the mass of retained dry shale  $m_F$  was then compared to the mass of initial cuttings  $m_i$  minus the initial water content %w to determine the percentage of shale retained %SR.

$$\%SR = \frac{m_F}{m_i * (100 - \%w)} * 100 \quad \text{Eq 5}$$

In the cases where polymeric solution was retained on the sieve, stuck to the cuttings, or could not be totally removed with DI water (see Figure 21), another method was used to calculate the percentage of shale retained: the mass of the shale in the filtrate was measured instead. This alternative procedure was used for some of the PEO solutions that had clouded out under the conditions of testing: 20% NaCl + 0.1% WSR-N10, 20% NaCl + 0.1% WSR-301, 20% NaCl + 0.1% WSR-301 + 0.5% PPG.



Figure 21 – A solution of 20% NaCl + 0.1% WSR-301 + 0.5% PPG retained on the sieve with the cuttings before (left) and after (right) the shale was dried out. It had been hot-rolled for 8 hours at 70°C.

The filtrate from the sieve was re-filtered on a paper filter that removed particles larger than 5  $\mu\text{m}$  and on a glass microfiber filter that retained particles larger than 1.5  $\mu\text{m}$ . The shale from the sieve filtrate that was retained on the filters was then dried, and its mass  $m_{F, \text{filtrate}}$  was recorded and compared to the initial mass of cuttings  $m_I$  as can be seen in Eq 6.

$$\%SR = \frac{m_I * (100 - \%w) - m_{F, \text{filtrate}}}{m_I * (100 - \%w)} * 100 \quad \text{Eq 6}$$

### 3.5 Fracture conductivity tests

To measure the effects of fluid sensitivity on fracture conductivity, proppant pack permeability measurements were performed. Fluids were flowed through a propped fracture in a shale core and the change in nitrogen permeability before and after the shale-fluid contact was quantified (Pedlow, 2013; Pedlow and Sharma, 2014).

#### 3.5.1 *Experimental design*

The core flood apparatus consisted of two flow paths. A schematic can be seen in Figure 22.

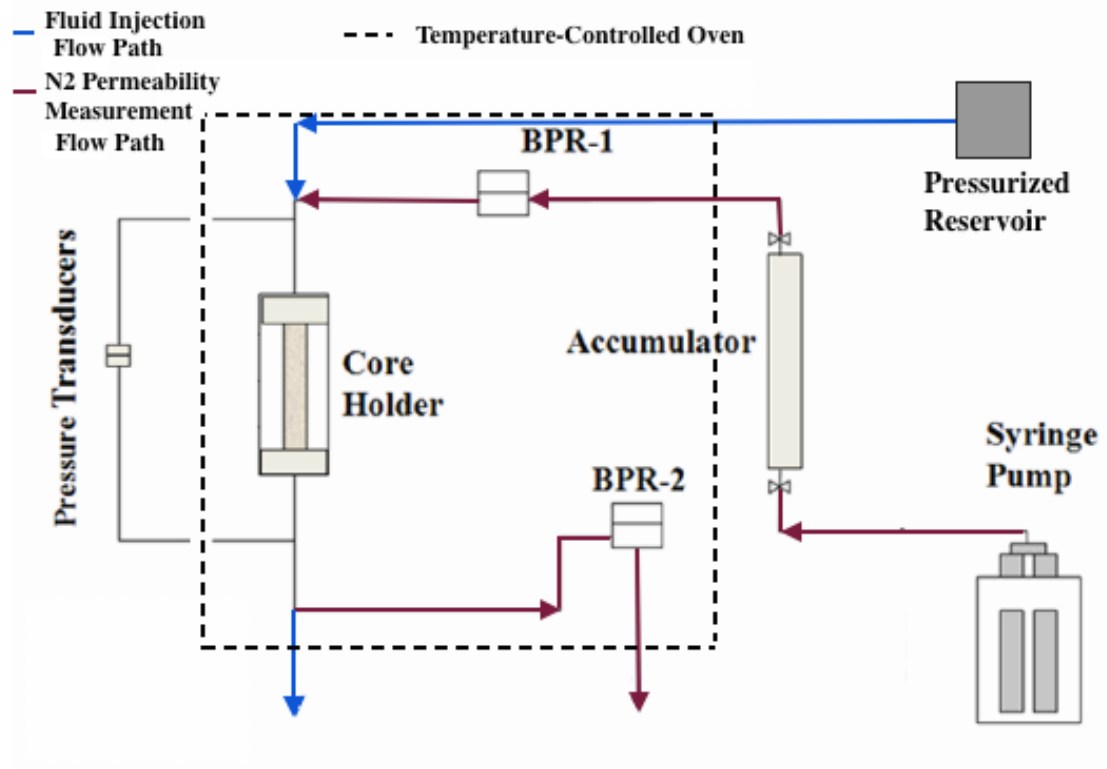


Figure 22 - Schematic of the core flood apparatus (Adapted from Pedlow, 2013)

The first flow path was used to inject the test solution through the propped fracture. It consisted of a pressurized reservoir, and a core holder. The test fluid was stored and pumped from the pressurized reservoir to the inlet of the loop at an average rate of 0.4L/h. The core was placed in a Viton sleeve, secured in the core holder, and confined at 2000 PSI by the means of hydraulic oil between the sleeve and the metal housing. A second flow path was employed to conduct the nitrogen permeability measurements. It was composed of a double syringe pump, an accumulator, two back pressure regulators (BPRs), and the core holder. The syringe pump allowed for a pulse-free precisely controlled flow rate. The accumulator was filled with tap water on one side of the piston and with nitrogen at 2500 psi on the other side. The pressure from the pump on the water, and thus on the piston, pushed the nitrogen into the fracture at the selected

flow rate. The first BPR (BPR-1) blocked the flow of nitrogen until the pressure at the outlet of the accumulator matched the pressure of the regulator (3000 psi). The second BPR (BPR-2) controlled the exit of the fluid from the loop: The pressure in the fracture was set to 500 psi, and nitrogen was forced to be at atmospheric pressure at the outlet of the core. Additionally, the pressure drop across the core was measured with two pressure transducers that were connected to the inlet and to outlet of the core. All the pressure readings were monitored via LabVIEW software. The BPRs and the core holder were placed in an oven where the temperature was maintained at 25°C.

Figure 23 and Figure 24 show the core flood apparatus in the oven, and the accumulator respectively.



Figure 23 - Core flood apparatus in oven



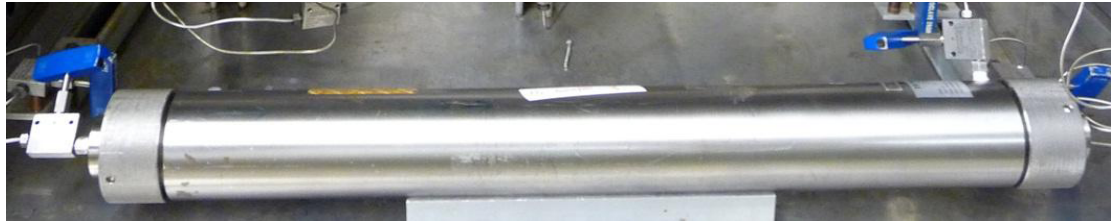


Figure 24 - Accumulator loaded with nitrogen

### 3.5.2 *Experimental procedure*

The shale was prepared into 3-inch long cylindrical cores, with a diameter of about 1 inch. The cores were cut into halves and stored in a vacuum sealed desiccator. Two 0.0325-inch diameter metal wires were used as spacers to separate the cores halves and Teflon tape was used to keep the two halves connected tightly. The diameter of the wires represented the width of the fracture. A 40/70 mesh white sand proppant was then poured between the two halves as can be seen in Figure 25. As the sand was packed, the wires were slowly pulled out. 200 mesh screens and 40 mesh screens were attached with Teflon tape to the top and to the bottom of the core to hold the proppant in place as shown in Figure 25. The core was then inserted into the rubber sleeve, which was placed in the core holder.

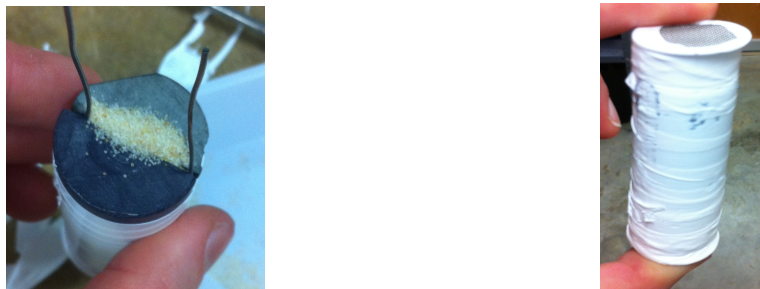


Figure 25 – Core preparation: Sand being packed between the half cores (left), and proppant pack, half cores, and screens tightly wrapped with Teflon tape (right)

The space between the sleeve and the metal housing was filled with hydraulic oil. Once the core holder was connected to the flow loop, the confining pressure was adjusted to 2000 psi with a hand pump. The confining pressure was always maintained at a pressure higher than the flowing pressure set by BPR-2 to prevent any leaks within the core holder of the test fluid from the fracture to the oil-containing space between the sleeve and metal housing.

The injections of DI water, 20% NaCl, 20% NaCl + 0.01% WSR-301; 20% NaCl + 0.1% DPFR and the corresponding permeability were conducted at 25°C and on cores that consisted of one shale half core and one plastic half core. To observe the effects of the CPT of PEOs solutions on fracture conductivity, an injection of a solution of 20% NaCl + 0.1% WSR-301 + 0.5% PPG was performed at 80°C. In this case, the two half cores were in plastic.

Setup for a new core in the core flood apparatus included equilibration time. The core was allowed to equilibrate overnight at the oven temperature and at the confining pressure. Meanwhile, air was flowed through the fracture pressure at air pressures ranged 90 and 100 PSI (shop air), to allow the sand pack to achieve a stable conformation within the fracture. To evaluate the effects of fluid sensitivity on fracture conductivity, the test fluid was allowed to be in contact with the shale for 2 hours and 30 minutes. The core was then dried out with shop air for 24 hours to remove as much liquid as possible from the fracture. A permeability measurement was performed before any fluid had been injected and after a fluid had been injected and then flushed out with air.

### Permeability measurement theory

The permeability was computed using the Forchheimer equation. It is an extension of Darcy's Law valid at high flow rates and high Reynolds number (Re). Eq 7 describes Darcy's Law, Eq 8 is the Forchheimer Equation and Eq 9 defines Re (Zeng & Grigg, 2006). P is the pressure (atm), X is the length of the porous media in the direction of the fluid flow (cm),  $\mu$  is the fluid viscosity (cP), v is the fluid velocity (cm/s), and k is the permeability (D). In the Forchheimer Equation,  $\beta$  is the non-Darcy coefficient (atm.s<sup>2</sup>/g),  $\rho$  is the fluid density (g/cm<sup>3</sup>). In the definition of the Reynolds number, D is the diameter of the particles (cm).

$$-\frac{dP}{dX} = \frac{\mu v}{k} \quad \text{Eq 7}$$

$$-\frac{dP}{dX} = \frac{\mu v}{k} + \beta \rho v^2 \quad \text{Eq 8}$$

$$Re = \frac{\rho D v}{\mu} \quad \text{Eq 9}$$

According to Darcy's law, when a fluid flows through a porous media, its pressure drop is proportional to its velocity, and the viscous resistance ( $\mu/k$ ) remains constant. However, when the flow is not laminar, the pressure drop increase is greater than predicted by the increase in velocity. To describe this behavior, Forchheimer (1901) added a quadratic term to Darcy's equation to account for the microscopic inertial effects. Even though no widely accepted criterion exists for the range of applicability of the Forchheimer equation, the critical Re values for the onset of the non-Darcy effects were found to range between 1 and 100 (Zeng and Grigg, 2006). It has been shown that the non-Darcy effects are significant in well performance evaluation (Holditch and Morse, 1976; Zeng and Grigg, 2006). As can be seen in Figure 26, the use of Darcy's Law in the



non-laminar region leads to a higher calculated permeability than the true permeability and thus an overestimation of production.

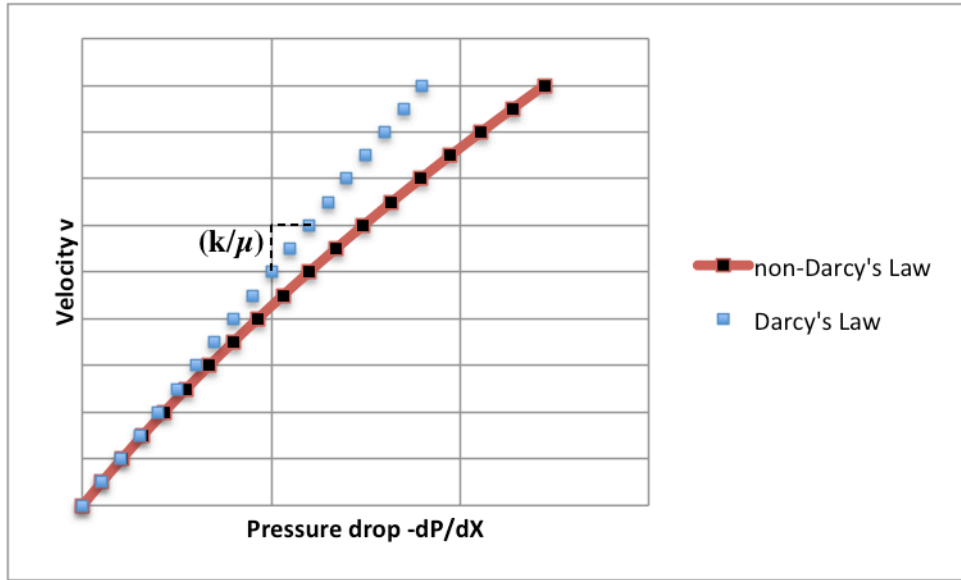


Figure 26 - Schematic of the deviation from Darcy's Law at high flow rates

The Forchheimer equation was used to calculate sand pack permeability. The pressure drops across the fracture corresponding to several flow rates were recorded. For each experiment, the permeability measurement was performed with nitrogen gas. The flow rate was increased until the observed stable pressure drop was about 20 psi. The flow rate was then gradually decreased and the corresponding pressure drops were measured. Generally, 6 flow rates were used, ranging between 1200 cm<sup>3</sup>/h and 3600 cm<sup>3</sup>/h, which led to good data correlation with the Forchheimer equation. The density of the flowing fluid in the accumulator and the density of the flowing fluid in the fracture were calculated using the pressure in BPR-1 and the pressure in BPR-2 respectively, and a Pressure-Volume-Temperature (PVT) analysis via a PVTSIM software. Using a mass

balance that accounted for the flow rate in the accumulator, the density of nitrogen in the accumulator, and the density of nitrogen in the fracture, the nitrogen flow rate in the fracture was calculated. Eq 8 can be rearranged in Eq 10 below.

$$-\frac{dP}{v} = \beta \rho dXv + \frac{\mu}{k} dX \quad \text{Eq 10}$$

The Darcy velocity  $v$ , i.e. the flow rate in the fracture divided by the cross-sectional area of the fracture, was plotted against the pressure drop divided by the Darcy velocity  $dP/v$ , as can be seen in Figure 27. Therefore, using Eq 10, the permeability  $k$  was directly given by the y-intercept as a function of the viscosity of the nitrogen fluid and of the length of the fracture.

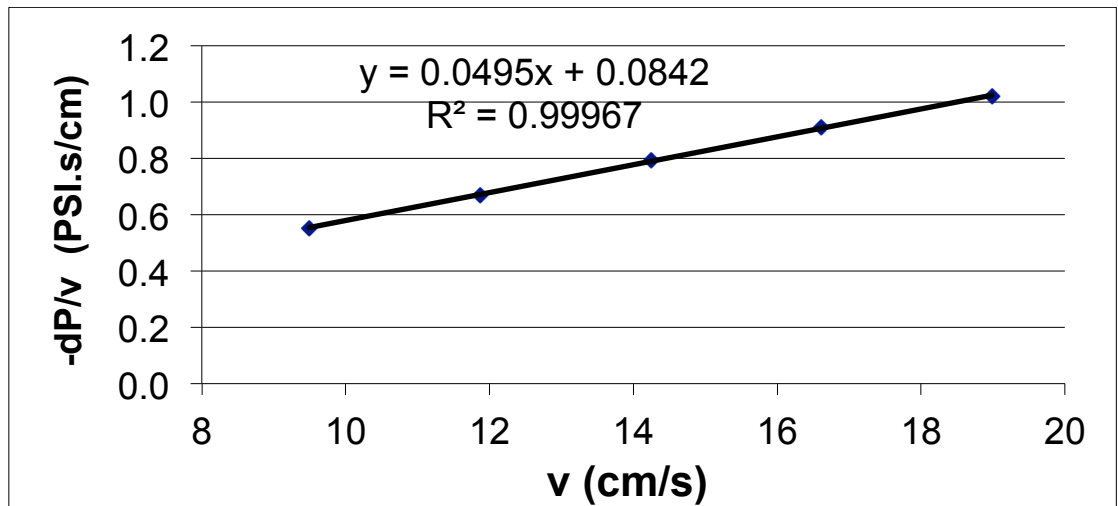


Figure 27 - Calculation of Y-intercept for permeability calculation

## Chapter 4: Results

In this chapter, the viscosity and the cloud point temperature of the fluids prepared were provided. The mineralogy of the shale samples was analyzed. Once the characteristics of the fluids and shales tested were determined, experiments were conducted to evaluate the effects of PA and PEO friction reducers on shale stability and fracture conductivity. Results of the beaker tests, swelling tests and hot rolling oven tests helped understand the shale stabilization generated by brines, PAs and PEOs. The effects of PEO and of the novel PA friction reducer in brines on fracture conductivity were found using the results of the permeability measurements.

### 4.1 Fluid and shale characterization

#### 4.1.1 *Fluid characterization*

The fluid characterization consisted of the study of the PEO solubility properties, and determination of the viscosity of PEO and PA solutions. The CPT of a PEO solution depends on its concentration, on its molecular weight, and on the salt composition of the solution.

Figure 28 shows the different aspects a PEO solution takes when heated.

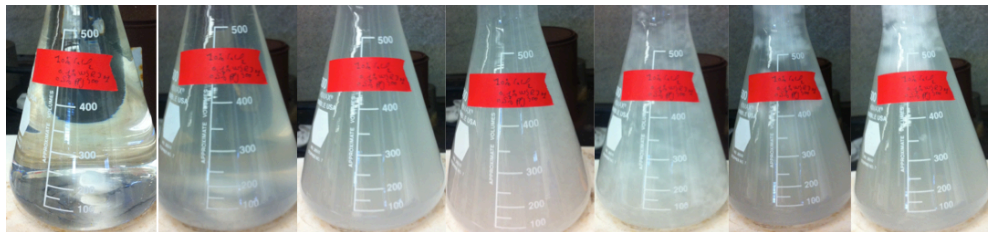


Figure 28 - Aspects of a PEO solution as the temperature increases (from the left to the right) - Solution of 10%  $\text{CaCl}_2$  + 0.1% WSR-301 + 0.5% PPG – The cloud point temperature (CPT) is the first temperature above which the solution becomes cloudy

The temperature of the solution was increased from the left to the right in the figure. Below the CPT, the PEO was fully soluble and the solution was transparent. As the temperature increased to the CPT, the solution became cloudier and opaque. With increasing temperature, the PEO came out of solution as a dispersed and homogeneous powder. Finally, small viscous lumps of white polymer began forming at higher temperature, and the PEO agglomerated at the top of the Erlenmeyer. The formation of agglomerates occurred at a temperature only a few degrees Celsius above the PEO solution CPT. The whole process was found to be reversible: when the temperature dropped, the PEO was soluble again.

The following results and discussions regarding CPT values only refer to the first temperature at which the solution became cloudy and not to the higher temperatures. As can be seen on Figure 29, the addition of NaCl had a major effect on the CPT. The CPT decreased linearly with increasing sodium chloride concentration. To a lesser extent, the CPT also depended on the molecular weight of the PEO, and on the PEO concentration. Even though solutions of high molecular weight PEOs had lower CPTs than solutions of lower molecular weight PEOs, this effect was small compared to the effects of salt concentration. For given NaCl and PEO concentrations, the CPT of PEO solutions with various molecular weights stayed within a range of 5°C. Moreover, solutions of 0.1% PEO had a lower CPT than solutions of 0.01% PEO for the same NaCl concentration and for the same PEO molecular weight. Once again, this PEO concentration effect is negligible compared to the effect of the NaCl concentration.

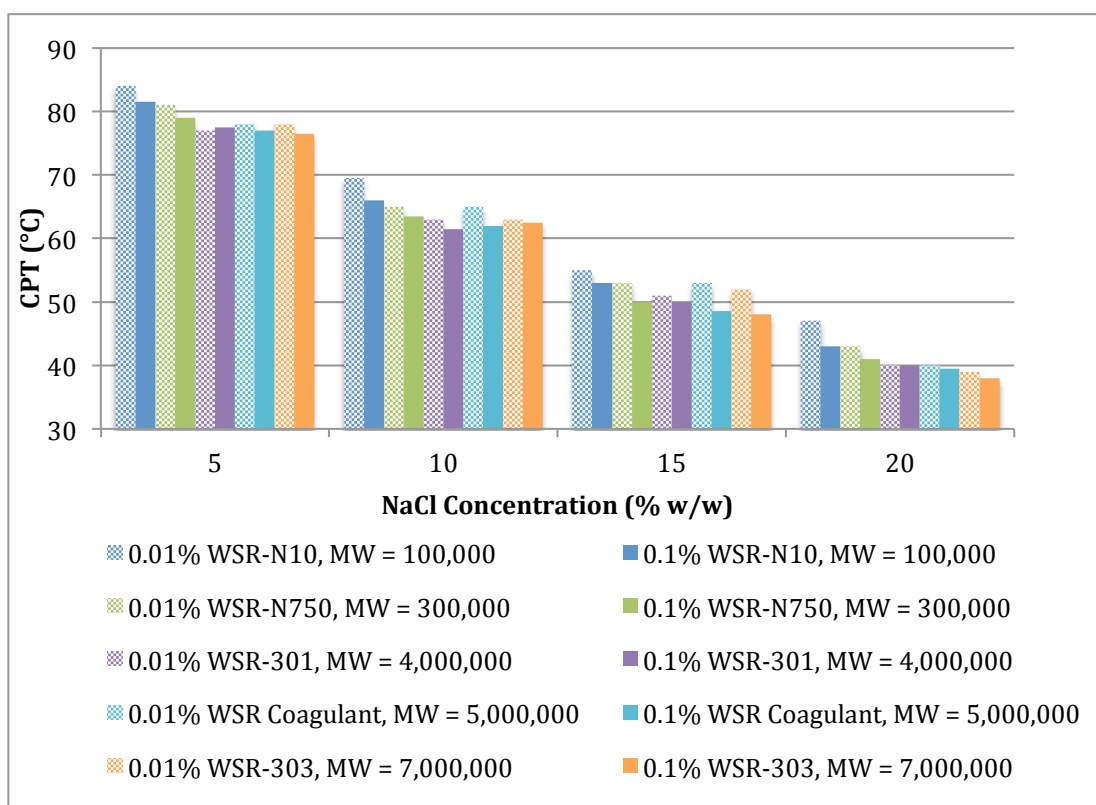


Figure 29 - Dependence of the CPT on NaCl concentration, the PEO concentration, and the PEO molecular weight

The CPT also depended on the salt species. As shown in Figure 30, NaCl was more effective at lowering the CPT than  $\text{CaCl}_2$ . The multi-solute brine, which was mainly composed of NaCl, had the same CPT as a NaCl solution of the same concentration. Therefore  $\text{CaCl}_2$  had very little effect on the CPT of PEO solutions. This result was in accordance with the series presented by Ataman and by Napper, which ranked the salting out power of cations. Sodium was found to have a greater ability to break water structure than calcium and this may explain its greater salting out power (Ataman, 1987).

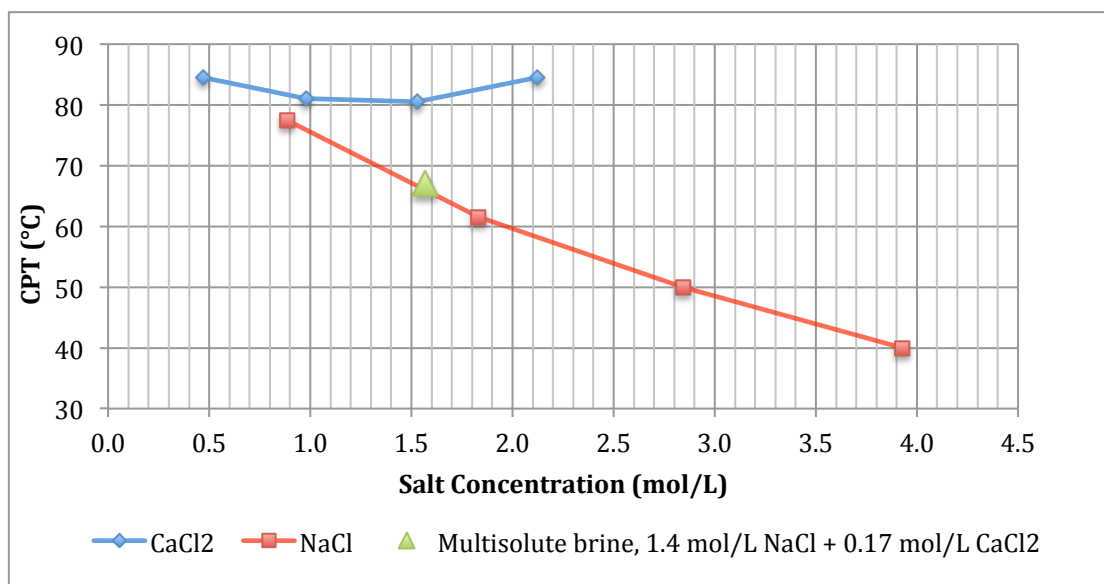


Figure 30 - Dependence of the CPT of 0.1% (w/w) WSR-301 on the salt species

Solutions containing PPG and PEO were tested as well. The addition of PPG lowered the CPT of PEO solutions. This was expected since PPG polymers have a chemical structure similar to PEO polymers and also are known to cloud out upon heating (Bland, 1992). The lowering of the CPT by PPG addition was greater at high NaCl concentrations as can be seen in Figure 31.

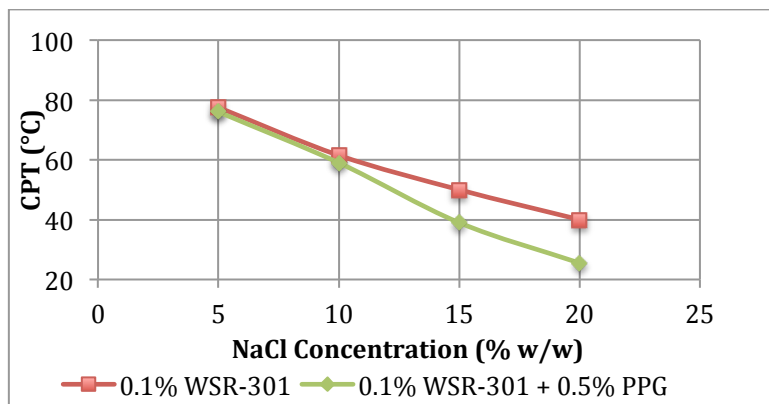


Figure 31 - Dependence of the CPT of 0.1% (w/w) WSR-301 on the addition of PPG

CPT results for other PEO solutions can be found in Appendix B. Additional results on the variation of pH with PEO addition in  $\text{CaCl}_2$  are provided in Appendix B.

The viscosity of each PA and PEO solution was measured. All the fluids tested were found to be Newtonian. Figure 32, which shows the viscosity values obtained for 20% NaCl solutions as a function of the shear rate and at 70°C, illustrates that the viscosity is independent of the shear rate. The viscosity values considered for analysis were the average of the viscosities measured when the shear rates varied between 10 and 100  $\text{s}^{-1}$ .

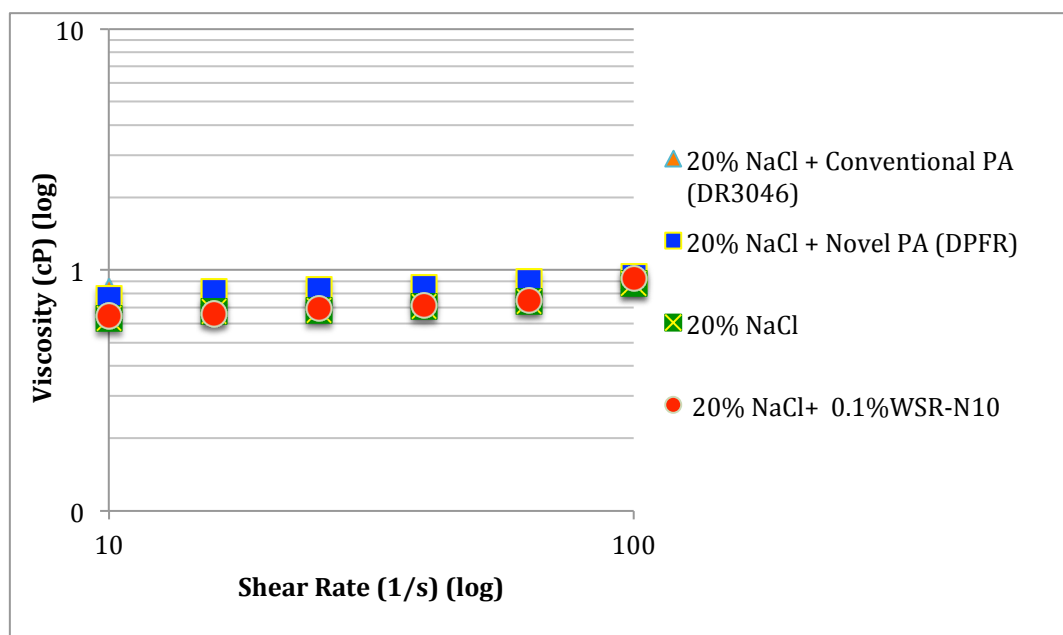


Figure 32 - Viscosity of 20% NaCl solutions with 0.1% PA and 0.1% PEO at 70°C

With the exception of the viscosity of the 0.1% DR3046 solution, the viscosities of all the solutions ranged between 0.5 and 1.9 cP at 70°C and between 0.8 and 5.1 cP at 25°C. Polymeric solutions showed higher viscosities than solutions composed only of salts, and this effect was more evident as the polymer concentration increased. For a

given salt concentration, the PEO solutions viscosities were on the same order of magnitude as the Dispersion Polymer Friction Reducer (DPFR) solution viscosities.

Due to higher densities, more concentrated salt solutions were more viscous. The viscosity of the 0.1% DR 3046 solution was 10 times higher than all other solutions: 14.1 cP at 25°C and 8.6 cP at 70°C. As salt was added to the solution of DR3046, its viscosity dropped significantly and reached the same level of magnitude as the other solutions. Without any salt, the negatively charged carboxyl groups on the polyacrylamide chains repel each other and this enhances viscosity by causing extension of the chain. When cations are present, the charges on the polymer chains are neutralized. Therefore, the chains don't stretch and the viscosity decreases compared to when cations are present (Choi, 2008).

When in DI water and at 25°C, the 0.1% DPFR solution was 3 times as viscous as the 0.01% DPFR solution. In the presence of 20% NaCl, the viscosities of the 0.01% and 0.1% DPFR solutions were the same. Therefore, the addition of salts controlled the viscosity of the PA solutions. In DI water and at 25°C, the increase of the PEO concentration from 0.01% WSR-301 to 0.1% WSR-301 caused the viscosity of the solution to increase by a factor of 5. The molecular weight of the PEO also had an impact on the viscosity: The viscosities of the 0.1% WSR-301 and of the 0.1% WSR-N10 solutions were respectively 4.5 cP and 0.9 cP at 25°C. The solutions of 0.1% WSR-301 and 0.1%-WSR-301 + 0.5%PPG had the same viscosity. In the presence of 20% NaCl and at 25°C, the same increases in PEO concentration and molecular weight caused the viscosity of the solution to triple.



As expected, the viscosities of the PA and salt solutions at 70°C were lower than the viscosities measured at 25°C, following the Arrhenius-type equation:

$$\mu(T) = \mu_0 e^{\frac{E}{RT}} \quad \text{Eq 11}$$

where the viscosity  $\mu$  exponentially decreases with increasing temperature  $T$ .  $\mu_0$  is the viscosity at some reference temperature,  $E$  is the temperature coefficient for viscosity and  $R$  is the ideal gas constant. Moreover, the changes resulting from increases in the PA or PEO concentrations, or from an increase in the PEO molecular weight were less significant at 70°C than at 25°C. At 70°C, it wasn't possible to measure the viscosities of some of the solutions which had their cloud point temperature below 70°C, because the reading was very unstable as lumps were forming. This was the case for all the solutions containing 20% NaCl and 0.1% PEO. All the viscosity measurements can be found in Appendix C.

The CPT of PEOs strongly decreased with salt concentration, and to a lesser extent, also depended on salt species, PEO molecular weight and concentration. The viscosity of PA and PEO based fluids increased with polymer concentration, molecular weight, and decreasing temperature, and varied with salt addition. With the exception of the 0.1% DR3046 solution, which viscosity was around 10 cP, all of the viscosities were on the same order of magnitude, close to 1 cP. The determination of the viscosity and CPTs of the fluids, as well as the mineralogy of the shale samples were useful to interpret the hot rolling oven results and fracture conductivity results. The desiccator used to store the shale was selected after adsorption isotherm tests had been conducted.

#### 4.1.2 Shale characterization

Samples of Pierre Shale I and GOM-12 were analyzed by X-Ray diffraction by Halliburton and by the Core Laboratories. The results are shown in Table 7.

Table 7 - X-Ray diffraction mineralogy of GOM-12 and Pierre Shale I

	<b>Whole Rock Mineralogy (Weight %)</b>							
Shale Sample	Quartz	K Feldspar	Plagioclase	Calcite	Dolomite	Pyrite	Siderite	Total Clay
GOM-12	26.4	2.4	1.9	2.1	0.0	0.6	1.2	65.5
Pierre I	38	18	0	Trace	4	1	0	39

	<b>Clay Mineralogy (Weight %)</b>				
Shale Sample	Illite/ Smectite	Smectite	Illite & Mica	Kaolinite	Chlorite
GOM-12	20.3	0.0	16.8	21.8	6.6
Pierre I	27	8	0	4	0

Both GOM-12 and Pierre Shale I were quartz-rich shales. GOM-12 appeared to have a much higher clay content than Pierre Shale I and thus to be more reactive. According to these results, due to its high illite/smectite content, Pierre shale I was classified in class 1 of the scheme presented in Table 4, with the soft and highly dispersive shales. GOM-12 was expected to be more brittle and harder because the presence of all illite, smectite and chlorite matched the description of classes 3 and 4 of Table 4.

The native water activity of the shale samples was determined to select the proper storage conditions (Chenevert, 1970a; Jung et al., 2013; Pedlow and Sharma, 2014). Therefore, adsorption isotherm tests were conducted. With a native water content of 5.2%, GOM-12 had a native water activity of 0.82. Therefore, it was stored in a desiccator in which water activity was maintained at 0.80. Pierre Shale I, which had a native water

content of 5.7% and a native water activity of 0.87, was stored in a desiccator at  $a_w=0.85$ .

Figure 33 shows the adsorption isotherm of Pierre Shale I.

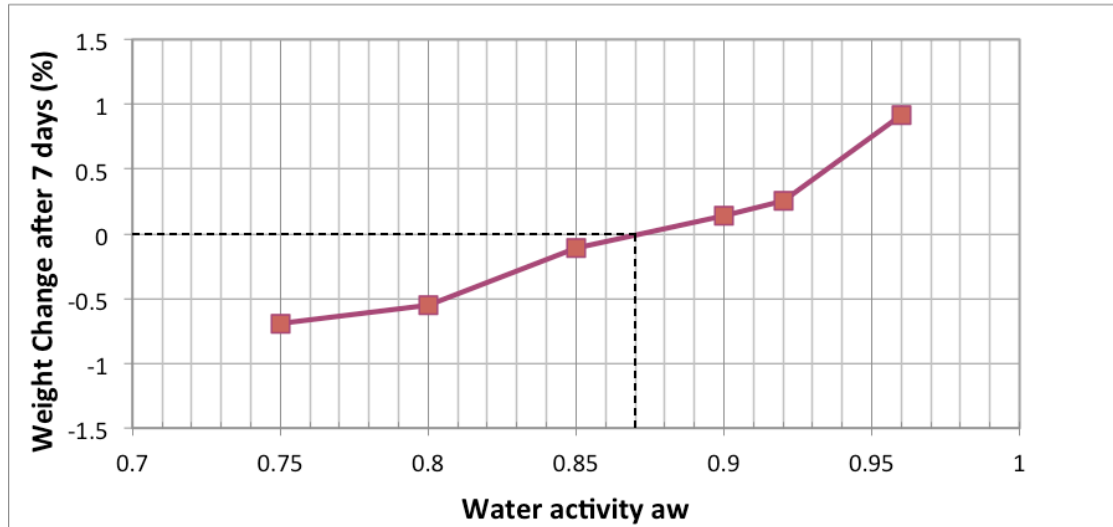


Figure 33 - Adsorption isotherm of Pierre Shale I with a native water content of 5.7%

## 4.2 Shale instability visualization

### 4.2.1 *Swelling tests results*

Swelling tests were performed to compare the effects of the contact of PEO, DI water, and a 4% NaCl solution with shale at ambient temperature (Chenevert, 1970b; Zhou et al., 2013). More swelling was observed in the direction perpendicular to bedding when GOM-12 was immersed in DI water and in DI water + 0.1% WSR-301 than in a 4%NaCl solution. The results are displayed in Figure 34. The salt solution was expected to be an effective shale inhibitor as salts delay the osmotic transport of water in the shale and thus reduce the swelling. Therefore, this preliminary result confirmed that reusing salty flowback water in hydraulic fracturing operations could be beneficial to shale stability. In addition to the effect of salts on shale swelling, the effect of PEO on shale

swelling was observed. The PEO solution caused swelling as important as the swelling caused by the contact of shale with DI water.

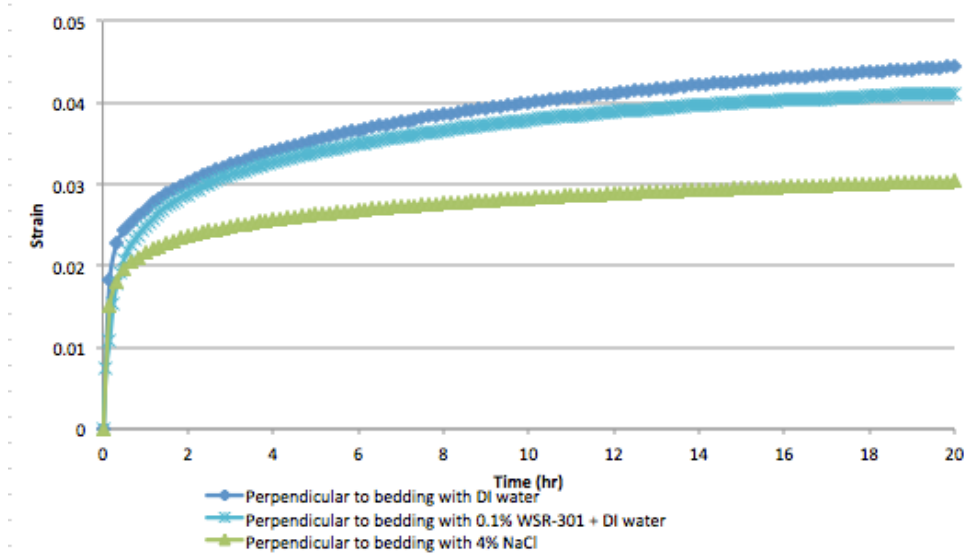


Figure 34 - Swelling of GOM-12 in DI Water, 0.1% WSR-301, and 4% NaCl. The strain is the ratio of the displacement of the clamp over the original length of sample shale.

#### 4.2.2 *Beaker tests results*

Beaker tests were conducted at ambient temperature in order to qualitatively compare the effects of PEO WSR-301 and DI water on GOM-12. As shown on Figure 35, small cracks appeared on the shale sample after 1.5 hours of immersion in DI water, while no sign of shale degradation was visible in the jar containing 0.01% PEO. This fracture was more apparent after 44 hours of immersion. This result could be interpreted as a demonstration of shale inhibition by the PEO solution.



Figure 35 - Beaker test on GOM-12 at ambient temperature for 0.01% WSR-301 in the left jar and DI water in the right jar at 0h (left), 1.5 (middle) and 44h (right) – The red circles indicate the noticeable shale degradation.

However, when 2.5% NaCl solutions were tested, the shale samples were damaged to a greater extent in the presence of PEO than without it. This result is shown in Figure 36. This degradation indicated that the association of PEO and salts might negatively impact shale stability while both PEO and NaCl had previously been found to be beneficial to GOM-12 stability on their own. It is important to note that these observations are qualitative and that the conclusions might have been different with a different shale, handling of the samples, or duration of the experiment.

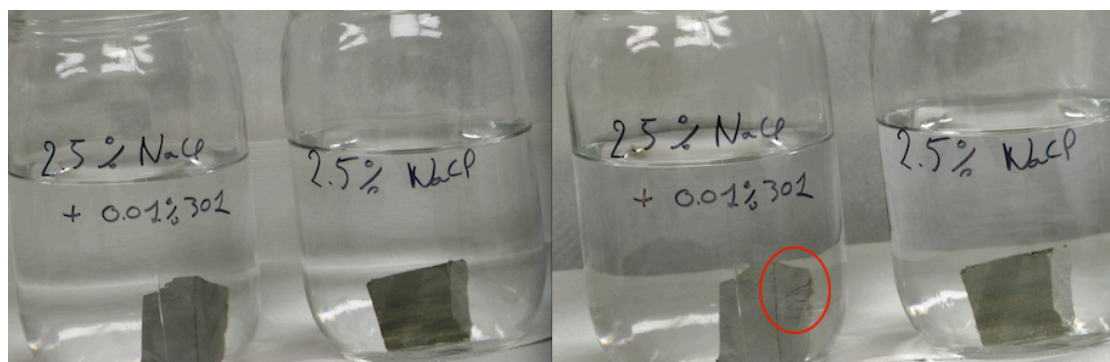


Figure 36 - Beaker test on GOM-12 at ambient temperature for 0.01% WSR-301 + 2.5% NaCl in the left jar and 2.5% NaCl in the right jar at 0h (left), and 1h30 (right) – The red circle indicates the noticeable shale degradation.

In order to simulate downhole temperatures and to activate the CPT property of PEOs, an attempt was made to do a beaker test at high temperature. The GOM-12

samples were immersed in boiling DI water and in a boiling solution of 0.01% PEO which had clouded out. The high temperature had an immediate impact on the shale: both samples broke apart as they contacted the hot solution. This sensitivity to temperature gradients, which was to be expected for any shale, was probably accentuated by the chlorite content of GOM-12, which made it hard and brittle. Therefore, this experiment was unsuccessful in that the immediate shale degradation due to the high temperature occurred before any effects of the PEO and of DI water on the shale was observed.

#### **4.2.3      *Conclusions***

The qualitative beaker tests and the swelling tests did not produce any conclusive results on the effects of the addition of PEO to DI water or salt water on shale stabilization at ambient temperature and high temperature but they showed that salt solutions were potential shale stabilizers. These results were expected since salts are already used for their clay stabilizing properties. These preliminary tests also pointed out the importance of using shale samples adapted to the experiments, ie, for which changes in properties are measurable within the timeframe of the experiment. Further study was necessary to quantitatively assess the effects of friction reducers on shale stabilization in more realistic conditions such as by controlling the temperature in hot rolling oven tests and by simulating the fluid-shale contact in a pressure and temperature controlled fracture with fracture conductivity tests.

### **4.3            Hot rolling oven dispersion results**

#### **4.3.1      *Effect of salt addition***

The first dispersion tests done were to prove the efficiency of salt solutions as shale inhibitors. These tests were done following the methods described by Arthur Hale (1991). As can be seen in Figure 37, both  $\text{CaCl}_2$  and  $\text{NaCl}$  were found to reduce the

dispersion of Pierre Shale I cuttings. After 3 hours in the hot rolling oven, only 61% of the cuttings immersed in DI water are of a size larger than 0.5 mm. This value drops to 38% after 12 hours in the oven. On the other hand, the percentage of shale retained, in all of the salts solutions tested – 10% NaCl, 20% NaCl, 10% CaCl<sub>2</sub>, and the multi-solute brine, is more than 63% even after 12 hours in the oven.

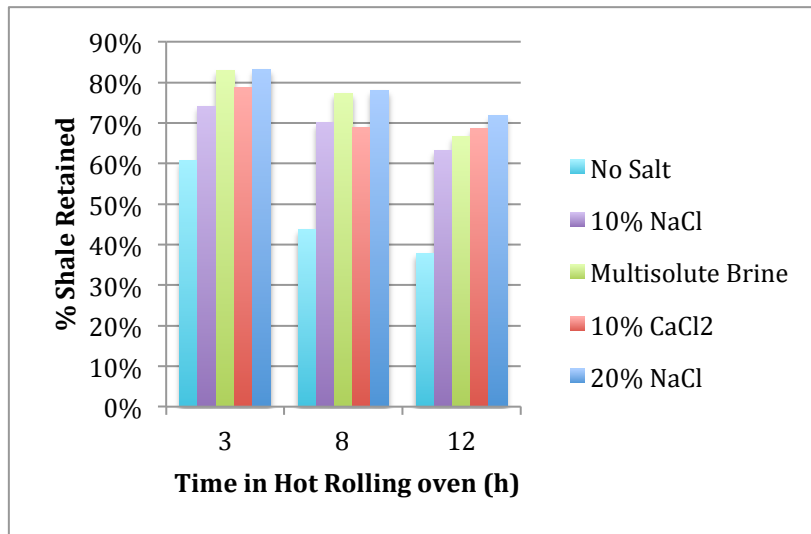


Figure 37 - Comparison of % shale retained in salt solutions (0, 10%, and 20% NaCl, 10% CaCl<sub>2</sub>, and the multi-solute brine) after 3h, 8h, and 12h in the HRO at 70°C

Variation in shale stability was observed for different salt concentrations and compositions. The very concentrated 20% NaCl solution consistently yielded higher shale retention. The multi-solute brine and the 10% CaCl<sub>2</sub> solution, both made up of CaCl<sub>2</sub>, were more efficient at preventing shale degradation than the 10% NaCl brine. Hale and colleagues suggested that the presence of divalent calcium cations could cause the formation of a precipitate on the shale that would prevent water from flowing in the shale and thus reduce shale degradation (Hale and Mody, 1993).

### **4.3.2      *Effects of PA addition***

The efficiency of polyacrylamide-based friction reducers at shale stabilization was then tested. At all salt concentrations, both the novel DPFR and the conventional DR3046 yielded higher percentages of shale retained than solutions containing only salts (see Figure 38). As described in Section 2.3.3, shale stabilization by PAs is mainly explained by the bridging between the carboxylic groups of the polymer and the structural cations on the clay surface, which blocks the entrance of water in the shale matrix. When salts are added to a PA solution, the inhibition of the shale is enhanced due to osmotic transport and because of the reduced hydration associated with interlayer exchangeable cations. This is the reason why the percentage of shale retained in the novel PA solution increased with the addition of salts. After 12 hours in the HRO, the novel PA-based friction reducer produced the highest retention with 74%, 88% and 89% of shale retained in DI water, 10% NaCl and 20% NaCl respectively. There are several possible reasons why the percentage of shale retained in the conventional PA solution decreased when 10% NaCl was added compared to when no salt was present. As seen in Section 4.1.1, the viscosity of 0.1% DR3046 was higher than all of the other polymeric solutions by a factor of 10 and dropped to a level similar to the other solutions when salts were added. Additionally, high viscosity fluids tend to delay the entrance of water in the shale matrix. Therefore, the variations of the viscosity of the conventional PA might explain the high percentage of shale retained when no salt was present, and its decrease when 10% NaCl were added. Moreover, since the addition of salts is known to neutralize some of the negatively charged carboxylic groups, they were not able to bridge with the clay as well. The increase in shale stability with the addition of the even more concentrated brine of 20% NaCl to a 0.1% conventional PA-based solution may be attributed to the inhibition power of the salts.



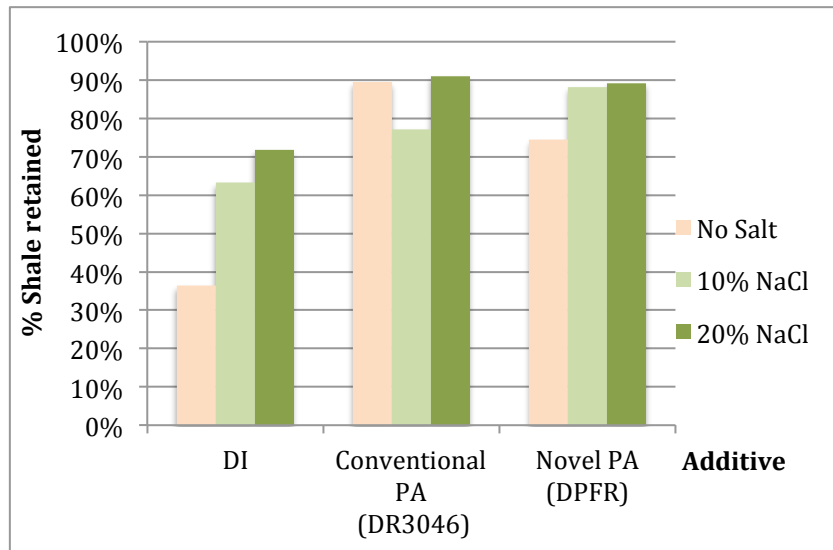


Figure 38 – Comparison of % shale retained in polyacrylamide-based solutions (0.1% DR3046 and 0.1% DPFR) with 0, 10% and 20% NaCl after 12 hours in the HRO at 70°C

Figure 39 shows the effects of PA concentration on the percentage of shale retained. High PA concentration helped stabilize the shale in DI water but did not have a significant effect in concentrated salt solutions. In a DI water based fluid, the 0.1% novel PA retained 13% more cuttings than the 0.01% novel PA. However, in 20% NaCl, the stabilization rates were high and close at both PA concentrations – 89% and 91%. This indicated that the salts together with the PA produced the maximum shale retention that couldn't be improved by any increase in the polymer concentration.

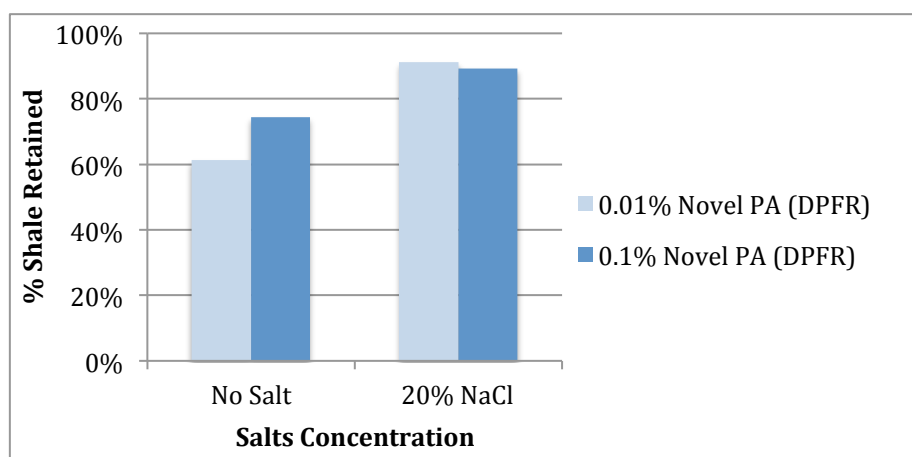


Figure 39 – Comparison of % shale retained with 0.01% DPFR and 0.1% DPFR after 12 hours in the HRO at 70°C

#### 4.3.3 *Effects of PEO addition*

The effects of the contact of PEO in brines with shale cuttings were tested in the HRO. As can be seen in Figure 40, both the addition of the PEO powder and the addition of the PEO-PPG dispersion to brines produced higher percentages of shale retained than without it. These results can be explained by the slight increase in viscosity observed with the addition of PEO to any salt solution, and by the hydrogen bonding between glycols and the clay surface. Moreover, shale stabilization was improved as salt concentration increased. These mechanisms and results are similar to the observations made with PAs.

The cloud point effect is the main difference between the experiments involving PAs and the experiments involving PEOs. Both PEO solutions were totally soluble in DI water at 70°C while they clouded out at a temperature below 70°C when 10 and 20% NaCl were added. The CPTs of these solutions are reported in Table 8. Moreover, the increase in the percentage of shale retained with NaCl addition is much greater when PEO is present than without it. Therefore, the PEO layer formed on the shale when the

PEO clouded out may be responsible for this shale stabilization. It protected the cuttings from abrasion and prevented water from entering the shale matrix. Additionally, the usual improvement of the shale stabilization process observed with increasing salts concentrations was not apparent because the clouding effect of the PEO was dominant: Once the PEO had clouded out, it retained the shale up to 88% - and this figure didn't increase more with further addition of NaCl.

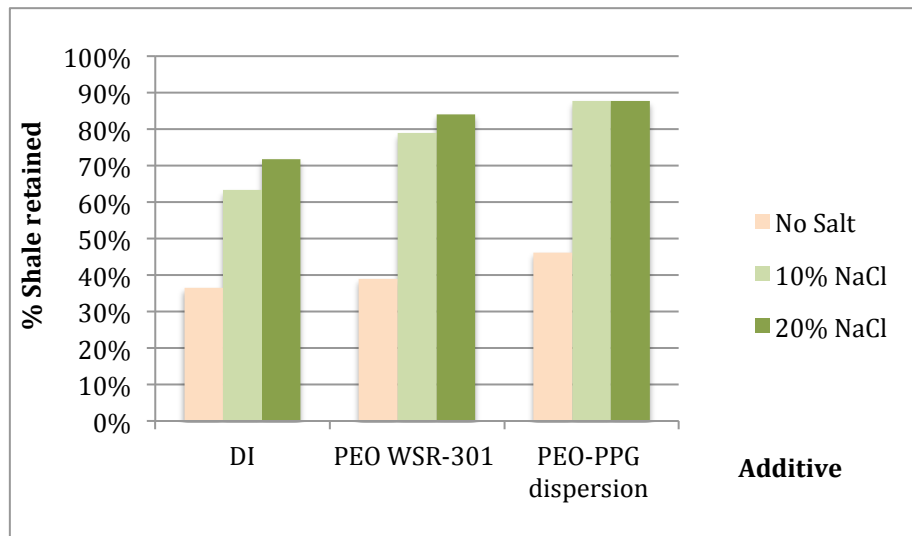


Figure 40 – Comparison of % shale retained in polyethylene oxide-based solutions (0.1% WSR-301 and PEO-PPG dispersion) with 0, 10, and 20% NaCl after 12 hours in the HRO at 70°C

Table 8 - CPT (°C) of 0.1% WSR-N10, 0.01% and 0.1% WSR-301, and 0.1% WSR-301 + 0.5% PPG in 10% and 20% NaCl

	PEO solutions of varying composition			
10% NaCl	66°C	61.5 °C	63°C	59 °C
20% NaCl	43°C	40°C	40°C	25.5°C

The effect of the CPT on shale stabilization is even clearer in Figure 41. The percentages of shale retained of various PEO-salt solutions are plotted versus the temperature difference between 70°C and their CPT. In the bottom left part of the graph,

the solutions that did not cloud out resulted in between 39% and 46% of shale retained. In the top right part of the graph, all the PEOs that precipitated out of the solutions are represented, and the percentage of shale retained was between 77% and 88%. This behavior is similar to a step function. There was no clear improvement of the shale stabilization at more advanced stages of the precipitation (cf Section 4.1.1) at higher temperatures. Once the HRO temperature was above the CPT of the solution, the percentage of shale retained increased and stabilized around 83%. Lower CPT solutions do not give rise to higher percentages of shale retained.

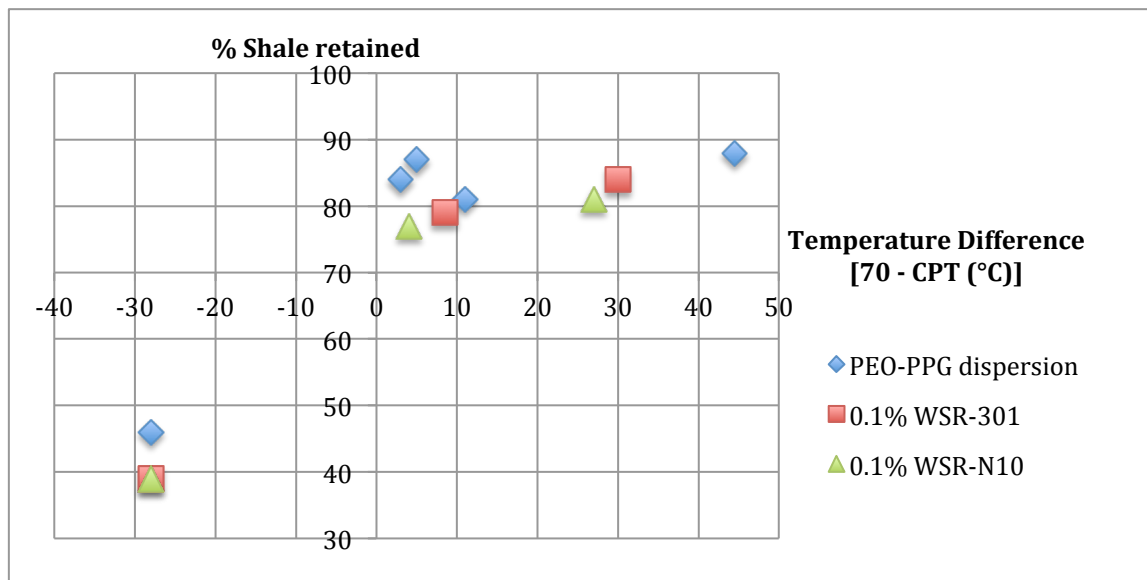


Figure 41 - % Shale retained after 12 hours in the HRO at 70°C vs the difference between 70°C and the CPTs of PEO-NaCl/CaCl<sub>2</sub> Solutions

Thus, the stabilization of the shale did not depend on the molecular weight nor on the concentration of the PEO. Figure 42 shows the results for 0.1% and 0.01% of WSR-301 and of the lower molecular weight PEO, WSR-N10 at 0.1%

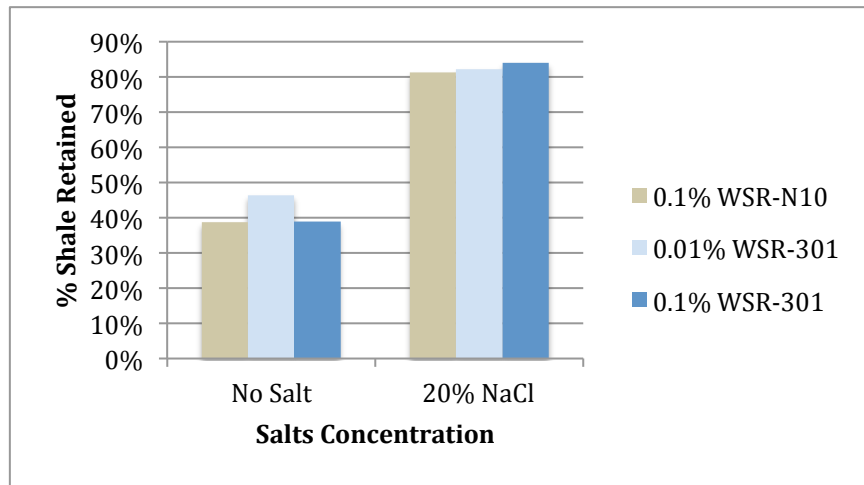


Figure 42 - Comparison of % shale retained with 0.1% WSR-N10, 0.01% WSR-301, and 0.1% WSR-301 after 12 hours in the HRO at 70°C

#### 4.3.4 Comparison of the effects of PA and PEO

While both the additions of PA and of PEO to brines enhanced shale stabilization, their effectiveness in protecting the shale from destabilization varied with salt concentration. These results are summarized in Figure 43. It is important to note that, as explained in Section 3.4, the methods used to compute the percentage of shale retained in PEO solutions with 10 and 20% NaCl, and in all the other solutions are different. This might have led to an underestimation of the percentage of shale retained in PEO solutions. When salts are present, all the polymeric solutions yielded between 77% and 91% shale retention. The novel PA-based solution showed the highest and most stable percentages of shale retained with and without salts. It had been shown to be efficient with all salt concentrations as a friction reducer (Kuzmyak, 2014) so it was expected to have relatively small interactions and sensitivity to salts. The conventional PA was the most effective at stabilizing the shale in DI water, but the addition of NaCl lowered its viscosity and thus reduced its stabilizing effects. However, further addition of NaCl maintained high shale retention because of the clay stabilizing capacity of the salts

themselves. Finally, PEO solutions were relatively poor shale stabilizers in DI water but the addition of NaCl triggered the precipitation of the polymers out of solution and onto the shale, and thus enhanced shale protection.

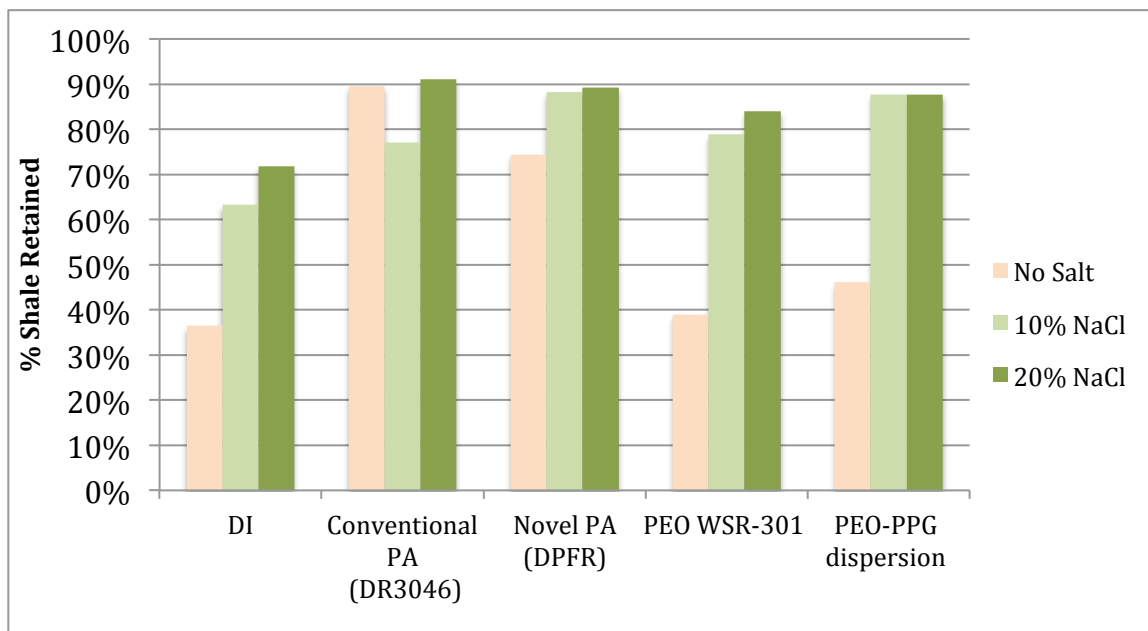


Figure 43 - Comparison of % shale retained in 0.1% PA and 0.1% PEO solutions with 0, 10, and 20% NaCl after 12 hours in the HRO at 70°C

Thus, the main mechanisms involved in shale cutting stabilization are the cloud point property of PEOs, the bridging between PA or PEO polymer chains and the clay surface, the osmotic transport and hydration in the presence of salts, and the viscosity of the solutions. The effects of viscosity were further investigated in Figure 44. Except for the 0.1% DR3046 solution, the range of viscosities was limited between 0.5 and 1.9 cP while the percentage of shale retained randomly ranged between 36% and 92%. Therefore, viscosity was not a controlling factor for shale stabilization. Only in the case of the solution of 0.1% DR3046, which was 10 times more viscous than all the other solutions, was the impact of viscosity apparent. With one of the highest percentages of

shale retained, the relatively high viscosity was likely to be controlling the HRO results for this polymer.

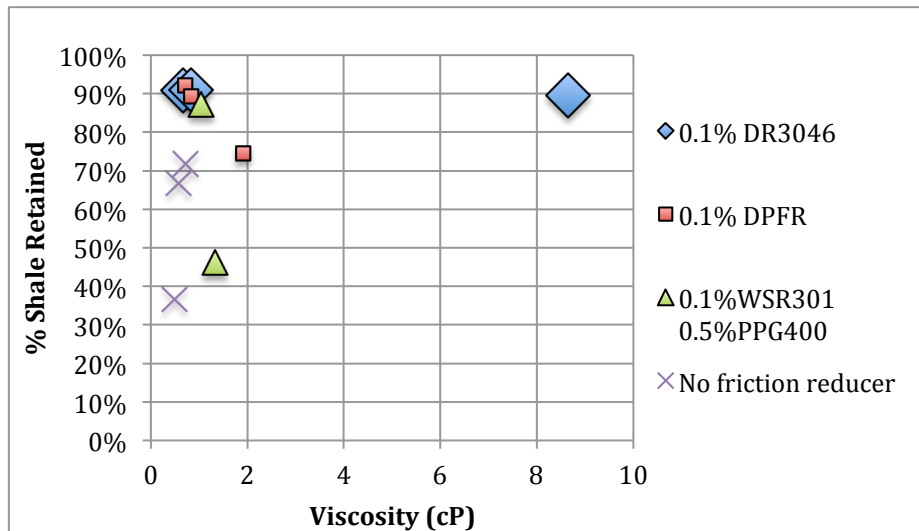


Figure 44 - % Shale retained after 12 hours in the HRO at 70°C vs viscosity at 70°C of the multi-solute brine, of 20% NaCl and in no salts

#### 4.3.5 Effects of salt composition

As shown in Figure 45, the percentage of shale retained in PA and PEO solutions depends on salt concentrations and the salt species in solution.

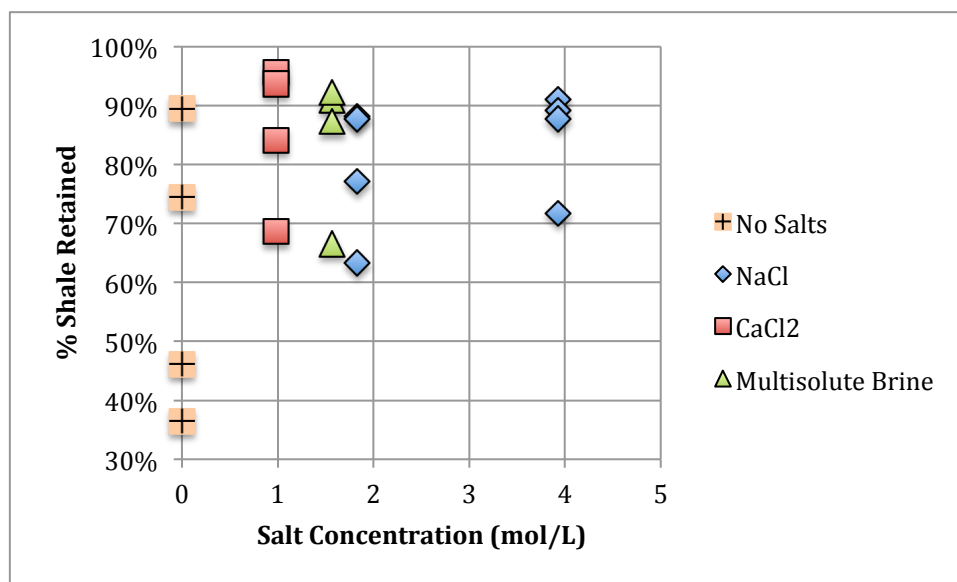


Figure 45 - % Shale retained after 12 hours in the HRO at 70°C vs salt concentrations and species (no salts, CaCl<sub>2</sub>, NaCl, multi-solute brine) for 0.1% DPFR, 0.1% DR3046, and 0.1% WSR-301 + 0.5% PPG

The percentage of shale retained in NaCl solutions increased with NaCl concentration. When comparing the HRO results obtained in brines that contained PA/PEO and NaCl/CaCl<sub>2</sub> at about 1.5 mol/L, the highest percentages of shale retained were achieved using brines with CaCl<sub>2</sub>. Even though the multi-solute brine and the pure CaCl<sub>2</sub> brine were less concentrated than the NaCl brine, they were more effective shale stabilizers than the NaCl brine. Therefore, Ca<sup>2+</sup> reduced the water uptake by the Pierre Shale I with and without PAs or PEOs in solution.

#### 4.3.6 *Effect of time*

As can be seen in Figure 37 and in Figure 46, the percentage of shale retained generally decreased with increasing time spent rolling in the HRO. This result was expected since more time in the HRO means longer contact times between the cuttings and the fluid and thus more opportunities for the clay to be degraded by the water and by the abrasion caused by rolling.



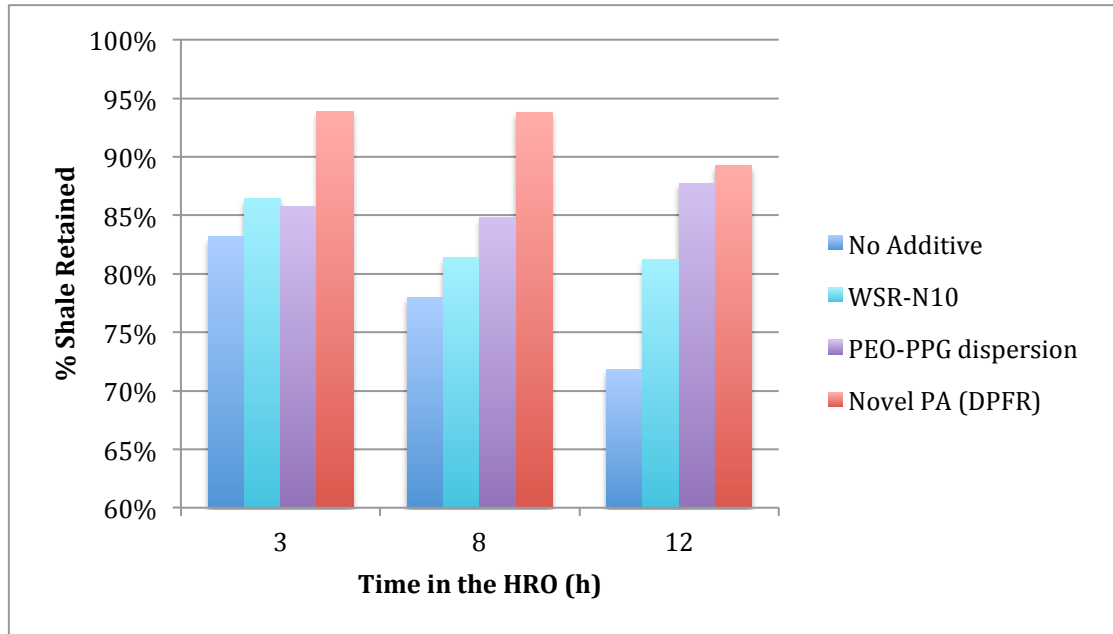


Figure 46 - Comparison of % shale retained in 20% NaCl and 0.1% WSR-N10, 0.1% WSR-301+ 0.5% PPG, 0.1% DPFR, and with no additive, after 3h, 8h, and 12h in the HRO at 70°C

It is interesting to note that, during the first 12 hours in the HRO, the shale in the pure brines and in the 20% NaCl solution with 0.1% of the low molecular weight PEO WSR-N10 degraded more rapidly than the shale cuttings in the 20% NaCl solution with the novel PA friction reducer or with the PEO-PPG dispersion. Therefore, the molecular weight and the concentration of the polymers are important parameters for delaying shale degradation. The polymer chains coat the shale and reduce the contact between the clay and water. If the polymer degrades due to heat and/or shear, water can begin to penetrate the shale, and the percentage of retained shale starts decreasing. This was observed with the 20% NaCl + novel PA series: the percentage of shale retained was 94%, 94% and 89% after 3, 8 and 12 hours respectively in the HRO. The results in the PEO solution showed a different trend. While the percentage of shale retained was stable at 86% and 85% after 3 and 8 hours respectively in the HRO, it increased to 89% after 12 hours. As

the PEO clouds out, it forms larger and larger agglomerates. With time, more cuttings are maintained in these aggregated clumps. Therefore, more cuttings are retained on the top of the sieves with the PEO clusters when the solutions are sieved after 12 hours compared to 8 hours. Therefore, this increase in the percentage of shale retained with time didn't mean that the cuttings dispersed less but that, independent of their sizes, the PEO agglomerates kept them together.

#### ***4.3.7 Conclusions on the efficiency of salt-tolerant friction reducers at preventing shale cuttings dispersion***

The above evaluation of shale stabilization by the additives tested in the HRO can be related to the friction reduction efficiency of these same additives, using the flow loop tests that were run to assess the compatibility of the conventional PA friction reducer DR3046, the novel PA DPFR and of the PEOs with various brines (Kuzmyak, 2014). The most efficient additive with regards to both shale stabilization and friction reduction efficiency and in all salt concentrations is the novel PA friction reducer. The results are shown in Figure 47. At all salt concentrations, it ensured a high percentage of shale retained and the highest friction reduction. The friction reduction efficiency of the PEO is high and constant but it shows the lowest percentage of shale retained when no salts were present. The shale stabilization process of PEOs is only activated when they cloud out, which is facilitated when salts are in solution and thus lower the CPT. As for the conventional PA solutions, they are efficient shale stabilizers over a wide range of NaCl and CaCl<sub>2</sub> brines but their friction reduction efficiency drops when CaCl<sub>2</sub> is in solution.

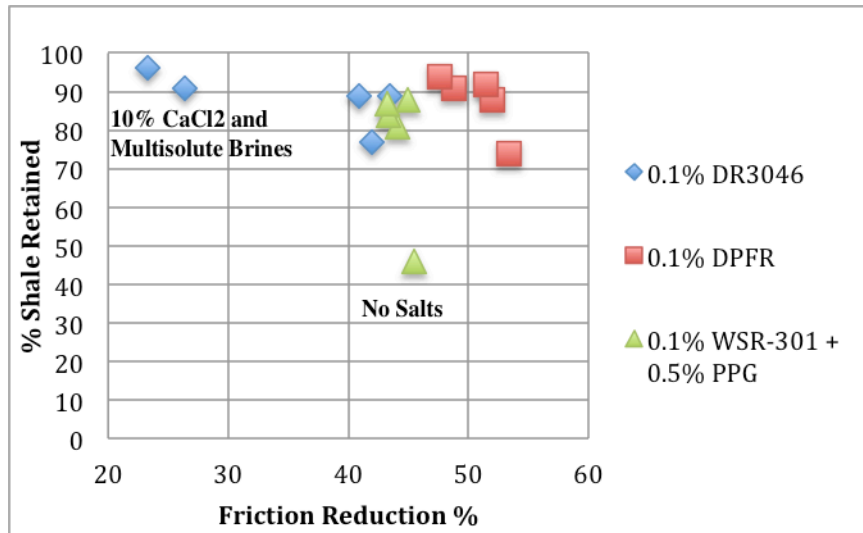


Figure 47 - % Shale retained after 12h in the HRO at 70°C vs friction reduction % in 0.1% DR3046, 0.1% DPFR, and PEO-PPG dispersion with DI water, 10% NaCl, 20% NaCl, 10% CaCl<sub>2</sub>, and the multi-solute brine

#### 4.4 Fracture conductivity results

Since shale degradation is one of the main causes of fracture conductivity reduction, fluids that are efficient shale stabilizers are often found to maintain fracture conductivity. Therefore, as the novel PA friction reducer and the PEO-PPG dispersion mixed with a 20% NaCl brine were shown to perform the best at preventing shale cuttings dispersion in the HRO, they were most likely to maintain fracture conductivity. The fracture conductivity experiments were designed to verify this assumption and compare the fracture conductivities retained after the shale had been in contact with a PEO solution, a novel PA based solution, a salt solution and DI water. These tests were conducted following John Pedlow's methods (2013).

#### **4.4.1      *Preliminary experiments***

The first experiments were designed to assess the effects of precipitation of the PEO on fracture conductivity. As shown in Section 4.3.3, the cloud point property helped enhance shale cuttings stability. Therefore, it was interesting to evaluate whether the contact between the shale and the precipitated PEO in the fracture would help maintain fracture conductivity. A 20% NaCl solution of 0.1% PEO-PPG dispersion was injected in the core flooding apparatus placed in the oven at 80°C. The first step was to check if the fluid would flow through the loop and the fracture despite the precipitation of the PEO. A plastic core was placed in the core holder. Upon the injection of the fluid with a pressurized reservoir at the shop air pressure (90-100 psi), a trickle of fluid flowed out of the system. Within an hour, it changed into droplets. As the flow of the fluid became smaller, it eventually stopped after more than 12 hours of pressurized injection and a total volume injected of 800 mL. The shop air was then directly connected to the entrance of the loop but no air came out from the outlet. Therefore, it appeared that the lines and the fracture were plugged and that no more fluid could be injected. It was concluded that the precipitation of the PEO was responsible for this plugging.

This experiment showed that, while the cloud point property is interesting for shale stabilizing purposes, it causes obstruction of the fractures and thus, is likely to drastically reduce gas production onsite. Moreover, in order to prevent any clogging of the equipment caused by PEOs precipitation, it was decided to perform the next experiments at 25°C and to lower the PEO concentration to 0.01% WSR-301; conditions designed to ensure that the PEO was below the cloud point.

#### 4.4.2 Shale fluid sensitivity to one fluid injection

The fracture conductivity tests were conducted on cores composed of half plastic and half shale propped with 40/70 white sand. The characteristics of the fractures are given in Table 9 and the details of the tests performed are summarized in Table 10.

*Table 9 –Propped fractures properties*

	Core 1	Core 2	Core 3	Core 4
Mass shale/plastic (g)	38.03/18.6	27.34/18.74	44.11/21.86	30.75/21.44
Fracture length (in)	2.45	2.45	2.83	2.83
Fracture diameter (in)	0.99	0.97	0.97	0.96
Fracture width (in)	0.0325	0.0325	0.0325	0.0325

*Table 10 - Fracture conductivity test matrix*

	Core 1	Core 2	Core 3	Core 4
1st Flood	DI water	20% NaCl	20% NaCl + 0.01% WSR-301	20% NaCl + 0.1% Novel PA
2nd Flood	/	20% NaCl	20% NaCl + 0.01% WSR-301	20% NaCl + 0.01% WSR- 301
3rd Flood	/	/	20% NaCl + 0.1% Novel PA	20% NaCl + 0.1% Novel PA
4th Flood	/	/	20% NaCl + 0.01% WSR-301	

The objective was to compare the changes in permeability due to shale-fluid contact i.e. shale fluid sensitivity. In order to compare the effects of fluid injections on different cores, the measured permeability after a fluid injection was normalized to the initial permeability of the proppant in the fractured core; this ratio was termed percentage of permeability retained. A comparison of the percentage of permeability retained after the first flood is shown in Figure 48. The 20% NaCl maintained a slightly higher fracture permeability than the DI water. This result was expected since the salt solution had been

shown to reduce the dispersion of the Pierre Shale in the HRO experiments and that DI water yielded the poorest performance in terms of shale stabilization. The biggest drop in proppant permeability was measured after the injection of the PEO solution. Only 22% of the initial permeability was measured in the proppant pack. As the salt concentration was 20% NaCl, one would expect this fluid to maintain at least a permeability to 34%, which is the level of performance observed for the pure 20% NaCl brine. The cation exchange and osmotic transport which benefitted the shale when it was flooded with the brine, seemed to be counterbalanced by some other effects of the PEO on the propped fracture. The low percentage of permeability retained may be explained by a coating of the sand or of the surface of the shale when the polymer dried out in the propped fracture. Finally, the brine that contained 0.1% DPFR was the most efficient at retaining proppant pack permeability with 43% of permeability retained.

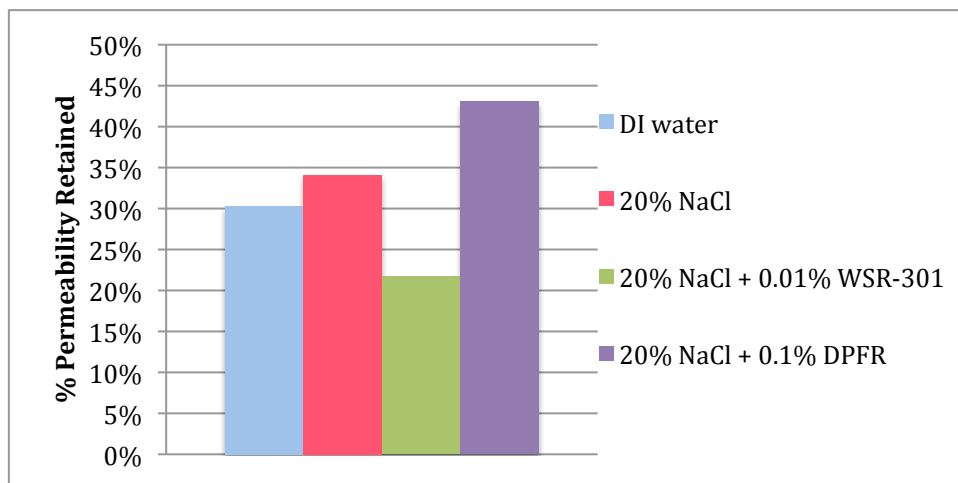


Figure 48 - Comparison of the percentages of permeability retained after a first flood

After completion of all the injections and nitrogen permeability measurements, the cores were removed from the core holder and taken apart to inspect the fracture faces. Since cores 1 and 2 were flooded only with one type of fluid, it was interesting to visually

examine them to quantitatively compare their degradation upon contact with the fluid. This analysis was not possible for cores 3 and 4 as they had successively been flooded with different fluids.

As can be seen in Figure 49, both faces contained black specks, and sand grains were attached to the surface. Based on Pedlow's similar description of embedment marks (Pedlow, 2013), it was concluded that proppant embedment had taken place. The round specks were below 300  $\mu\text{m}$  in diameter after NaCl contact and 400  $\mu\text{m}$  after DI water contact. Moreover, it appeared that the sand grains in Core 1 were more regularly spread on the surface of the fracture than on Core 2 and that they were harder to remove.



Figure 49 – Fracture faces of cores 1 (left) and 2 (right) at the end of the test

These observations indicated that the sand had embedded deeper in the shale after it had been in contact with DI water. Finally, many smaller white particles were visible on the surface of this latter core. These were assumed to be shale or proppant fines. All these observations showed that more fracture conductivity damage occurred after DI water flood than after the 20% NaCl flood and, therefore, confirmed the permeability measurements. Additionally, a SEM-EDX analysis was performed on core 2 to

corroborate these findings. An SEM image can be seen on Figure 51. The results showed that what were thought to be sand grains were mainly composed of silicon. The surface of the black pores contained a larger amount of sodium and chloride than their surroundings. This confirmed that these specks were cavities. Therefore, it is very likely that these small holes formed when the proppant embedded in the shale. Due to surface tension and gravity, the concentrated brine may have accumulated in these cavities.

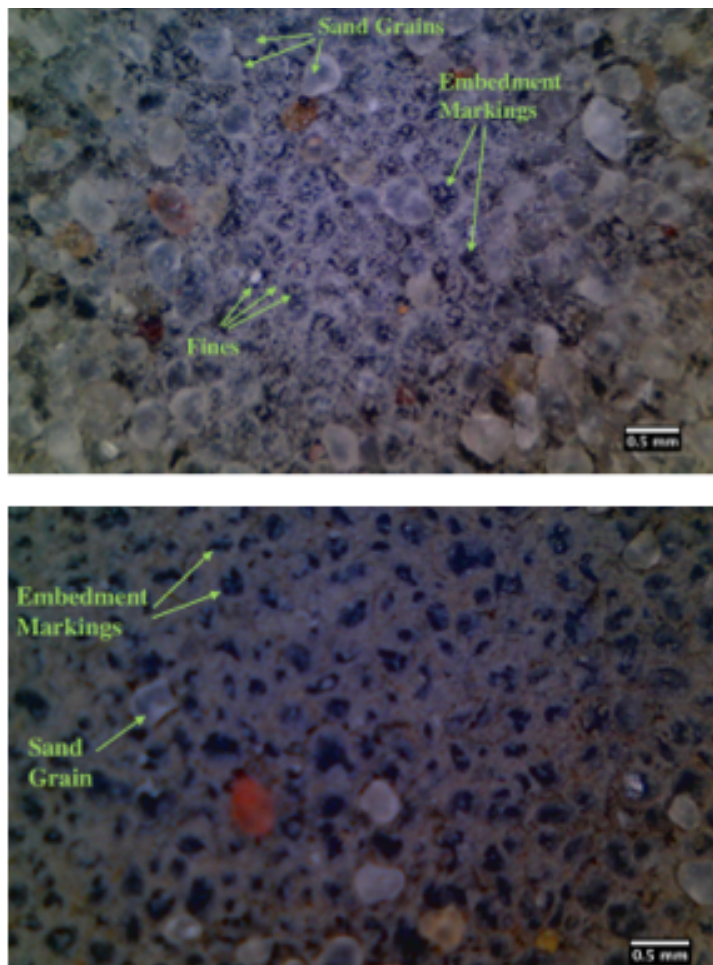


Figure 50 - Microscope images showing faces of cores 1 (top) and 2 (down) after floods



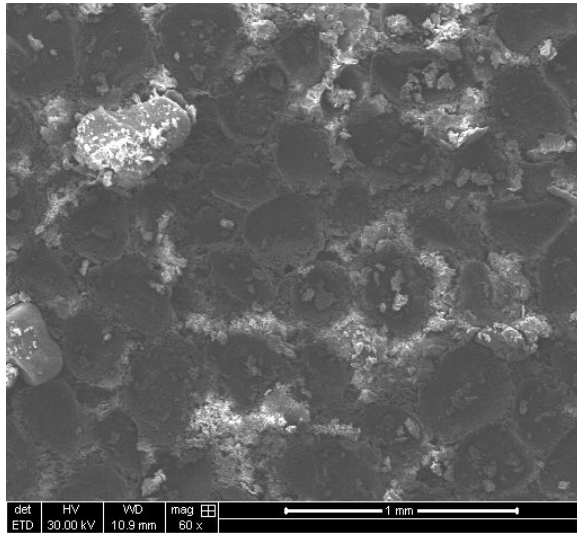


Figure 51 - SEM image of core 2 after flood with fresh water

Finally, oxygen, magnesium, aluminum, silicon, potassium, and iron were detected in between the pores and on the sand grains. They are the main elements that compose quartz and illite present in Pierre Shale. The SEM-EDX results confirmed the structure of the core surfaces that had been determined visually.

#### ***4.4.3 Shale fluid sensitivity to successive fluid injections***

Successive fluid injections and permeability measurements were conducted on cores 3 and 4 (see Figure 52 and Figure 53, respectively). This was done in order to corroborate the above results, to determine if the fluid shale sensitivity depended on fluid contact time, and to differentiate polymer coating, from true embedment resulting from shale degradation upon contact with the fluid. The second injection of PEO into core 3 (previously flooded with PEO) did not significantly change the permeability of the propped fracture. The percentage of retained permeability was 2% higher than the percentage of retained permeability measured after the first PEO injection. This slight increase should not be considered significant given the uncertainties associated with the computation of the permeability using the Forchheimer correlation. It was concluded that

the Pierre Shale was not sensitive to a longer contact time with PEO after the 2.5 hours of contact during the first injection. The third fluid injection of DPFR didn't lead to any change in the permeability of the proppant pack. This result was expected since, as explained in Section 4.4.2, it was shown to be more efficient at preventing fracture conductivity damage than the PEO-based fluid. Therefore, it did not degrade the permeability more than what the PEO solution had already done. After the fourth injection of PEO in core 3, the measured permeability strongly increased. This result was unexpected. One possible explanation is that there is a reaction between the PEO and PA solutions, which dissolved some residues - coating or fines - that were obstructing the nitrogen flow during the permeability measurements. It is also possible that the product of this reaction created a film on the surface of the shale and changed its wettability. Therefore, the following PEO injection would generate a higher measured permeability if the sand coating was eliminated and/or a polymeric film was preventing shale degradation. It is likely that both a PA-PEO reaction and a change in the surface wettability are involved. This experiment shows that a coating occurs with the injection of PEO and with the injection of PA. Indeed, both need to have been flowed through the fracture and to be in contact for the reaction to take place.

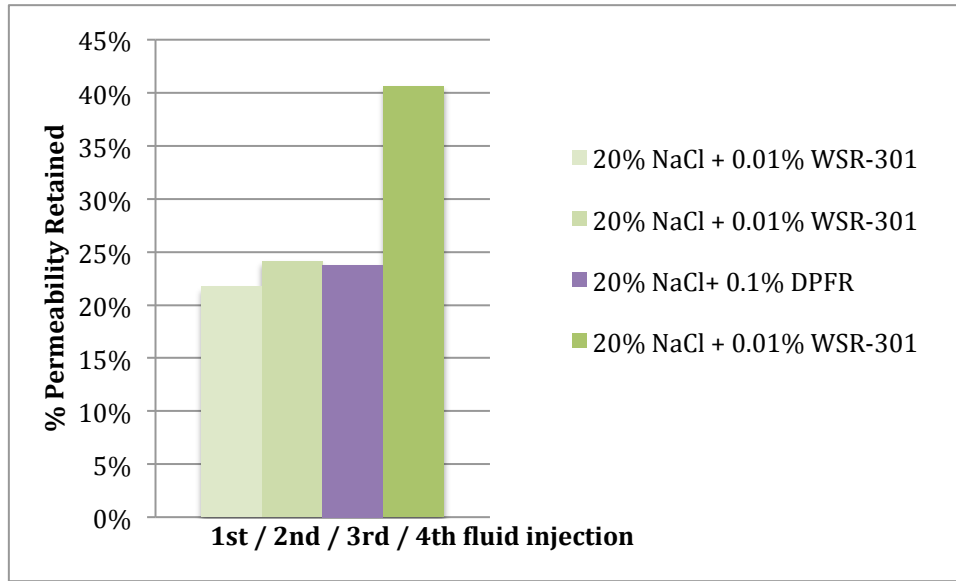


Figure 52 – Percentages of permeability retained after the successive injections in core 3

In the last experiment, the novel PA, PEO WSR-301, and the novel PA were sequentially injected. The percentage of permeability retained for these are summarized in Figure 53. Again, the results were rather unexpected but they confirmed the trends observed on Core 3. The permeability measured after the injection of PEO rose and was much higher than the permeability retained after the injection of the novel PA. It was calculated that the percentage of permeability retained was of 110%. However, it is very unlikely that the permeability of the proppant pack after two injections was higher than its initial permeability. A possible reason for the percentage of permeability retained to be higher than 100% is that the fracture was not completely dry and that the pressure drops across the fracture were not stable. Therefore, the assessment of the differential pressure for a given nitrogen flow rate during the permeability measurements might have contained some error. It did not allow enough time for the pressure to reach its equilibrium value. In any case, this result was similar to the observed increase of the percentage of permeability retained in the fracture of core 3 after the successive injections

of the novel PA and PEO WSR-301, and thus showed that it was reproducible. In addition to this mechanism, which possible explanations have already been discussed, this outcome points out that these measurements are relative. They are useful to compare the increase or the decrease of permeabilities but cannot be used as absolute numbers due to the uncertainties related to these experimental methods.

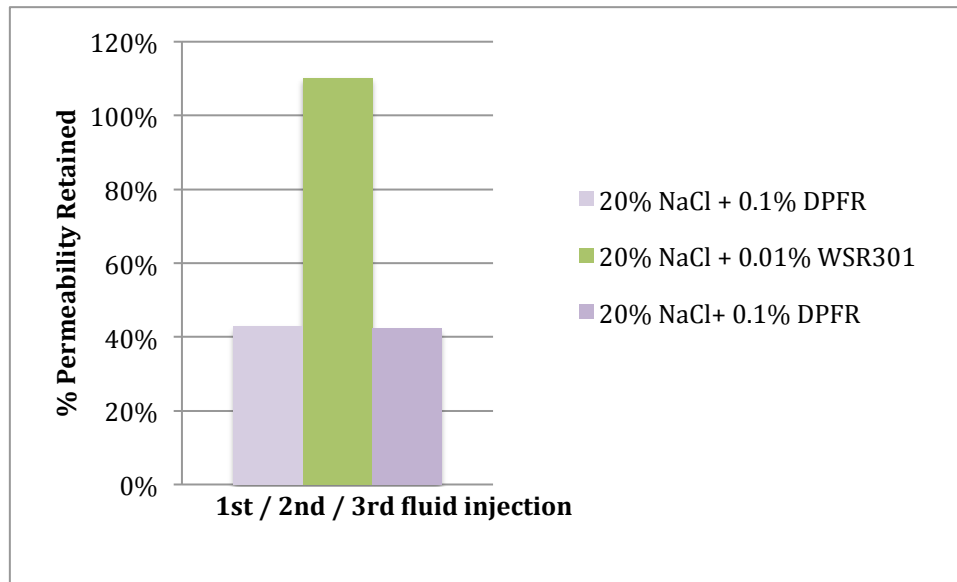


Figure 53 – Percentages of permeability retained after the successive injections in core 4

The last injection in this core was of a solution containing NaCl and the novel PA friction reducer. The permeability dropped to the same level as its initial value after the first injection of the same fluid. Therefore, it was concluded that neither the second injection (PEO solution) nor the third one (novel PA solution) degraded the fracture conductivity more than what the initial injection of novel PA did. The degradation of the fracture conductivity of the Pierre Shale core did not depend on the contact time between the novel PA (DPFR) solution and the shale. Finally, the decrease in permeability after the novel PA injection showed that the reaction that may have occurred between PA and

PEO depended on the order of injection of these products. More precisely, it only occurred if PEO was injected on the top of PA. Additionally, the last injection of PA created coating or fines again so that the permeability was reduced to its previous level but no embedment, which would have led a lower percentage of permeability retained. This last injection cancelled the effects of the injection of PEO and therefore is likely to have removed the polymeric film if there was any.

#### ***4.4.4 Conclusions on the efficiency of salt-tolerant friction reducers at maintaining fracture conductivity***

Although the mechanisms that control the increase of the proppant pack permeability after the successive contacts with a 20% NaCl + 0.1% DPFR solution and a 20% NaCl + 0.01% WSR-301 solution are still unclear, the fracture conductivity measurements showed that:

- A high salinity fluid allowed for a higher fracture conductivity and demonstrated the advantage to using flowback water.
- Above its CPT, the PEO solution plugged the fracture and below its CPT, the addition of PEO to a 20% NaCl solution reduced fracture conductivity. These experiments pointed out that the HRO tests were not adapted to fully understand shale stabilization by PEOs. Though the CPT of PEOs prevented cuttings dispersion, it deteriorated fracture conductivity. Moreover, the effects of the soluble PEO on shale swelling and softening had not been evaluated with the HRO tests.
- The DPFR friction reducer was the most efficient additive at maintaining fracture conductivity in a 20% NaCl brine. While only 22% and 34% of the initial permeability of the proppant pack were retained after a first injection

with 0.01% WSR301 + 20% NaCl and 20% NaCl respectively, 43% permeability was retained after a first injection with DPFR in the NaCl brine.

- Successive floods with a novel PA friction reducer brine and with a PEO brine generated a significant permeability recovery. Even though the underlying mechanism was not fully explained, it was likely to involve a reaction between PA and PEO that changed the wettability of the clay surface and cleared fines.

## Chapter 5: Conclusions

### 5.1 Summary

The swelling tests and beaker tests provided preliminary results showing that NaCl solutions were promising fluids to enhance shale stabilization at ambient temperature. However, they did not yield conclusive results about the effects of PEO-based fluids on shale degradation. It was noted that PEO performance was dependent on salt concentrations.

The dispersion tests, conducted at 70°C, confirmed the shale stabilization effects of the salts. They showed that stabilization increased with salt concentration and varied with salt species. CaCl<sub>2</sub> was found to be more effective than NaCl at stabilizing Pierre Shale I. The results were consistent with the hypothesis that salts favored shale stabilization because they enhanced osmotic transport of water out of the shale and reduced hydration. The addition of salt-tolerant friction reducers – the conventional PA based friction reducer DR3046, the novel PA based friction reducer called Dispersion Polymer Friction Reducer (DPFR), and PEOs – limited shale cuttings dispersion. The stabilization mechanisms proposed rely on chemical bridging between the polymer chains and the shale surface, the viscosity of the DR3046 solution, and the cloud point property of PEOs. For both PEO and PA based fluids, the concentration and the molecular weight of the polymers did not significantly impact shale stabilization. Salts controlled the PEO cloud point value, and therefore, the onset of the PEO stabilization mechanism for a given reservoir temperature. As the PEO precipitates on the shale surface, it prevents fluids from entering the shale and reduces shale degradation. Salts also improved shale stabilization by PAs. Shale cuttings dispersion increased with longer contact times but the

addition of PEO-PPG and of the novel PA based friction reducer delayed shale degradation. Overall, the DPFR friction reducer generated the best and most consistent results in all salt conditions. The PEO-PPG dispersion was very efficient at reducing shale cuttings dispersion in the presence of salts and the addition of the conventional friction reducer DR3046 produced the best shale retention results in DI water.

Finally, fracture conductivity experiments were carried out at 25°C and 70°C. The precipitation of PEOs at high temperature clogged the core flood apparatus. The results suggest that even though they are efficient friction reducers and shale stabilizers, PEOs cannot maintain fracture conductivity in reservoirs in which temperatures exceed the CPT of the PEO. Permeability measurements performed at 25°C showed that the contact of the shale with DI water or with 20% NaCl reduced the permeability of the propped fracture by 70%. The novel PA based NaCl brine was found to be the most efficient at maintaining fracture conductivity with up to 43% of permeability retained. Even below its cloud point temperature and at its lowest concentration to be an efficient friction reducer, the PEO solution in 20% NaCl degraded the permeability of the proppant pack the most.

The objective of this research was to assess the capability of friction reducers to maintain shale integrity and fracture conductivity in flowback waters. The typical polyacrylamide based friction reducer provides adequate shale stabilization but is not an efficient friction reducer in the presence of  $\text{CaCl}_2$ . While PEOs are cheaper than PAs and good friction reducers that perform similarly regardless of the salt concentration, their effects on shale stabilization strongly depend on salt composition and temperature. Moreover, the permeability measurements showed that PEOs damage fracture



conductivity at temperature above as well as below the cloud point temperature. At all salt concentrations, the novel DPFR was consistently shown to be the most efficient additive for both friction reduction and shale stabilization.

## **5.2 Future work**

The mechanism that generated the increase in the proppant permeability after successive injections of DPFR and WSR-301 would need to be further investigated. If, what is likely to involve a reaction between the PA and PEO additives, proves to actually protect the shale and maintain such a high fracture conductivity, the mixing of PA and PEO could greatly improve the productivity of hydraulic fracturing operations.

In order to minimize the uncertainties related to the permeability measurement and to confirm the encouraging results obtained with the DPFR, the fracture conductivity experiments would need to be repeated. The main sources of uncertainty are due to unstable pressure measurements and incorrect data correlation to the Forchheimer equation. Additionally, proppant embedment tests such as the measurement of shale deformation and the penetration of proppant when the shale samples are subjected to various loads and immersed in the same test fluids would confirm the results of this research on fracture conductivity. Special care should be taken to ensure similar storage conditions of the shale and core preparation. The use of preserved shale and actual flowback water samples would make the observations more directly applicable to ongoing hydraulic fracturing operations. If the DPFR is confirmed to maintain fracture conductivity, it should be tested at higher temperatures.

To take advantage of the consistent performance of PEOs as friction reducers even though they reduce fracture conductivity, more research could potentially be done

on its heat and shear degradation within the well. Therefore, a fracture conductivity experiment would have to be conducted on a PEO solution that has previously been submitted to the high shear of a flow loop test. If the shear in the flow loop degrades the PEO chains enough to maintain a reasonable conductivity in the fracture, PEOs may be able to provide a cheap alternative to the DPFR product in the hydraulic fracturing industry.

## Appendix A - Cloud point temperatures in NaCl and CaCl<sub>2</sub> solutions at 0.1 % and 0.01 % PEO

*Table 11 - CPT (°C) of 0.1% PEO solutions in NaCl and CaCl<sub>2</sub>*

0.1% PEO						
Salt Composition	WSR-N10	WSR-N750	WSR-301	WSR Coagulant	WSR-303	0.1% WSR-301 + 0.5% PPG
No Salt	> 97	> 98	> 97.5	> 97.5	> 98	- <sup>(a)</sup>
5% NaCl	81.5	79	77.5	77	76.5	76
10% NaCl	66	63.5	61.5	62	62.5	59
15% NaCl	53	50	50	48.5	48	39
20% NaCl	43	41	40	39.5	38	25.5
25% NaCl	< 29	< 27	< 26	< 26	< 26	-
5% CaCl <sub>2</sub>	87	85.5	84.5	84	84	-
10% CaCl <sub>2</sub>	83	81	81	80.5	80.5	67
15% CaCl <sub>2</sub>	82	81.5	80.5	80	80	-
20% CaCl <sub>2</sub>	86	85	84.5	84	84	-
7.4% NaCl + 1.8% CaCl <sub>2</sub>	71	68.5	67	67	67	65

(a): Measurement not available

*Table 12 - CPT (°C) of 0.01% PEO solutions in NaCl and CaCl<sub>2</sub>*

0.01% PEO					
Salt Composition	WSR-N10	WSR-N750	WSR-301	WSR Coagulant	WSR-303
No Salt	> 98	> 98	> 98	> 98	> 98
5% NaCl	84	81	77	78	78
10% NaCl	69.5	65	63	65	63
15% NaCl	55	53	51	53	52
20% NaCl	47	43	40	40	39
3.7% CaCl <sub>2</sub>	91	89.5	87.5	88.5	88.5
7.1% CaCl <sub>2</sub>	89	86	84.5	84.5	85
10.4% CaCl <sub>2</sub>	87	85	83	83.5	83
13.5% CaCl <sub>2</sub>	86	84	83	83.5	83.5

## Appendix B - Effect of PEO addition on the pH of CaCl<sub>2</sub> solutions

*Table 13 - pH of CaCl<sub>2</sub> solutions with and without 0.1% PEO*

% CaCl <sub>2</sub>	0		5		10		15		20	
PEO (Yes/No)	No	Yes	No	Yes	No	Yes	No	Yes	No	Yes
WSRN-10	6.0	9.3	5.7	7.5	5.7	7.0	5.8	6.7	5.5	6.0
WSRN-750	5.7	9.3	5.5	7.3	5.5	6.9	5.8	6.7	5.5	6.0
WSR-301	5.4	8.8	5.5	7.2	5.6	7.0	5.4	6.4	5.3	6.1
WSR Coagulant	5.7	8.6	5.5	7.2	5.6	6.9	5.3	6.3	5.5	6.2
WSR-303	5.8	8.9	5.5	7.3	5.5	6.6	5.5	6.3	5.6	6.2
% Increase	57		32		24		17		11	

## Appendix C – Viscosity data

*Table 14 - Viscosity (cP) of PA and PEO solutions with no salt present and with 20% NaCl, at 25°C and 70°C*

25°C/70°C	No Additive	0.01% DPFR	0.01% WSR-301	0.1% WSR-N10	0.1% DR3046	0.1% DPFR	0.1% WSR-301 + 0.5% PPG	0.1% WSR-301
No Salt	0.8/0.5	1.3/0.8	0.9/0.5	0.9/0.5	14.1/8.7	3.2/1.9	3.6/1.3	4.5/1.6
20% NaCl	1.2/0.7	1.3/0.7	1.4/0.7	1.4/ND	2.6/0.8	1.6/0.8	2.4/ND	3.2/ND

*Table 15 - Viscosity (cP) of PA and PEO solutions with 10% NaCl, 10% CaCl<sub>2</sub> and the multi-solute brine, at 25°C and 70°C*

25°C/70°C	No Additive	0.1% DR3046	0.1% DPFR	0.1% WSR-301 + 0.5% PPG
10% NaCl	-(a)	1.2/0.7	1.3/0.7	-
10% CaCl <sub>2</sub>	1.1/0.6	1.4/0.8	1.4/0.8	5.1/1.6
7.4% NaCl + 1.8% CaCl <sub>2</sub>	0.9/0.6	1.1/0.7	1.2/0.7	5.0/1.1

ND: Not determined due to instability

(a): Measurement not available

## **Bibliography**

- Acharya, H.R., Henderson, C., Matis, H., Kommepalli, H., Brian, M., Wang, B., 2011. Cost Effective Recovery of Low-TDS Frac Flowback Water for Re-use.
- Al-Muntasheri, G.A., 2014. A Critical Review of Hydraulic Fracturing Fluids over the Last Decade. Soc. Pet. Eng.
- Alramahi, B., Sundberg, M., 2012. Proppant embedment and conductivity of hydraulic fractures in shales. ARMA 1–6.
- Aston, M.S., Elliott, G.P., 1994. Water-based glycol drilling muds: shale inhibition mechanisms. Eur. Pet. Conf. 107–113.
- Ataman, M., 1987. Properties of aqueous salt solutions of poly(ethylene oxide). Colloid Polym. Sci. 265, 19–25. doi:10.1007/BF01422658
- Back, D., Schmitt, R., 2000. Ethylene oxide polymers, in: Kirk-Othmer Encyclopedia of Chemical Technology. John Wiley & Sons.
- Bailey, F., Callard, R., 1959. Some properties of poly(ethylene oxide) in aqueous solution. J. Appl. Polym. Sci. I, 56–62.
- Barbot, E., Vidic, N.S., Gregory, K.B., Vidic, R.D., 2013. Spatial and temporal correlation of water quality parameters of produced waters from devonian-age shale following hydraulic fracturing. Environ. Sci. Technol. 47, 2562–9. doi:10.1021/es304638h

- Beihoffer, T.W., Dorrough, D., Schmidt, D.D., 1988. The Separation of Electrolyte Effects from Rheological Effects in Studies of Inhibition of Shales with Natural Moisture Contents. Soc. Pet. Eng.
- Bland, R., 1992. Water-based glycol systems acceptable substitute for oil-based muds. Oil Gas J. 1–9.
- Bland, R., 1994. Quality criteria in selecting glycols as alternatives to oil-based drilling fluid systems. Soc. Pet. Eng. SPE 27141, 1–13.
- Bland, R., Smith, G., Eagark, P., van Oort, E., Dharma, N., n.d. Low Salinity Polyglycol Water-Based Drilling Fluids as Alternatives to Oil-Based Muds. Soc. Pet. Eng. IADC/SPE 3, 273–285.
- Blauch, M., Houston, N., Seyman, M., Reese, R., 2009. Technique Reuses Frac Water In Shale. Am. Oil Gas Teporter.
- Blauch, M.E., 2010. Developing Effective and Environmentally Suitable Fracturing Fluids Using Hydraulic Fracturing Flowback Waters. Soc. Pet. Eng.
- Blauch, M.E., Services, S.W., Myers, R.R., Moore, T.R., Lipinski, B.A., North, E., Energy, C., 2009. Marcellus Shale Post-Frac Flowback Waters – Where is All the Salt Coming From and What are the Implications ? 1–20.
- Bradley, W., 1945. MOLECULAR ASSOCIATIONS BETWEEN MONTMORILLONITE AND SOME POLYFUNCTIONAL ORGANIC LIQUIDS. J. Am. Chem. Soc. 67.

- Bruff, M., Jikich, S., 2011. Field Demonstration of an Integrated Water Treatment Technology Solution in Marcellus Shale. SPE East. Reg. Meet. 1–9.
- Caulfield, M.J., Hao, X., Qiao, G.G., Solomon, D.H., 2003. Degradation on polyacrylamides. Part I. Linear polyacrylamide. *Polymer (Guildf)*. 44, 1331–1337. doi:10.1016/S0032-3861(03)00003-X
- Caulfield, M.J., Qiao, G.G., Solomon, D.H., 2002. Some aspects of the properties and degradation of polyacrylamides. *Chem. Rev.* 102, 3067–84.
- Chenevert, M., 1970a. Shale alteration by water adsorption. *J. Pet. Technol.* 1141–1148.
- Chenevert, M., 1970b. Shale control with balanced-activity oil-continuous muds. *J. Pet. Technol.*
- Choi, S., 2008. PH sensitive polymers for novel conformance control and polymer flooding applications. The University of Texas at Austin.
- Cinco-Ley, H., Samaniego-V., F., 1981. Transient Pressure Analysis: Finite Conductivity Fracture Case Versus Damaged Fracture Case. *Soc. Pet. Eng.* doi:10.2118/10179-MS
- Clark, C., Burnham, A., Harto, C., Horner, R., 2013. Hydraulic Fracturing and Shale Gas Production: Technology, Impacts, and Regulations.
- Clark, R.K., Scheuerman, R.F., 1976. Polyacrylamide/potassium-chloride mud for drilling water-sensitive shales. *J. Pet. Technol.*



- D’Almeida, A.R., Dias, M.L., 1997. Comparative study of shear degradation of carboxymethylcellulose and poly (ethylene oxide) in aqueous solution. *Polym. Degrad. Stab.* 56, 331–337.
- Dow company, 2002a. POLYOX Water-soluble resins. doi:10.1016/0016-0032(62)90965-1
- Dow company, 2002b. Polyox Water-Soluble Resins - Degradation of Water-Soluble Resins.
- Downs, J., van Oort, E., Redman, D., 1993. TAME: A new concept in water-based drilling fluids for shales. *Soc. Pet. Eng. SPE* 26699.
- Dowwolff Cellulosics, n.d. POLYSLIP OF-50 Polymer.
- EIA, 2011. Review of Emerging Resources: U.S. Shale Gas and Shale Oil Plays.
- Elbel, J., Britt, L., 2000. Fracture Treatment Design, in: *Reservoir Stimulation*. Wiley, pp. 1–50.
- Evangelou, V.P., 1998. *Environmental soil and water chemistry*. John Wiley & Sons.
- FDA, 2013a. CFR Code of Federal Regulations Title 21.
- FDA, 2013b. CFR Code of Federal Regulations Title 21.
- FDA, 2013c. CFR Code of Federal Regulations Title 21.

FDA, 2013d. CFR Code of Federal Regulations Title 21 CFR Code of Federal Regulations Title 21.

Ferguson, M.L., Anderson, C.C., Eichelberger, P.B., Hallock, J.K., Qiu, X., Roell, R., 2013. Innovative Friction Reducer Provides Improved Performance and Greater Flexibility in Recycling Highly Mineralized Produced Brines. Soc. Pet. Eng.

Fiume, M.M., Bergfeld, W.F., Belsito, D. V, Hill, R. a, Klaassen, C.D., Liebler, D., Marks, J.G., Shank, R.C., Slaga, T.J., Snyder, P.W., Andersen, F.A., 2012. Safety assessment of propylene glycol, tripropylene glycol, and PPGs as used in cosmetics. Int. J. Toxicol. 31, 245S–60S. doi:10.1177/1091581812461381

Florin, E., Kjellander, R., Eriksson, J.C., 1984. Salt Effects on the Cloud Point of the Poly(ethylene oxide) + Water System. J. Chem. Soc. Faraday Trans. 80, 2889–2910.

Gautreau, Z., Griffin, J., Peterson, T., Thongpradit, P., 2006. Characterizing viscoelastic properties of polyacrylamide gels.

Gidley, J., Penny, G., McDaniel, R., 1995. Effect of proppant failure and fines migration on conductivity of propped fractures. SPE Prod. Facil.

Green, V., Stott, D., 1999. Polyacrylamide: A review of the use, effectiveness, and cost of a soil erosion control amendment. 10th Int. Soil Conserv. Organ. Meet. 384–389.

Gregory, K.B., Vidic, R.D., Dzombak, D. a., 2011. Water Management Challenges Associated with the Production of Shale Gas by Hydraulic Fracturing. Elements 7, 181–186. doi:10.2113/gselements.7.3.181

- Hale, A., 1991. Method to quantify viscosity effects on dispersion test improves testing of drilling-fluid polymers. SPE Drill. Eng.
- Hale, A., Mody, F., 1993. Mechanism for Wellbore Stabilization With Lime-Based Muds. SPE/IADC Drill. Conf. 4–7.
- Haluszczak, L.O., Rose, A.W., Kump, L.R., 2013. Geochemical evaluation of flowback brine from Marcellus gas wells in Pennsylvania, USA 28, 55–61.
- Hammouda, B., 2006. Solvation Characteristics of a Model Water-Soluble Polymer. Wiley Intersci. 3195–3199. doi:10.1002/polb.20967
- Hayes, T., 2009. Sampling and Analysis of Water Streams Associated with the Development of Marcellus Shale Gas.
- Holditch, S.A., Morse, R.A., 1976. The Effects of Non-Darcy Flow on the Behavior of Hydraulically Fractured Wells. J. Pet. Technol.
- Jung, C.M., Zhou, J., Chenevert, M., Sharma, M., 2013. The Impact of Shale Preservation on the Petrophysical Properties of. Soc. Pet. Eng.
- Khodja, M., Khodja-saber, M., Canselier, J.P., Cohaut, N., Bergaya, F., 2010. Drilling Fluid Technology : Performances and Environmental Considerations, in: Products and Services from R&D to Final Solutions.
- Kimball, R., 2011. Key considerations for frac flowback/produced water reuse and treatment. NJWEA Annu. Conf.

- Kjellander, R., Florin, E., 1981. Water structure and changes in thermal stability of the system poly (ethylene oxide)–water. *J. Chem. Soc. Faraday Trans.* 2053–2077.
- Kutz, M., 2005. Handbook of environmental degradation of materials.
- Kuzmyak, N.J., 2014. Evaluation of Friction Reducers for Use in Recycled Fracturing Flowback and Produced Water. The University of Texas at Austin.
- L'Hôte-gaston, J.L., Tocce, E., Li, Q., Karas, C., Levina, M., Vuong, H., Hitt, J., n.d. Improvements in Oxidative Stability of Polyethylene Oxide and the Impact in Oral Solid Dosage Forms.
- LaFollette, R., Carman, P., 2010. Proppant Diagenesis: Results So Far. SPE Unconv. Gas Conf.
- Leung, H.-W., Ballantyne, B., Hermansky, S.J., Frantz, S.W., 2000. Peroral Subchronic, Chronic Toxicity, and Pharmacokinetic Studies of a 100-Kilodalton Polymer of Ethylene Oxide (Polyox N-10) in the Fischer 344 Rat. *Int. J. Toxicol.* 19, 305–312. doi:10.1080/10915810050178752
- Leung, W.M., Axelson, D.E., Syme, D., 1985. Determination of charge density of anionic polyacrylamide flocculants by NMR and DSC. *Colloid Polym. Sci.* 263, 812–817. doi:10.1007/BF01412958
- Liebert, M.A., 1991. Final Report on the Safety Assessment of Polyacrylamide. *J. Am. Coll. Toxicol.* 10, 193–203. doi:10.3109/10915819109078629

- Likos, W.J., 2004. Measurement of crystalline swelling in expansive clay. *ASTM Geotech. Test. J.* 27, 1–7.
- Madsen, F., Müller-Vonmoos, M., 1989. The swelling behaviour of clays. *Appl. Clay Sci.* 4, 143–156.
- McLaughlin, J., 2013. Key Considerations for Frac Flowback/Produced Water Reuse and Treatment, in: *NYWEA Spring Technical Conference*. Syracuse, NY.
- Mitchell, J.K., 1993. *Fundamentals of soil behaviors*. Wiley.
- Muecke, T.W., 1979. Formation Fines and Factors Controlling Their Movement in Porous Media. *J. Pet. Technol.* 31, 144–150. doi:10.2118/7007-PA
- Norrish, K., 1954. The swelling of montmorillonite. *Discuss. Faraday Soc.* 18, 120. doi:10.1039/df9541800120
- O'Brien, D., Chenevert, M., 1973. Stabilizing sensitive shales with inhibited, potassium-based drilling fluids. *J. Pet. Technol.* 1089–1100.
- Osisanya, S., 1991. *Experimental studies of wellbore stability in shale formations*. The University of Texas at Austin.
- Paktinat, J., O'Neil, B., Aften, C., Hurd, M., 2011a. High Brine Tolerant Polymer Improves the Performance of Slickwater Frac in Shale Reservoirs. *Soc. Pet. Eng.*
- Paktinat, J., O'Neil, B., Aften, C., Hurd, M., 2011b. Critical Evaluation of High Brine Tolerant Additives Used in Shale Slick Water Fracs. *Soc. Pet. Eng.*

- Paktinat, J., O'Neil, B., Tulissi, M., 2011c. Case Studies : Impact of high Salt Tolerant Friction Reducers on Fresh Water Conservation in Canadian Shale Fracturing Treatments. Soc. Pet. Eng.
- Paktinat, J., O'Neil, B., Tulissi, M., 2011d. Case Studies : Improved Performance of High Brine Friction Reducers in Fracturing Shale Reservoirs. Soc. Pet. Eng.
- Palisch, T., Duenckel, R., Bazan, L., Heidt, H.J., Turk, G., 2007. Determining Realistic Fracture Conductivity and Understanding Its Impact on Well Performance—Theory and Field Examples. Proc. SPE Hydraul. Fract. Technol. Conf. doi:10.2523/106301-MS
- Patel, A., Gomez, S., 2013. Shale Inhibition : What Works ? Soc. Pet. Eng.
- Patel, A., Stamatakis, S., 2007. Advances in Inhibitive Water-Based Drilling Fluids—Can They Replace Oil-Based Muds? Soc. Pet. Eng.
- Pedlow, J., 2013. A study of the effect of stress and fluid sensitivity on propped fracture conductivity in preserved reservoir shales. The University of Texas at Austin.
- Pedlow, J.W., Sharma, M., 2014. Changes in Shale Fracture Conductivity due to Interactions with Water-Based Fluids. Soc. Pet. Eng.
- Rabiee, A., Zeynali, M., Baharvand, H., 2005. Synthesis of high molecular weight partially hydrolyzed polyacrylamide and investigation on its properties. Iran. Polym. J. 14, 603–608.

- Sheu, J.J., Perricone, A.C., 1988. Design and Synthesis of Shale Stabilizing Polymers for water-Based Drilling Fluids. Soc. Pet. Eng.
- Silva, J., Matis, H., Kostedt IV, W., Watkins, V., 2012. Produced Water Pretreatment for Water Recovery and Salt Production.
- Smith, E. a, Prues, S.L., Oehme, F.W., 1996. Environmental degradation of polyacrylamides. 1. Effects of artificial environmental conditions: temperature, light, and pH. *Ecotoxicol. Environ. Saf.* 35, 121–35. doi:10.1006/eesa.1996.0091
- SNF, 2013. FLOJET® DR Series - Application Guide.
- SNF, n.d. Polyacrylamide Emulsions handbook.
- Sung, J.H., Lim, S.T., Kim, C.A., Chung, H., Choi, H.J., 2004. Mechanical degradation kinetics of poly (ethylene oxide) in a turbulent flow. *Korea-Australia Rheol. J.* 16, 57–62.
- Taylor, K.C., Nasr-El-Din, H. a., 1994. Acrylamide copolymers: A review of methods for the determination of concentration and degree of hydrolysis. *J. Pet. Sci. Eng.* 12, 9–23. doi:10.1016/0920-4105(94)90003-5
- Terracina, J., Turner, J., Collins, D., Spillars, S., 2010. Proppant Selection and Its Effect on the Results of Fracturing Treatments Performed in Shale Formations. *Proc. SPE Annu. Tech. Conf. Exhib.* doi:10.2118/135502-MS

- Van Oort, E., 2003. On the physical and chemical stability of shales. *J. Pet. Sci. Eng.* 38, 213–235. doi:10.1016/S0920-4105(03)00034-2
- Van Oort, E., Bland, R., 1997. Improving HPHT stability of water based drilling fluids, in: *SPE/IADC Drilling Conference*. Amsterdam.
- Van Oort, E., Hale, A.H., Mody, F.K., Roy, S., 1996. Transport in Shales and the Design of Improved Water-Based Shale Drilling Fluids. *SPE Drill. Complet.* SPE 28309, 137–146.
- Van Oort, E., Ripley, D., Chapman, J.W., Williamson, R., Aston, M., 1996. Silicate-based drilling fluids: competent, cost-effective and benign solutions to wellbore stability problems. *Soc. Pet. Eng.* SPE 35059.
- Wayllace, A., 2008. Volume change and swelling pressure of expansive clay in the crystalline swelling regime. University of Missouri.
- Weaver, J.D., Nguyen, P.D., Parker, M.A., van Batenburg, D., 2005. Sustaining Fracture Conductivity. *Soc. Pet. Eng.* 1–10.
- Wever, D.A.Z., Picchioni, F., Broekhuis, A.A., 2011. Polymers for enhanced oil recovery: A paradigm for structure–property relationship in aqueous solution. *Prog. Polym. Sci.* 36, 1558–1628. doi:10.1016/j.progpolymsci.2011.05.006
- Wingrave, J.A., Kubena, E., Douty, C.F., Cords, D.P., 1987. New Chemical Package Produces an Improved Shale Inhibitive Water-Based Drilling Fluid System. *Soc. Pet. Eng.*



- Winston, P., Bates, D., 1960. Saturated solutions for the control of humidity in biological research. *Ecology* 41, 232–237.
- Woodrow, J.E., Seiber, J.N., Miller, G.C., 2008. Acrylamide release resulting from sunlight irradiation of aqueous polyacrylamide/iron mixtures. *J. Agric. Food Chem.* 56, 2773–9. doi:10.1021/jf703677v
- Xu, L., 2013. A Preliminary Simulation of Membrane Distillation for Treatment of Hydraulic Fracturing Produced Waters.
- Yoxtheimer, D., n.d. Potential Water Quality Issues from Natural Gas Development Potential Water Quality Impact Pathways.
- Zeng, Z., Grigg, R., 2006. A Criterion for Non-Darcy Flow in Porous Media. *Transp. Porous Media* 63, 57–69. doi:10.1007/s11242-005-2720-3
- Zeynali, M.E., Rabbii, A., 2002. Alkaline Hydrolysis of Polyacrylamide and Study on Poly (acrylamide-co-sodium acrylate) Properties 11, 269–275.
- Zhou, J., Jung, C.M., Pedlow, J.W., Chenevert, M.E., Sharma, M.M., 2013. A New Standardized Laboratory Protocol to Study the Interaction of Organic-Rich Shales with Drilling and Fracturing Fluids. *Soc. Pet. Eng.*
- Zhou, M., Baltazar, M., Qu, Q., Sun, H., 2014. Water-Based Environmentally Preferred Friction Reducer in Ultrahigh-TDS Produced Water for Slickwater Fracturing in Shale Reservoirs. *Soc. Pet. Eng.*